ON COUPLED LIBRATIONAL DYNAMICS OF GRAVITY ORIENTED AXI-SYMMETRIC SATELLITES

by

SHASHI KANT SHRIVASTAVA
B. Tech. (Hons.), Indian Institute of Technology,
Kharagpur, 1967

A THESIS SUBMITTED IN PARTIAL FULFILMENT OF

THE REQUIREMENT FOR THE DEGREE OF

DOCTOR OF PHILOSOPHY

in the Department
of

MECHANICAL ENGINEERING

We accept this thesis as conforming to the required standard

THE UNIVERSITY OF BRITISH COLUMBIA

September, 1970

In presenting this thesis in partial fulfilment of the requirements for an advanced degree at the University of British Columbia, I agree that the Library shall make it freely available for reference and study. I further agree that permission for extensive copying of this thesis for scholarly purposes may be granted by the Head of my Department or by his representatives. It is understood that publication, in part or in whole, or the copying of this thesis for financial gain shall not be allowed without my written permission.

SHASHI KANT SHRIVASTAVA

Department of Mechanical Engineering

The University of British Columbia
Vancouver 8, Canada

Date October, 29, 1970

Dedicated to my parents

Sri Bhaiya Lal Shrivastava (1901-1970)

and

Srimati Siyarani Shrivastava (1912-1968)

who passed away witnessing my involvement in the process of education which they valued most

ABSTRACT

The influence of inertia, eccentricity and atmospheric forces on the attitude dynamics of gravity oriented, non-spinning, axi-symmetric satellites, executing general librational motion is investigated using analytical, numerical and analog techniques. The problem is studied in the increasing order of complexity.

For the case of a circular orbit, the autonomous, conservative system represented by constant Hamiltonian yields zero-velocity curves and motion envelopes which identify regions of instability from conditional and guaranteed stable motion. The non-linear, coupled equations of motion are solved using approximate analytical techniques: Butenin's variation of parameter method and invariant integral approach. A comparison with the numerical response, establishes their suitability in studies involving motion in the small. The invariant integral method maintains reasonable accuracy even for larger, predominantly planar, disturbances. However, for a general motion in the large, the analytical solutions provide only qualitative information and one is forced to resort to numerical, analogic or hybrid procedures.

The analysis suggests strong dependence of system response on the in-plane disturbances and satellite inertia. The librational and orbital frequencies are of the same

order of magnitude. It also shows that the stable solution, when represented in a three dimensional phase space may lead to 'regular', 'ergodic' or 'island' type regions. The limiting integral manifolds, given here for a few representative values of Hamiltonian, provide all possible combinations of initial conditions, which a satellite can withstand without tumbling. The results, for a range of satellite inertia, are condensed in the form of design plots, indicating allowable disturbances for stable motion. In general, the slender satellites exhibit better stability characteristics.

The presence of aerodynamic torque destroys the symmetry properties of the integral manifolds. The stability of the equilibrium configuration, which now deviates from the local vertical, is established through Routh's as well as Liapunov's criteria. As the system is still autonomous and conservative, the Hamiltonian remains constant leading to the bounds of libration. Numerical analysis of the system response indicates increased sensitivity to planar disturbances. The distortion and contraction of the regular, ergodic and island type stability regions show the adverse effects of aerodynamic torque. The design plots suggest that the shorter satellites, normally not preferred from gravity-gradient considerations, could exhibit better stability characteristics in the presence of large aerodynamic torque.

An alternate, economical approach to the dynamical analysis of the satellites is attempted using an analog

computer. A comparison with the digital data establishes the suitability of the method for design purposes and real time simulation.

As the regular surface represents the only usable stability region from design considerations, a detailed study to establish the bound between regular and ergodic type stability was undertaken. The periodic solutions, obtained numerically using variable secant iteration show their spinal character with the body of stability region built around them. Of particular significance is the fundamental periodic solution P_{21} (two planar oscillations in one out-of-plane cycle) associated with the regular region, suitable for practical operation of a satellite. The remaining periodic solutions represent degeneration of the island-like areas surrounding the mainland. The results lead to a set of fundamental periodic solutions over a wide range of system parameters. Floquet's variational analysis is used to establish the critical disturbance ($C_{H_{cr}} \simeq 0.8$), beyond which no stable motion can be expected. The periodic solutions together with the regular stability region are presented here as functions of Hamiltonian, satellite inertia and aerodynamic torque. The case study of GEOS-A satellite is also included.

In elliptic orbit, the Butenin's analysis of coupled forced systems is found to give an approximate solution of good accuracy. However, for this non-autonomous situation,

where Hamiltonian is no longer a constant of the motion, the concept of integral manifold breaks down. Fortunately, the design plots can still be generated by direct utilization of the response characteristics. In general the stability region diminishes with increasing eccentricity and disappears completely for $e > 0.35$.

The presence of atmosphere adds to the complex behaviour of this non-autonomous system, where even the equilibrium configuration now becomes periodic in character. The stability regions are further reduced with instabilities normally initiating in the planar degree of freedom.

Finally, a possibility of using the atmospheric forces in attitude control is explored. The use of a set of horizontal flaps in conjunction with a semi-passive, velocity-sensitive controller appears to be promising. With a suitable choice of system parameters even a large disturbance can be damped in approximately two orbits.

TABLE OF CONTENTS

CHAPTER PAGE

CHAPTER PAGE

LIST OF TABLES

LIST OF FIGURES

FIGURE PAGE

FIGURE PAGE

FIGURE PAGE

FIGURE PAGE

ACKNOWLEDGEMENT

The author wishes to express his gratitude to Dr. V.J. Modi for guidance given throughout the preparation of the thesis. His help and encouragement have been invaluable.

The suggestions by Dr. A.C. Soudack, Dr. J.E. Neilson and Mr. C. Tschann are appreciated.

The investigation reported in the thesis was supported (in part) by the National Research Council, Grant No. A-2181, and the Defence Research Board of Canada, Grant No. 9551-18.

LIST OF SYMBOLS

a	amplitude of libration in orbital plane
a_1, a_2	constants, equation (2.22)
b	amplitude of libration across orbital plane
e	eccentricity of orbit
f, g	nonlinear functions, equation (2.10)
f^*, g^*	approximations to f and g, respectively, due to constraints, equation (2.15)
f_1, g_1	nonlinear functions, equation (5.3)
f_1^*, g_1^*	approximations to f_1 and g_1, respectively, due to constraints, equation (5.9)
$\bar{g}$	acceleration due to gravity
h_θ	angular momentum per unit mass of satellite
k_1, k_2	moduli of Jacobian elliptic functions, equation (2.24)
l	distance of a mass element from satellite's mass center
l_m	moment arm, equation (6.4)
m	mass of satellite
n_1	frequency of libration in orbital plane, $(3K_i)^{1/2}$
n_2	frequency of libration across orbital plane, $(3K_i+1)^{1/2}$
p_{q_i}	momentum conjugate to generalized coordinate q_i
r	distance between center of attraction and satellite's center of mass

t	time
$\bar{u}_{x_2}$	unit vector along x_2-axis, equation (3.2b)
v	orbital velocity
x,y,z	principal body coordinate with z along the axis of symmetry
x_0,y_0,z_0 x_1,y_1,z_1 x_2,y_2,z_2	intermediate body coordinates with origin at center of mass during modified Eulerian rotations ψ,ϕ,λ, respectively
A_1,A_2,A_3,A_4 B_1,B_2,B_3,B_4	periodic coefficients in variational equation (4.1)
A_f	flap area
$\bar{A}$	surface area of satellite
A,B,C,D,E	coefficients in characteristic equation (3.15)
B_f,B_{f_E},B_{f_p}	aerodynamic coefficient in circular orbit, elliptic orbit and at perigee, respectively
C_1	ratio of transverse to axial cross-sectional areas of satellite, $\pi D_o/4L_o$
C_D,C_L	drag and lift coefficients, respectively
C_H	non-dimensionalized Hamiltonian
C.P.	center of pressure
D_o,L_o	cylindrical satellite's diameter and length, respectively
H	Hamiltonian
I	$I_{xx}=I_{yy}>I_{zz}$
I_{xx},I_{yy},I_{zz}	moments of inertia about x,y,z axes, respectively
K,K_1	amplitude scaling factors appearing in analog simulation

K_i	inertia parameter, $(I-I_{zz})/I$
L	Lagrangian
M_a	aerodynamic moment
O	center of attraction
P	normal pressure due to atmosphere
$P_{x_2}, P_{y_2}, P_{z_2}$	components of P along x_2, y_2, z_2 axis, respectively
P_{ij}	periodic solution, i planar oscillations (ψ) corresponding to j out of plane cycles (ϕ)
R	universal gas constant
Re	radius of the earth
S	centre of mass of the satellite
S_o	ratio of satellite velocity to average molecular velocity, $v/(2\bar{g}RT_\alpha)^{1/2}$
S_o'	$S_o \sin \xi$
T	kinetic energy
T_α	ambient temperature
T_P	dimensionless time, librational period/ orbital period
$Tr[\Theta(t)]$	trace of the condition matrix Θ at time t
T_w	wall temperature of the satellite
U_a	aerodynamic potential
U_g	gravitational potential
V_L	Liapunov function
$erf(S_o')$	$2(\pi)^{-0.5} \int_o^\infty e^{-(S_o')^2} dS_o'$

α	scaling factor appearing in analog simulation
β	dependent variable, equation (2.22)
β_1, β_2	phase angles, equations (2.12), (5.6)
δq_i	infinitesimal increment of q_i
ε	distance between center of mass and center of pressure of satellite
ζ	$n_1\theta+\beta_1$
η	$n_2\theta+\beta_2$
θ	angular position of the satellite, measured from pericenter
$\theta^*, \theta_1^*, \theta_2^*$	phase angles, equations (2.22), (2.24)
λ	rotation about axis of symmetry
λ_i	eigen values
μ	gravitational constant
μ_i	proportionality constant in controller characteristic relation
ξ	angle between satellite surface and air velocity
ρ	atmospheric density
σ	surface reflection coefficient for tangential momentum transfer
σ'	surface reflection coefficient for normal momentum transfer
τ	shear stress due to atmosphere
$\tau_{1_{max}}, \tau_{2_{max}}$	nondimensionalized maximum stabilizing torque in ψ and ϕ degrees of freedom, respectively
ϕ	rotation across the orbital plane
ψ	rotation in the orbital plane

Subscripts

cr	critical value of parameter for stability
e	value of parameter at stable equilibrium configuration
o	initial condition
p	value of parameter at pericenter
v	variational
P	periodic
R	limiting value of parameter for guaranteed regular stability

Dots and primes indicate differentiation with respect to t and θ, respectively; ▼ ▲ in diagrams represent critical value for stability as given by the Floquet theory.

1. INTRODUCTION

1.1 Preliminary Remarks

The advent of the space age has brought promise of a new world to mankind. Some of its innovations are already here, others are yet to come. Among the numerous facets of this exciting new era, communication, earth-resources, navigation and military (implying public safety) are the aspects likely to involve and affect major portion of humanity. In this respect the remarks of Arthur C. Clarke[1], directed particularly to the communication satellite, are pertinent:

> . . . . What we are building now is the nervous system of mankind, which will link together the whole human race, for better or worse, in a unity which no earlier age could have imagined . . . .

Accompanying this new world is a "restructuring of political, scientific and business thinking"[1] leading to an open global society.

However, scientific success demands scientific precision. All of the above mentioned missions normally require satellites to maintain preferred orientations relative to the earth. Among the numerous methods proposed for station keeping, gravity-gradient stabilization has gained much attention primarily due to the passive nature of the system. The earth's natural satellite, the moon, provides an excellent

example of such attitude control. The lunar globe is a triaxial ellipsoid with its longer axis captured by the earth's gravitational field.

The key to this stabilization principle is the fact that the gravitational field varies over a satellite resulting in a restoring moment tending to align its long axis (axis of minimum moment of inertia) with the local vertical. Unfortunately, a gravity gradient stabilized satellite, even though positioned correctly in the beginning, deviates with time from this desired orientation due to perturbing environmental forces such as aerodynamic and radiation pressures, gravitational and magnetic field interactions, micrometeorite impacts, etc.

Design of a satellite capable of proper functioning in such a "hostile" environment demands thorough understanding of its dynamical behaviour. Such a study, with a particular reference to an axi-symmetric satellite, forms the subject of this thesis.

1.2 Literature Review

A survey of the pertinent literature reveals a vast body of information in this area. The bulk of the investigation, however, is devoted to the restricted problem of librations in the plane of the orbit. The dynamic analysis of a general motion has gained relatively little attention,

probably due to the non-linear, coupled character of governing equations.

The pioneering work on pure gravity oriented satellites was carried out by Klemperer[2] (1960), who obtained the exact solution for planar librations of a dumbbell satellite in a circular orbit, and by Baker[3] (1960) who found periodic solutions of the problem for small orbit eccentricity. Beletskiy[5] (1963) focused the attention on resonance effects for satellites in elliptic orbits while Schechter[5] (1964) attempted, with limited success, to extend Klemperer's solution to non-circular orbital motion by perturbation methods. Zlatousov et al.[6] (1964) and more recently, Brereton and Modi[7] (1967) successfully employed numerical methods, involving the use of the stroboscopic phase plane, to analyze the stability of planar motion in the large for orbits of arbitrary eccentricity. They also investigated the corresponding periodic motion[8,9] (1969) and showed that at the critical eccentricity for stability, the only available solution is a periodic one. Brereton[10] (1967) has presented an excellent review of the work on planar librations.

Thomson[11] (1962) analyzed, through linearization, the related problem of slowly spinning satellites in circular orbits. Kane and Barba[12] (1966) attempted to study the motion in elliptic orbits using Floquet theory while Wallace and Meirovitch[13] (1967) used, with questionable success, asymptotic analysis in conjunction with Liapunov's direct method. Modi

and Neilson investigated roll dynamics of a spinning satellite using the W.K.B.J.[14] (1968) and numerical[15] (1968) methods. The concept of integral manifolds was successfully extended to the study of three degrees of freedom motion in circular orbit[16] (1969). The periodic solutions were found and their variational stability was established[17] (1970). The literature on slowly spinning satellites has been summarized, quite effectively, by Neilson[18] (1968).

The presence of various perturbing forces and their influence on satellite dynamics has been discussed in some detail by Roberson[19] (1958), Wiggins[20] (1964), Moyer and Katucki[21] (1966), Anand et al.[22] (1969) and Flanagan and Modi[23] (1970). At higher altitudes, normally used for communication satellites, the solar radiation pressure becomes quite significant. Sohn[24] (1959) indicated the use of solar radiation to orient the satellite with respect to the sun while Ule[25] (1963) considered its application to spin an array of mirrors to achieve attitude stability. A more complete analysis accounting for solar as well as the earth and earth reflected radiations was attempted by Clancy and Mitchell[26] (1964). In addition to the inherent limitations of the approach, the resulting force expression, given in an integral form, required numerical evaluation. This rendered their application to any comprehensive study of satellite attitude dynamics impractical. Modi and Flanagan[27,28,29] evaluated these forces, quite accurately, using the concept of cutting-

plane distance ratios and used them to analyze the environmental effect on the satellite planar dynamics. A critical review of the developments in this field is presented by Flanagan[30] (1969).

Schrello[31] (1961) pointed out the predominance of aerodynamic torque for satellites at altitude below 350 miles with variations in equilibrium configurations discussed by Debra[32] (1959). The effect of small aerodynamic and gravitational torques were treated by Beletskiy[33] (1960) as independent perturbations to the motion of rapidly spinning satellites. Evans[34] (1962) presented the aerodynamic and radiation disturbances in the fundamental form of pressure and shear stress. Using infinitesimal analysis, Garber[35] (1963) treated the effect of constant disturbing torques on the librational motion of a rigid, gravity oriented system in a circular orbit. More directly, Meirovitch and Wallace[36] (1966) established the regions of guaranteed stability for a slowly spinning, axi-symmetric satellite in a circular orbit with constant aerodynamic force. For two satellite configurations, equilibrium positions were tested for stability in the small through Liapunov's direct method. No attempt was made to obtain response of the system to an arbitrary disturbance or the limiting bounds for stability. Nurre[37] (1968) considered a more complex model of an asymmetric satellite in a circular orbit and investigated the stability

of its equilibrium position using linearized analysis. The results of the study were substantiated for an infinitesimal disturbance, by numerical solution of the exact equations of motion.

Exploitation of gravitational, magnetic and solar radiation forces for damping the librations and controlling the attitude has been suggested by many authors. The feasibility of such a concept in terms of solar sailing was investigated by Garwin[38] as early as 1958. Several configurations of mechanical dampers have been evolved and analyzed by Debra[39] (1962), Kamm[40] (1962), Paul[41] (1963), Modi and Brereton[42] (1969), Tschann and Modi[43,44] (1970), etc. Paul et al.[45] (1963) suggested the use of magnetic hysteresis damper, while Mallach[46] (1966), Modi et al[47,48,49] (1970) proposed controllers using solar radiation pressure. A stability theorem, derived by Pringle[50] (1963) for a damped autonomous system, involving the Hamiltonian as a Liapunov function, is of considerable significance. A critical analysis of the literature on the subject, as presented by Tschann[51] (1970), forms a useful contribution to the field.

1.3 Purpose and Scope of the Investigation

From the foregoing, it is apparent that the general motion of a gravity gradient stabilized satellite and the effects of environmental forces on it have received, relatively, little attention. The reason for this limited effort could,

perhaps, be attributed to the complexity of the problem. The non-linear non-autonomous, coupled equations of motion involving large number of parameters are not amenable to any simple concise analysis. Such an investigation, however, is important because, as pointed out by Kane[52] (1966) strong coupling exists between the planar and transverse motions. The main purpose of this investigation, therefore, is to gain a fundamental understanding of the dynamics of the general motion and to obtain the limiting initial conditions for stable motion, in arbitrary orbits, as a function of design parameters. The effect of aerodynamic forces, which become significant for near-earth satellites, on the librational response and stability is also investigated. The possibility of aerodynamic damping and attitude control is examined. From cost considerations, the applicability of analog simulation as well as analytical methods is explored.

The problem is analyzed in five stages, representing, in general, an increasing order of complexity. In the beginning, coupled librational motion of a pure gravity-gradient, axi-symmetric satellite is considered for the autonomous case of a circular orbit. The work is essentially an extension of the study initiated by Modi and Brereton[53] (1968). It helps establish methods of approach for subsequent research.

The influence of constant aerodynamic torque on equilibrium configurations, librational response, nature of

solutions and stability bounds of near-earth satellites is investigated in the third chapter.

A determination of the periodic solutions, which form the spines of stability bounds, is the main objective in the next stage. The peculiar ergodic behaviour of the trajectories, not reported in the case of planar librations, is analyzed. The critical conditions and practically usable bounds of stability are also obtained. A case study of Geodetic Earth Orbiting Satellite[54] (GEOS-A) emphasize the usefulness of the results.

In Chapter 5, the analysis is extended to the case of elliptic orbits. The non-autonomous character of the system increases the complexity of the problem, especially in presence of atmosphere. The parametric study of the response and stability in the large has particular relevance to the geophysical, earth resources, and military satellites.

Finally, the feasibility of using aerodynamic forces in the librational damping through a semi-passive controller is explored. The response analysis over a large range of system parameters establishes its effectiveness.

Figure 1-1 schematically illustrates the various stages involved in the proposed plan of study. It is felt that the approach represents a coherent program to explore the subject.

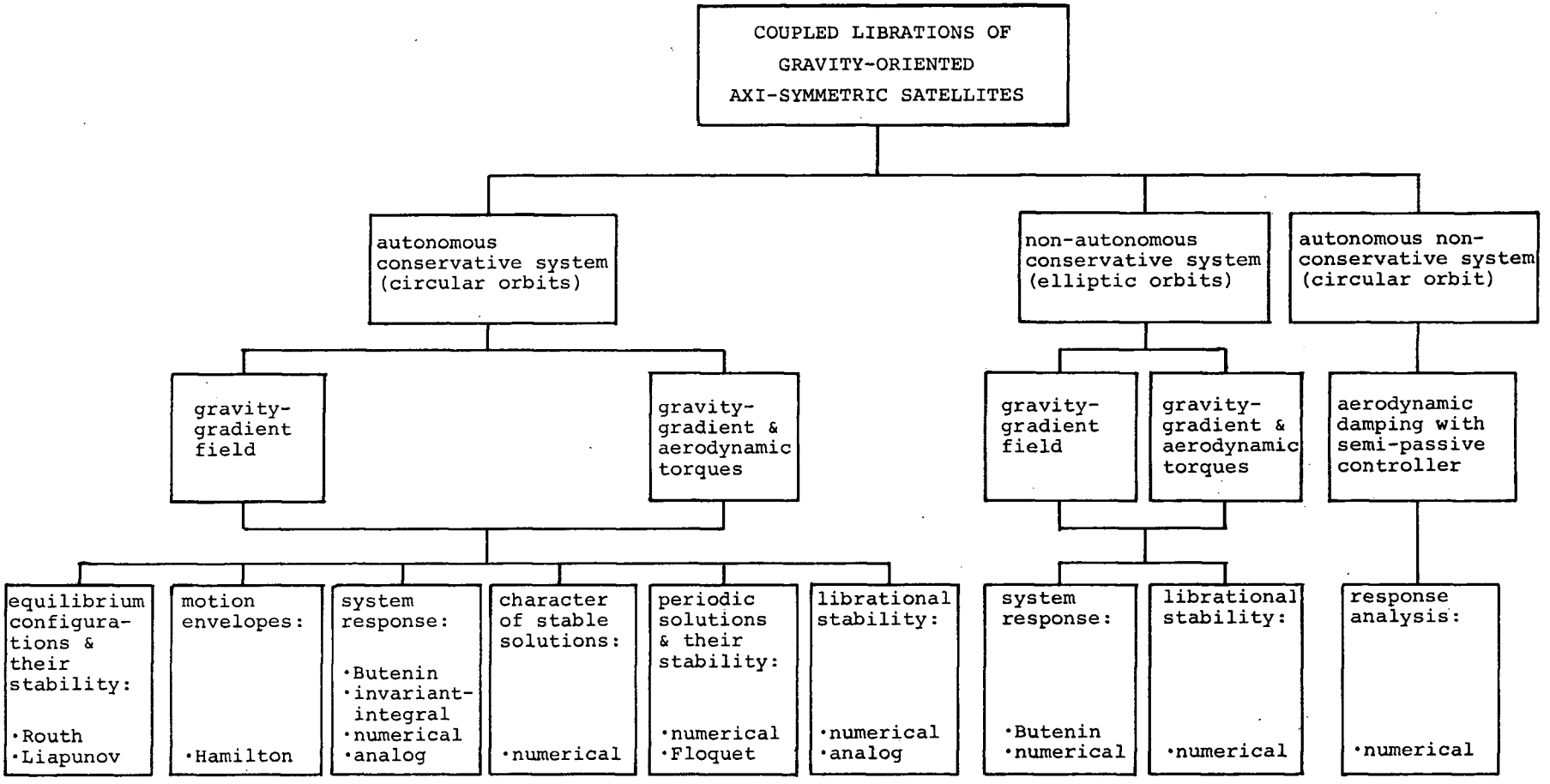

Figure 1-1 Schematic diagram of the proposed plan of study

2. LIBRATIONAL RESPONSE AND STABILITY IN CIRCULAR ORBIT

2.1 Preliminary Remarks

Gravity-gradient stabilization of axi-symmetric non-spinning satellites, moving in circular orbits and free to librate both in and across the orbital plane is analyzed here. The study, initiated by Modi and Brereton[53], emphasizes the effect of satellite inertia on the bounds of possible motion, response and stability characteristics. The invariant Hamiltonian, representing the first integral, yields regions of possible motion through zero velocity curves[55] and establishes conditions for stability.

As the second order, non-linear, coupled equations of motion do not possess any known closed form solution, an approximate analysis is undertaken using an extension of the Krylov and Bogoliubov method[56] (variation of parameter) as suggested by Butenin[57] with certain modifications. A response study establishes the acceptability of the solution for small amplitude librations.

The Hamiltonian is also used to reduce the order of the system and to obtain another approximate solution in terms of Jacobian elliptic functions.

For a motion in the large, the equations are solved numerically using Adams Bashforth predictor corrector integration[58] with a Runge-Kutta starter. The concept of integral

manifolds[16,53,59,60,61] in a three dimensional phase-space is adopted for concise presentation of the solution. Three classes of stable trajectories exist: 'regular', 'ergodic' and 'island' type. The limiting manifolds establish the stability bounds. The effect of the inertia parameter, Hamiltonian and initial conditions are studied by their systematic variations. The massive information generated is condensed in the form of design plots, which give allowable disturbances for non-tumbling motion.

2.2 Formulation of the Problem

Consider an arbitrarily shaped, rigid satellite with mass center at S in an orbit about center of force O (Figure 2-1). Let S-xyz be the principal body axes of the satellite with the triad $S\text{-}x_0y_0z_0$ so chosen as to direct z_0-axis outward along the local vertical and the y_0-axis parallel to the orbital angular momentum vector. The orientation of the satellite may be specified by a set of successive rotations: ψ about y_0-axis giving $x_1y_1z_1$-axes; ϕ about x_1-axis resulting in the $x_2y_2z_2$ triad; and λ about z_2-axis yielding xyz.

The expression for potential and kinetic energies to $O(1/r^3)$ can be written as:[10]

$$U_g = -\mu m/r + \mu (I_{xx} + I_{yy} + I_{zz})/4r^3 - 3\mu [\sin^2\psi \{I_{zz} - (I_{xx} - I_{yy})(\cos^2\lambda - \sin^2\lambda) + 4\sin\psi\cos\psi\sin\lambda\cos\lambda\sin\phi(I_{xx}$$

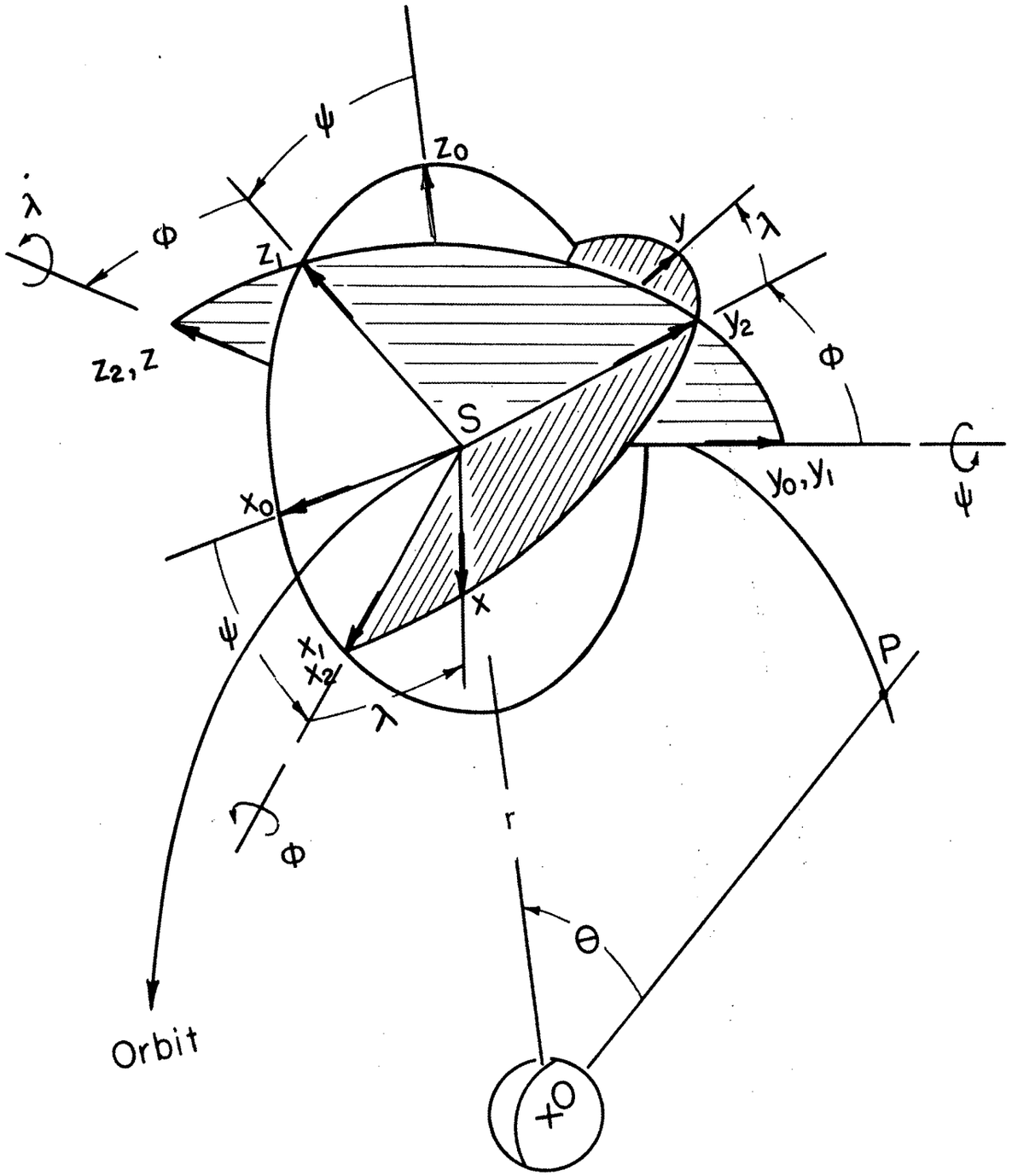

Figure 2-1 Geometry of satellite motion

$$-I_{yy}) + \cos^2\psi \sin^2\phi \{ I_{zz} - (I_{xx} - I_{yy})(\sin^2\lambda - \cos^2\lambda)\} + \cos^2\psi \cos^2\phi (I_{xx} + I_{yy} - I_{zz})]/4r^3 \quad \ldots\ldots (2.1a)$$

$$T = m(\dot{r}^2 + r^2\dot{\theta}^2)/2 + \dot{\phi}^2(I_{xx}\cos^2\lambda + I_{yy}\sin^2\lambda) + \dot{\phi}(\dot{\theta} + \dot{\psi})\cos\phi \sin\lambda\cos\lambda(I_{xx} - I_{yy}) + (\dot{\theta} + \dot{\psi})^2\cos^2\phi(I_{xx}\sin^2\lambda + I_{yy}\cos^2\lambda)/2 + [\dot{\lambda} - (\dot{\theta} + \dot{\psi})\sin\phi]^2 I_{zz} \quad \ldots\ldots (2.1b)$$

As for an axi-symmetric satellite, $I_{xx}=I_{yy}=I$, λ does not appear explicitly in the expression for Lagrangian thus rendering the conjugate momentum p_λ a constant of the motion, i.e.,

$$p_\lambda = \partial L/\partial\dot{\lambda} = I_{zz}[\dot{\lambda} - (\dot{\theta} + \dot{\psi})\sin\phi] = \text{constant} \quad \ldots\ldots (2.1c)$$

For a non-spinning satellite the constant must be zero, therefore equations (2.1a) and (2.1b) assume the simpler forms:

$$U_g = -\mu m/r + \mu(I - I_{zz})(1 - 3\cos^2\psi\cos^2\phi) \quad \ldots\ldots (2.2a)$$

$$T = m(\dot{r} + r^2\dot{\theta}^2)/2 + I[\dot{\phi}^2 + (\dot{\theta} + \dot{\psi})^2\cos^2\phi]/2 \quad \ldots\ldots (2.2b)$$

Using the Lagrangian formulation, the governing equations of motion in r, θ, ψ and ϕ degrees of freedom can be written as:

$$\ddot{r} - r\dot{\theta}^2 + \mu/r^2 - 3\mu(I - I_{zz})(1 - 3\cos^2\psi\cos^2\phi)/2mr^4 = 0 \quad \ldots\ldots (2.3a)$$

$$r^2\ddot{\theta} + 2r\dot{r}\dot{\theta} + I[(\ddot{\theta} + \ddot{\psi})\cos^2\phi - 2(\dot{\theta} + \dot{\psi})\dot{\phi}\sin\phi\cos\phi]/m = 0 \quad \ldots\ldots (2.3b)$$

$$\ddot{\psi} + \ddot{\theta} - 2\dot{\phi}(\dot{\theta} + \dot{\psi})\tan\phi + 3\mu K_i \sin\psi\cos\psi/r^3 = 0 \quad \ldots\ldots (2.3c)$$

$$\ddot{\phi} + [(\dot{\theta} + \dot{\psi})^2 + 3\mu K_i \cos^2\psi/r^3]\sin\phi\cos\phi = 0 \quad \ldots\ldots (2.3d)$$

Neglecting perturbations of the orbital motion due to librations,[62,63 et al.] the equations (2.3a) and (2.3b) lead to the classical Keplerian relations:

$$r^2\theta = h_\theta \quad \ldots\ldots (2.4)$$

$$r = h_\theta^2/\mu(1 + e\cos\theta) \quad \ldots\ldots (2.5)$$

For a circular orbit (e=0), with θ as an independent variable, the equations (2.3c) and (2.3d) transform to:[53]

$$\psi'' - 2\phi'(\psi' + 1)\tan\phi + 3K_i \sin\psi\cos\psi = 0 \quad (2.6a)$$

$$\phi'' + \{(\psi' + 1)^2 + 3K_i\cos^2\psi\}\sin\phi\cos\phi = 0 \quad (2.6b)$$

The governing equation in the λ degree of freedom is represented by (2.1c).

These second order, coupled, and highly non-linear equations do not appear to possess any known closed-form solution. However, before proceeding to seek an approximate solution it would be worthwhile to gain some insight into the problem by examining the Hamiltonian of the system.

2.3 Bounds of Libration

For circular orbits, the Lagrangian function associated with the librational motion does not involve time explicitly. Hence, the corresponding Hamiltonian of this conservative system is a constant of the motion:

$$
\begin{aligned}
H &= p_\psi \dot{\psi} + p_\phi \dot{\phi} + p_\lambda \dot{\lambda} \\
&= I\left[\dot{\phi}^2 + (\dot{\psi}^2 - \dot{\theta}^2)\cos^2\phi\right]/2 - 3\mu(I - I_{zz}) \\
&\quad \cos^2\psi \cos^2\phi / 2r^3 \\
&= \text{constant}
\end{aligned}
$$

i.e.,

$$
\begin{aligned}
C_H &= 2H/I\dot{\theta}^2 = \phi'^2 + \cos^2\phi\,(\psi'^2 - 1 - 3K_i\cos^2\psi) \\
&= \text{constant} \qquad \ldots\ldots (2.7)
\end{aligned}
$$

Setting $\psi'=\phi'=0$ results in a set of zero-velocity curves[55], symmetrical with respect to ψ and ϕ axes (Figure 2-2), enclosing regions of possible motion. Consistent with the stability criterion of nontumbling motion, the zero-velocity curves are presented only over the range ψ, $\phi=\pm\pi/2$. It may be observed that for:

$C_H \leq -(1+3K_i)$	,	no motion is possible;
$-(1+3K_i) \leq C_H \leq -1$	,	the motion is bounded;
$-1 < C_H \leq 0$	,	the motion is bounded in ϕ only;
$0 < C_H$	,	unbounded motion is possible in both directions.

. . . . (2.8)

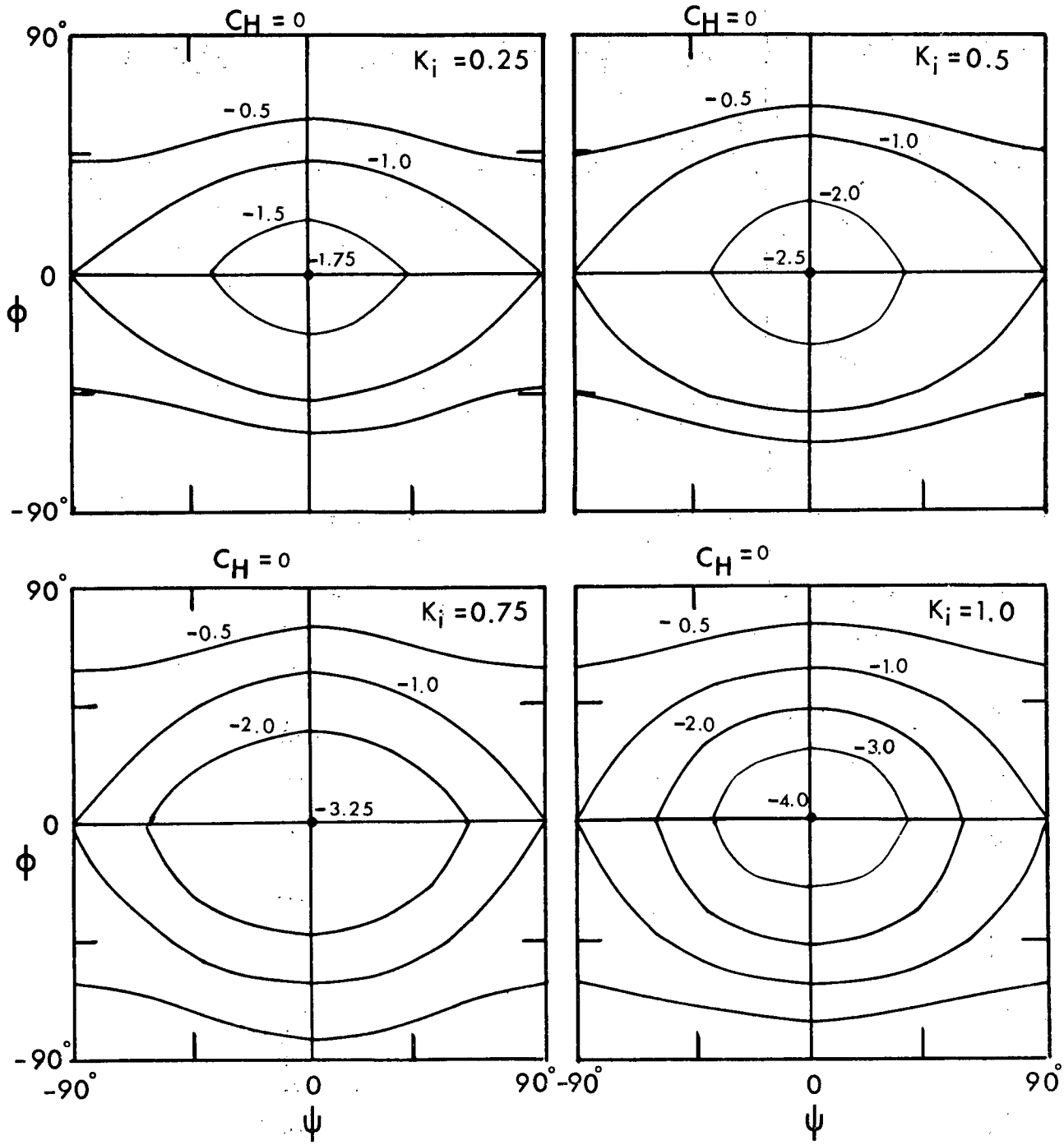

Figure 2-2 Effect of satellite inertia and Hamiltonian on zero-velocity curves

Furthermore, with constant Hamiltonian any one of the four state parameters (ψ,ψ',ϕ,ϕ') can be eliminated thus permitting a three-dimensional state-space representation of the motion. Within the bounds imposed by the zero-velocity curves, relations defining surfaces in ψ,ψ',ϕ or ϕ,ϕ',ψ space can be obtained by equating the eliminated velocity to zero. For example, in ψ,ψ',ϕ-space motion is bounded by

$$\cos^2\phi\,(\psi'^2 - 1 - 3K_i\cos^2\psi) - C_H = 0 \quad \ldots \quad (2.9)$$

Figure 2-3 illustrates these surfaces. They represent envelopes of possible motion in the state space for a given value of Hamiltonian. Note that the zero-velocity curves are merely cross-sections of these surfaces at $\psi'=0$. A growth of the limiting closed envelope ($C_H=-1.0$) with increasing K_i (Figure 2-3(a)) suggests a more stable performance. The envelopes are open in ψ direction for $C_H>-1.0$ (Figure 2-3(b)) indicating possibility of unbounded planar librations.

The actual motion of the system, however, is dependent upon the initial conditions as well as the Hamiltonian. Hence to establish the character of the motion, such as amplitude and frequency, it is essential to solve the governing equations. In the absence of any known closed form solution, approximate analytical methods and numerical techniques have to be resorted to.

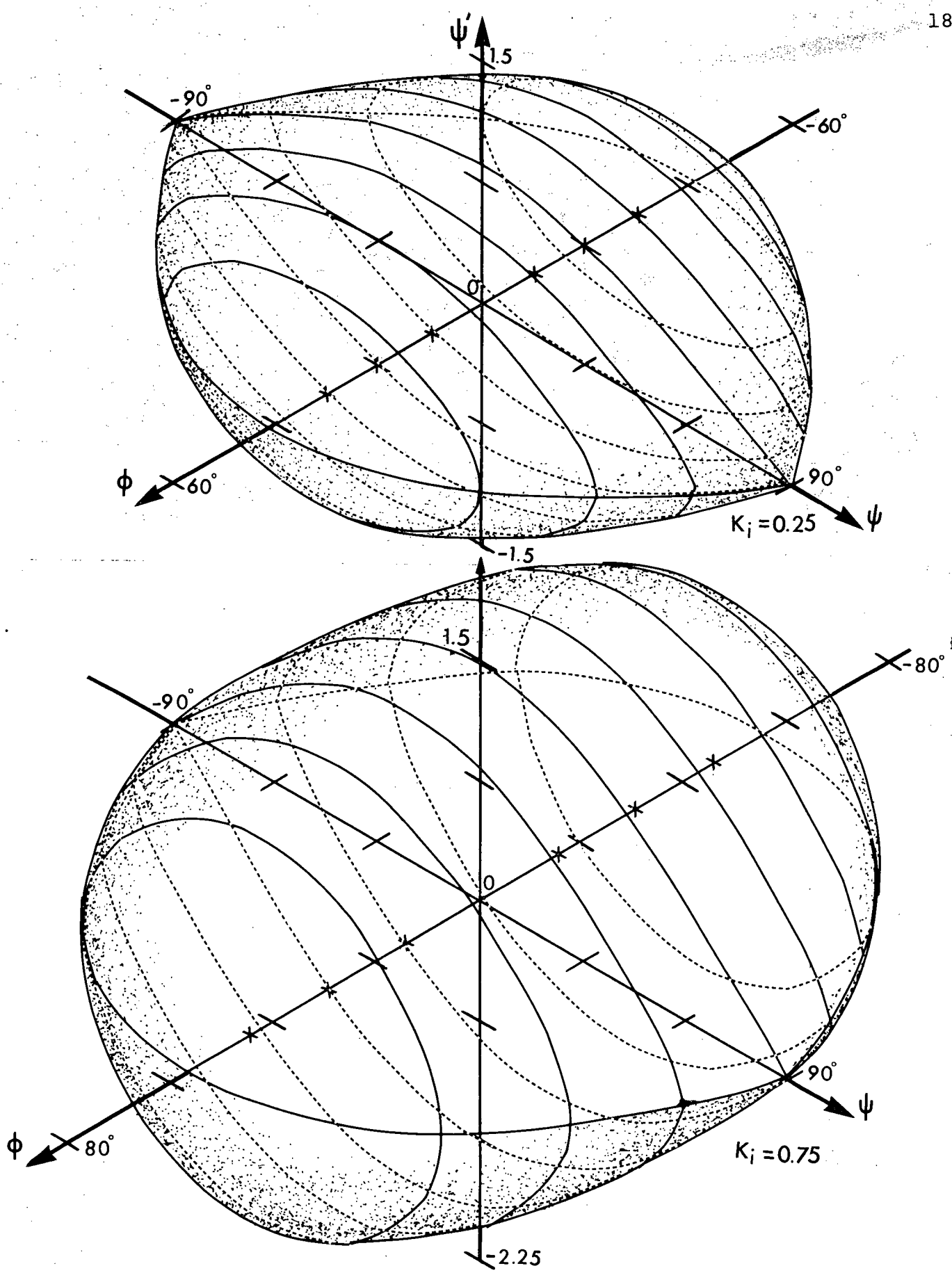

Figure 2-3 Effect of satellite inertia and Hamiltonian on motion-envelope ($\phi'=0$): (a) limiting region for guaranteed bounded librations ($C_H=-1.0$)

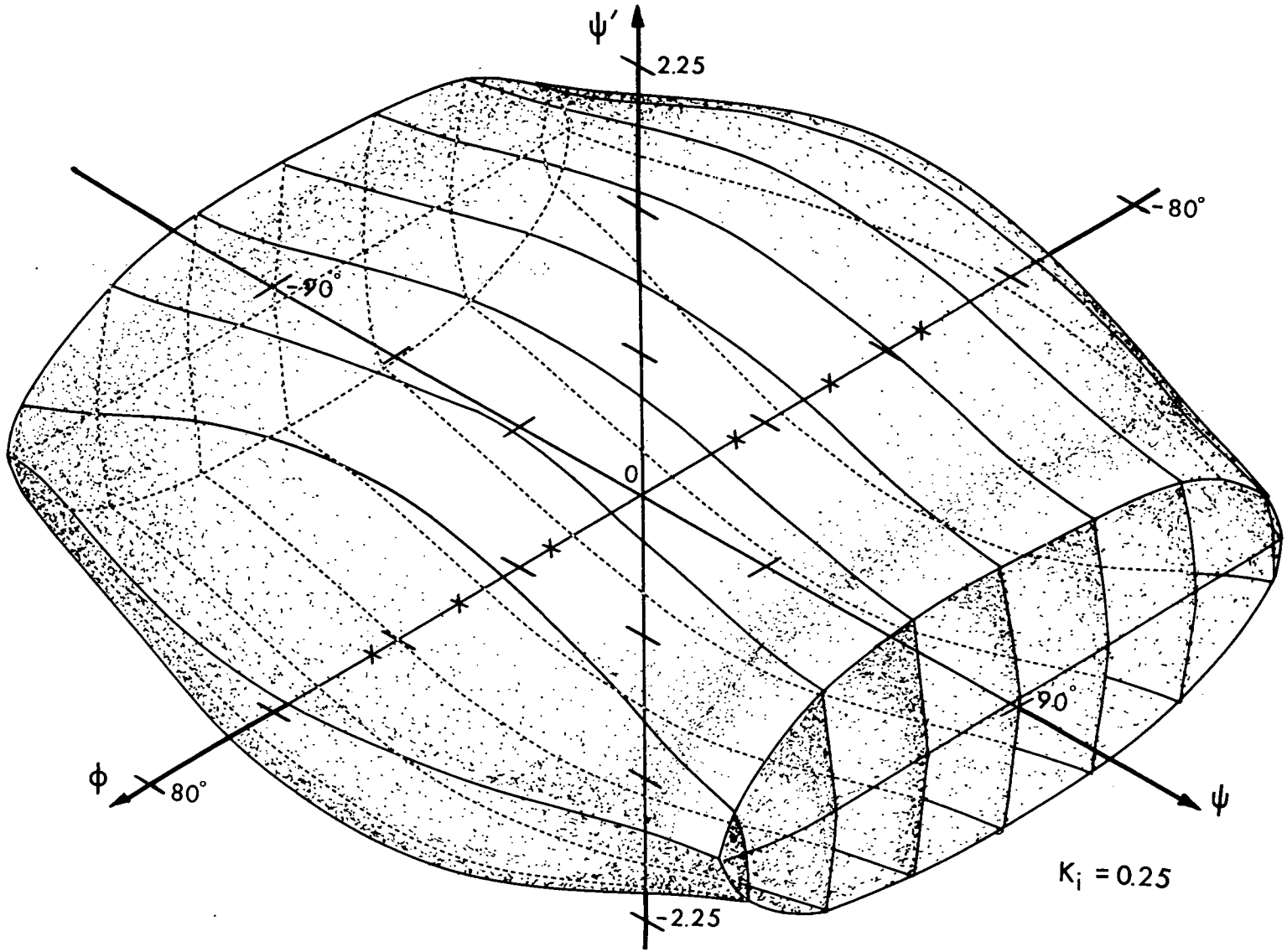

Figure 2-3 Effect of satellite inertia and Hamiltonian on motion envelope ($\phi'=0$): (b) librations bounded in ϕ only ($C_H=-0.5$)

2.4 Approximate Solutions and System Response

2.4.1 Variations of Parameter Method (Butenin[57])

Representing the trigonometric functions by their series, neglecting fifth and higher degree terms in ψ, ϕ and their derivatives, and collecting the nonlinear terms on the right hand side the equations of motion take the form

$$\psi'' + 3K_i\psi = 2\phi'\psi'\phi + 2\phi'\phi + 2\phi'\phi^3/3 + 2K_i\psi^3$$

$$\phi'' + (1+3K_i)\phi = -\psi'^2\phi - 2\psi'\phi + 3K_i\psi^2\phi + 4\phi^3\psi'/3 + 2(1+3K_i)\phi^3/3 \quad \ldots\ldots (2.10)$$

or

$$\psi'' + n_1^2\psi = f(\psi, \psi', \phi, \phi')$$

$$\phi'' + n_2^2\phi = g(\psi, \psi', \phi, \phi') \quad \ldots\ldots (2.11)$$

For small amplitude motion each term in f and g is small as compared to the terms on the L.H.S. of the equation (2.10), hence their approximate solution can be found using the method of variation of parameters.

The complementary solution of this system of equations is given by a set of harmonic functions

$$\psi = a\sin(n_1\theta + \beta_1)$$

$$\phi = b\sin(n_2\theta + \beta_2) \quad \ldots\ldots (2.12)$$

It is intended here to obtain the solution essentially in the same form as the complementary solution, but now permitting the amplitudes and phase angles to be functions of θ, i.e.,

$$\begin{aligned} \psi &= a(\theta)\sin\left[n_1\theta + \beta_1(\theta)\right] \\ \phi &= b(\theta)\sin\left[n_2\theta + \beta_2(\theta)\right] \end{aligned} \qquad \ldots\ldots (2.13)$$

Note that n_1 and n_2 represent the principal frequencies given by the solution of the homogeneous equations and a, b, β_1, β_2 are unknowns to be determined. Each of the functions $a(\theta)$, $b(\theta)$, $\beta_1(\theta)$, $\beta_2(\theta)$ may be expressed as a function of θ plus a constant. Thus the solution in this form involves eight unknowns and hence is over specified. It will be, therefore, necessary to obtain four more relations in addition to those given by the initial conditions. This is achieved by introducing logical constraints.

Equating the first derivative of equation (2.13) to that of the homogeneous solution (2.12) gives the two constraint relations:

$$a'\sin\zeta + a\beta_1'\cos\zeta = 0 \qquad \ldots (2.14a)$$

$$b'\sin\eta + b\beta_2'\cos\eta = 0 \qquad \ldots (2.14b)$$

Mathematically this implies that the nonlinearities are small. Physically it means that the satellite is executing small

amplitude motion. Normally this condition is satisfied by most communication, weather, or earth-resources satellites.

The other two relations are obtained by differentiating once again with respect to θ and substituting in the equations of motion giving

$$a' n_1 \cos\zeta - a n_1 \beta_1' \sin\zeta = f^* \quad \ldots (2.14c)$$

$$b' n_2 \cos\eta - b n_2 \beta_2' \sin\eta = g^* \quad \ldots (2.14d)$$

where

$$f^* = f(a \sin\zeta, a n_1 \cos\zeta, b \sin\eta, b n_2 \cos\eta)$$
$$g^* = g(a \sin\zeta, a n_1 \cos\zeta, b \sin\eta, b n_2 \cos\eta) \quad \ldots (2.15)$$

Solving the four algebraic equations in (2.14) for the unknowns $a', b', \beta_1', \beta_2'$ gives

$$\begin{aligned} a' &= 1/n_1 \; f^* \cos\zeta \\ b' &= 1/n_2 \; g^* \cos\eta \\ a\beta_1' &= -1/n_1 \; f^* \sin\zeta \\ b\beta_2' &= -1/n_2 \; g^* \sin\eta \end{aligned} \quad \ldots (2.16)$$

Here f^* and g^* are known nonlinear functions in a, b, β_1, β_2, and θ. For small amplitude motion (say 10°), f^* and g^* are quite small (5-10%) compared to the remaining terms in the equations of motion. Hence a, b, β_1, β_2 are slowly varying

parameters. Using their average values over a period in ψ and ϕ degrees of freedom yields

$$da/d\theta = (1/4\pi^2 n_1) \int_0^{2\pi} \int_0^{2\pi} f^* \cos\zeta \; d\zeta \, d\eta$$

$$db/d\theta = (1/4\pi^2 n_2) \int_0^{2\pi} \int_0^{2\pi} g^* \cos\eta \; d\zeta \, d\eta$$

$$d\beta_1/d\theta = -(1/4\pi^2 n_1 a) \int_0^{2\pi} \int_0^{2\pi} f^* \sin\zeta \; d\zeta \, d\eta$$

$$d\beta_2/d\theta = -(1/4\pi^2 n_2 b) \int_0^{2\pi} \int_0^{2\pi} g^* \sin\eta \; d\zeta \, d\eta \qquad \ldots\ldots (2.17)$$

Evaluating the integrals and using the conditions of orthogonality gives

$$\begin{aligned} a', b' &= 0 \\ \beta_1' &= -\frac{a^2 n_1}{4} \\ \beta_2' &= -\frac{b^2 n_2}{4} \end{aligned} \qquad \ldots\ldots (2.18)$$

i.e., solution represented by equation (2.18) becomes

$$\psi = (\psi_0^2 + \psi_0'^2/3K_i)^{1/2} \sin\left[\{1 - (\psi_0^2 + \psi_0'^2/3K_i)/4\}(3K_i)^{1/2}\theta + \tan^{-1}\{(3K_i)^{1/2}\psi_0/\psi_0'\}\right]$$

$$\phi = \left\{\phi_o^2 + \phi_o'^2/(1+3K_i)\right\}^{1/2} \sin\left[\left\{1 - (\phi_o^2 + \phi_o'^2/(1+3K_i))/4\right\}(1+3K_i)^{1/2}\theta + \tan^{-1}\left\{(1+3K_i)^{1/2}\phi_o/\phi_o'\right\}\right] \quad \ldots . (2.19)$$

To establish the validity of the analytical solution the equations of motion (2.6) were rewritten as a set of four first order relations:

$$d\psi/d\theta = \psi' \quad ; \quad d\phi/d\theta = \phi'$$

$$d\psi'/d\theta = 2\phi'(\psi'+1)\tan\phi - 3K_i \sin\psi\cos\psi$$

$$d\phi'/d\theta = -\left\{(\psi'+1)^2 + 3K_i\cos^2\psi\right\}\sin\phi\cos\phi \quad \ldots . (2.20)$$

and were integrated numerically using Adams-Bashforth predictor-corrector procedure[58] with a Runge-Kutta starter. The step size of 3° gave results of sufficient accuracy without involving excessive computation time[64]. The use of symmetry properties, as exhibited by the invariant nature of the equations under transformation (θ,ψ,ϕ) to $(\theta,\psi,-\phi)$, $(-\theta,-\psi,\phi)$ or $(-\theta,-\psi,-\phi)$ substantially reduced the effort.

The librational response of a wide range of satellites to a broad spectrum of disturbances was obtained, over fifty orbits, by systematically varying the inertia parameter K_i and initial conditions, and is compared with that given by the approximate closed form solution in Figure 2-4. For conciseness only initial and terminal regions are shown.

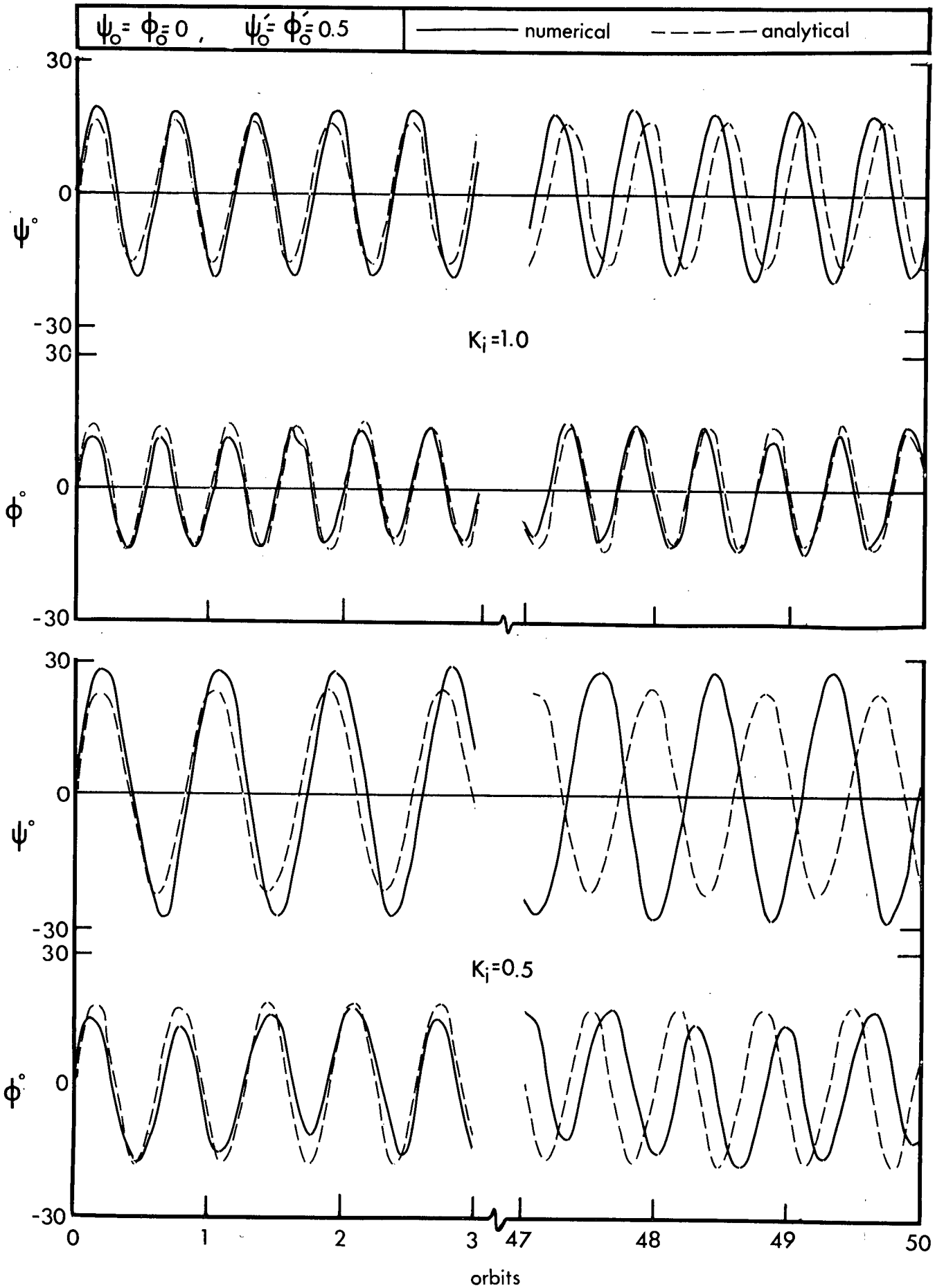

Figure 2-4 Effect of satellite inertia on librational response obtained using numerical and variation of parameter methods: (a) impulsive disturbance

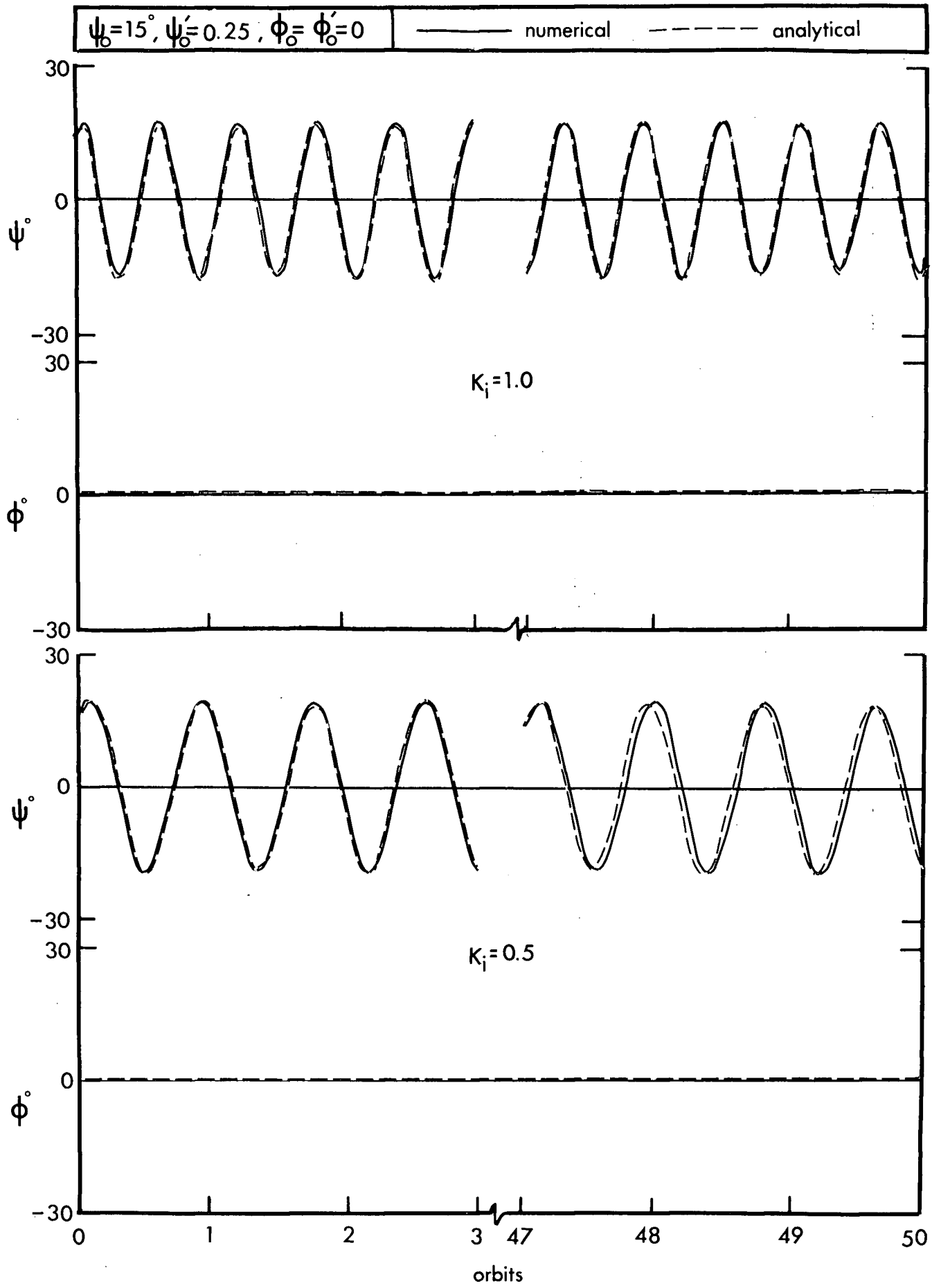

Figure 2-4 Effect of satellite inertia on librational response obtained using numerical and variation of parameter methods: (b) disturbance in the orbital plane

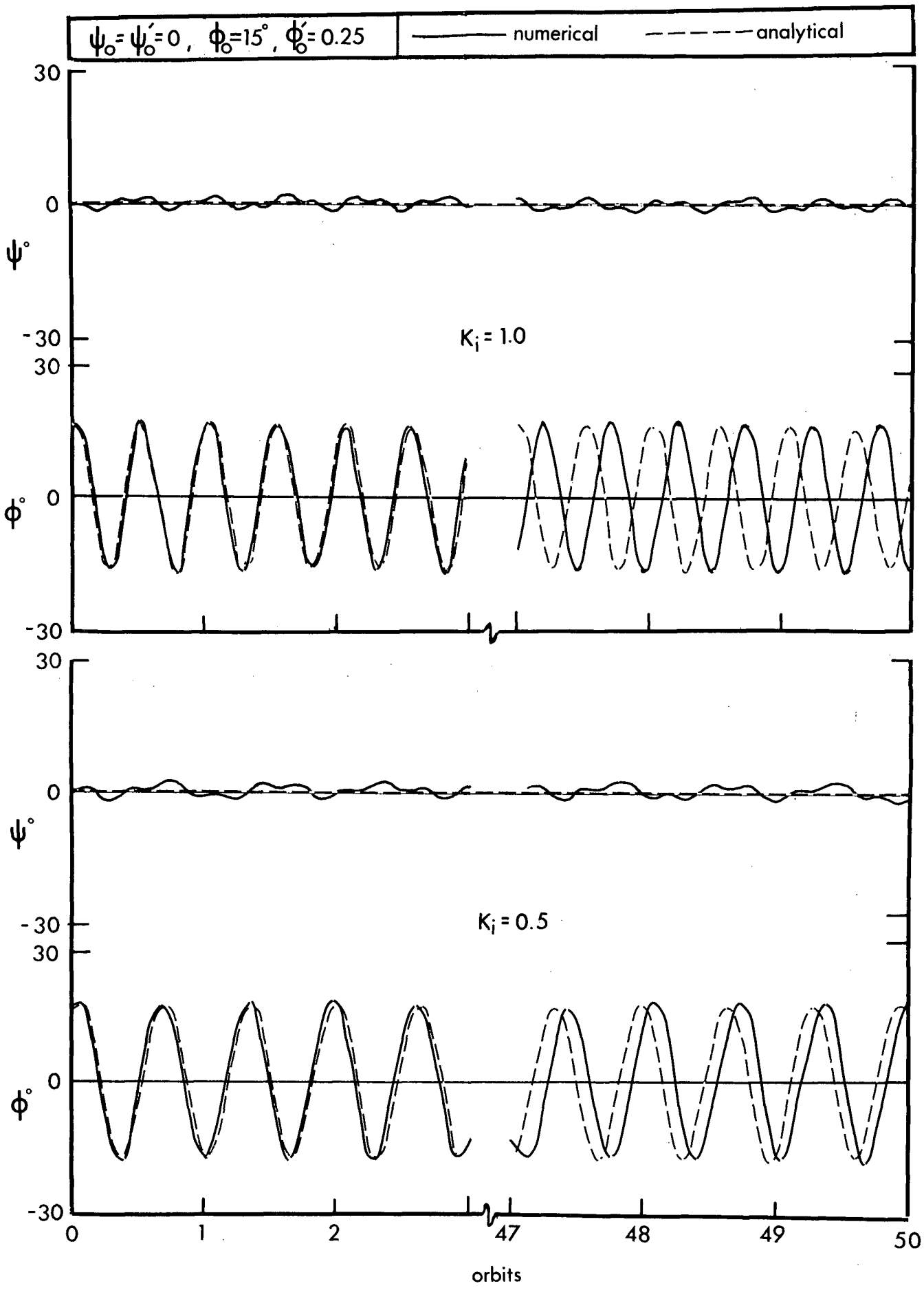

Figure 2-4 Effect of satellite inertia on librational response obtained using numerical and variation of parameter methods: (c) disturbance across the orbital plane

Figure 2-4(a) indicates that the analytical method determines the amplitude and frequency of the motion with considerable accuracy. For a disturbance of appreciable magnitude ($\psi_o'=\phi_o'=0.5$), the main discrepancy is in the phase which appears to be cumulative. From the practical application point of view this may not be a serious limitation as amplitude and frequency of motion provide sufficient information needed in preliminary structural design of a satellite.

The agreement, in general, is better for slender satellites ($K_i \simeq 1.0$) which are normally preferred for gravity-gradient stabilization. The librational frequency, which depends on the disturbances encountered as well as the inertia parameter, is of the order of orbital frequency. For an identical disturbance in the two degrees of freedom, a larger amplitude and smaller frequency motion is excited across the orbital plane (ϕ). Both the analytical and numerical solutions indicate decrease in frequency and increase in amplitude, particularly for planar motion (ψ), with decreasing K_i.

The accuracy of the analytical solutions improves when the disturbance is restricted to one degree of freedom only. As apparent from the equations (2.6), the planar disturbances ($\phi_o=\phi_o'=0$) do not excite a transverse motion (Figure 2-4(b)). However, librations in ϕ direction lead to small ripples in the ψ degree of freedom, which increase with decreasing inertia (Figure 2-4(c)). The analytical

method fails to predict this behaviour as well as small amplitude modulations, perhaps due to the assumed form of the solution.

The periodic nature of the independent variable provides yet another standard for comparison between the solutions. On the stroboscopic phase plane (Figure 2-5), the points shown represent the state of the system at $\theta=2\pi n (n=0,1 \ldots,50)$. A few of the points are labelled. Here again the correlation between the two methods appears to be quite satisfactory. Any error in the phase results only in circumferential rotation (as against the radial departure) of the point of intersection of the trajectory with the plane. The agreement suggests a possibility of using the analytical solution for stability analysis by the integral manifold technique.

It may be pointed out that the two solutions are compared here under adverse situations. In actual practice, the communication satellites demand extreme pointing accuracy. So in that case the predictions made by the approximate theory are likely to be more accurate. The simple analysis presented here provides considerable insight into the physical nature of the coupled motion and appears to be adequate for preliminary design purposes.

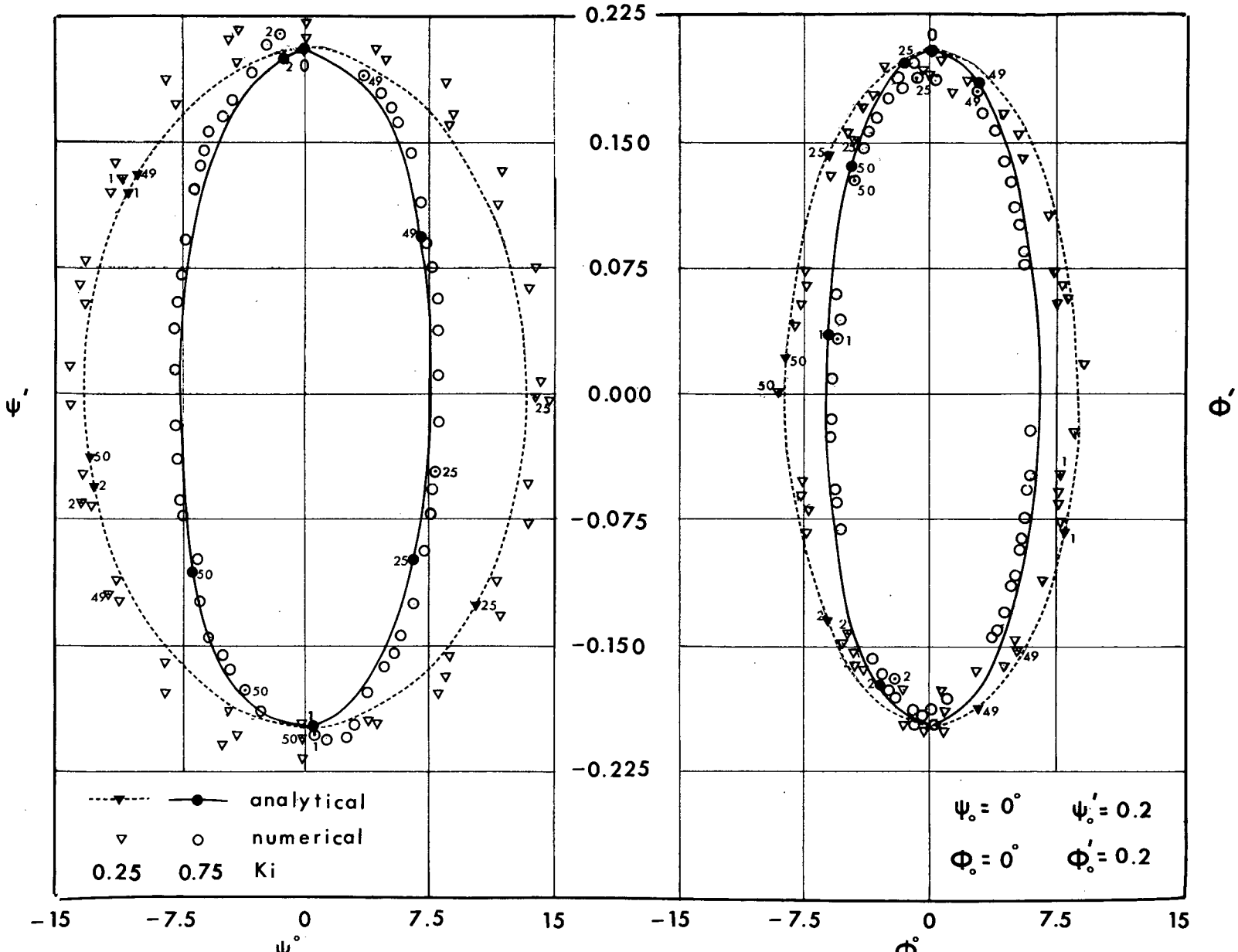

Figure 2-5 Stroboscopic phase-plane (θ=0), obtained using numerical and variation of parameter methods: (a) impulsive disturbance

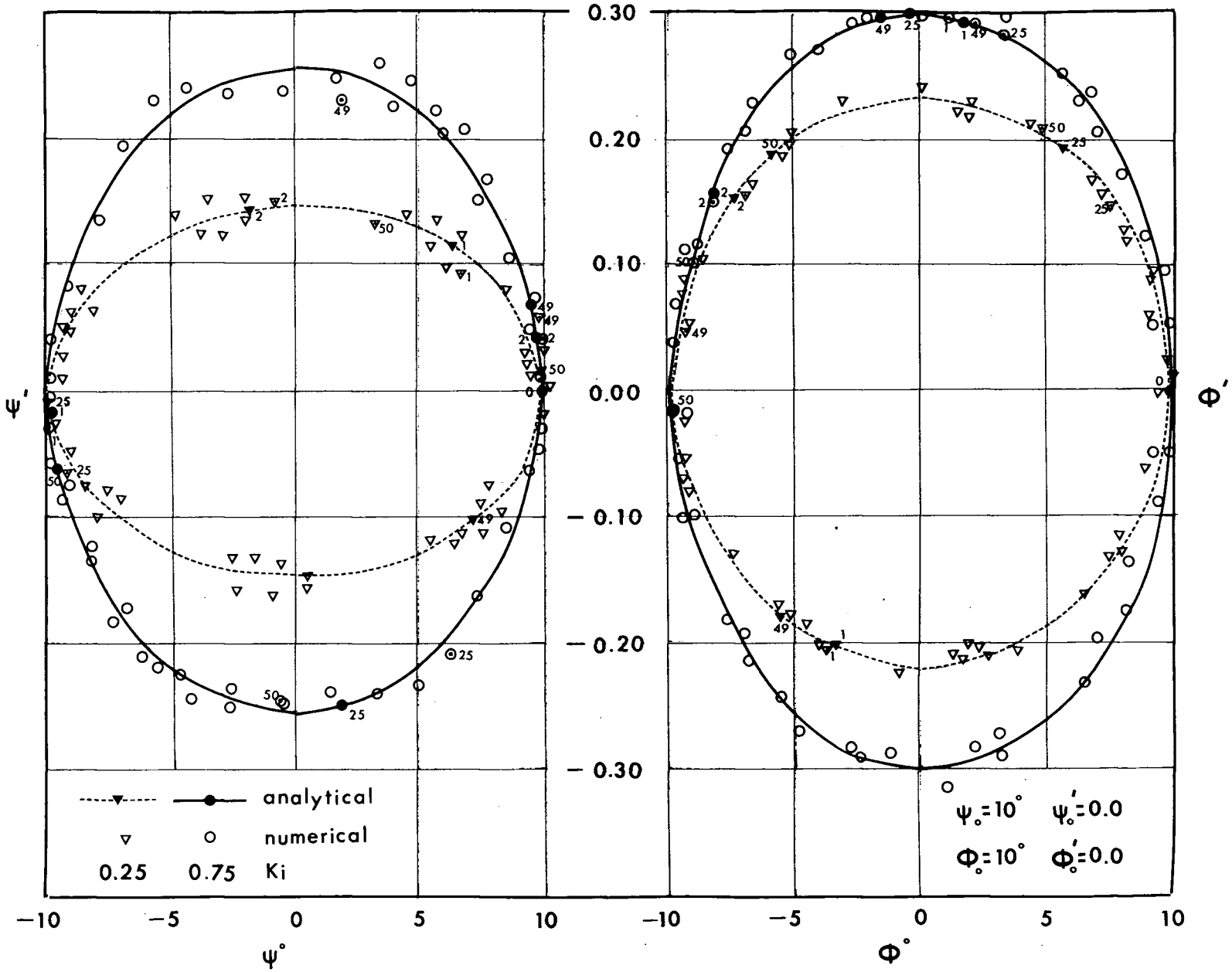

Figure 2-5 Stroboscopic phase-plane (θ=0), obtained using numerical and variation of parameter method: (b) angular disturbance

2.4.2 Invariant Integral Method

The Hamiltonian, a constant of the motion, which gave the bounds of libration, can be used to reduce the order of the system leading to yet another approximate analytical solution.

Multiplying equations of motion (2.6a) and (2.6b) by $2\psi'\cos^2\phi$ and $2\phi'$, respectively, adding and integrating once yield the normalized Hamiltonian (equation 2.7), which can be rearranged as,

$$\psi'^2 = [(C_H - \phi'^2)/\cos^2\phi + 1 + 3K_i] - 3K_i \sin^2\psi \qquad \text{. . . . (2.21a)}$$

$$\phi'^2 = [C_H + 1 + 3K_i \cos^2\psi - \psi'^2] - [1 + 3K_i \cos^2\psi - \psi'^2] \sin^2\phi \qquad \text{. . . . (2.21b)}$$

As is well-known, the solution of an equation of the form,

$$\beta'^2 = a_1 - a_2 \sin^2\beta$$

where a_1 and a_2 are constants, is a Jacobian elliptical function:[65]

$$\beta = \sin^{-1}\left[(a_1/a_2)^{1/2}\, \mathrm{Sn}\left\{(a_2)^{1/2}(\theta - \theta^*),\ a_1/a_2\right\}\right] \qquad \text{. . . . (2.22)}$$

where $\beta=0$ at $\theta=\theta^*$.

Thus equation (2.21) can be solved approximately in the form (2.22) provided,

$$d/d\theta \left\{ (C_H - \phi'^2)/\cos^2\phi \right\} \simeq 0$$

$$d/d\theta \left\{ 3K_i \cos^2\psi - \psi'^2 \right\} \simeq 0$$

Note that these conditions are equivalent and correspond to (from equation 2.6a):

$$4\phi'\psi'(\psi'+1)\tan\phi \simeq 0 \qquad \ldots\ldots (2.23)$$

thus implying that the coupling terms may be ignored. Hence for systems satisfying this condition, the solution can be approximated by:

$$\psi = \sin^{-1}\left[k_1 \, Sn\left\{(3K_i)^{1/2}(\theta - \theta_1^*), k_1^2\right\}\right]$$

$$\phi = \sin^{-1}\left[k_2 \, Sn\left\{(1 + 3K_i\cos^2\psi_o - \psi_o'^2)^{1/2}(\theta - \theta_2^*), k_2^2\right\}\right]$$

where, $\ldots\ldots (2.24)$

$$k_1^2 = 1 + \left\{1 + (C_H - \phi_o'^2)/\cos^2\phi_o\right\}/3K_i$$

$$k_2^2 = 1 + C_H/(1 + 3K_i\cos^2\psi_o - \psi_o'^2)$$

$$\psi(\theta_1^*) = \phi(\theta_2^*) = 0$$

The solution becomes exact in the absence of disturbances across the orbital plane (Figure 2-6(a)i), however, the planar motion excited by a transverse disturbance is not exhibited by the analytical solution (Figure 2-6(a)ii).

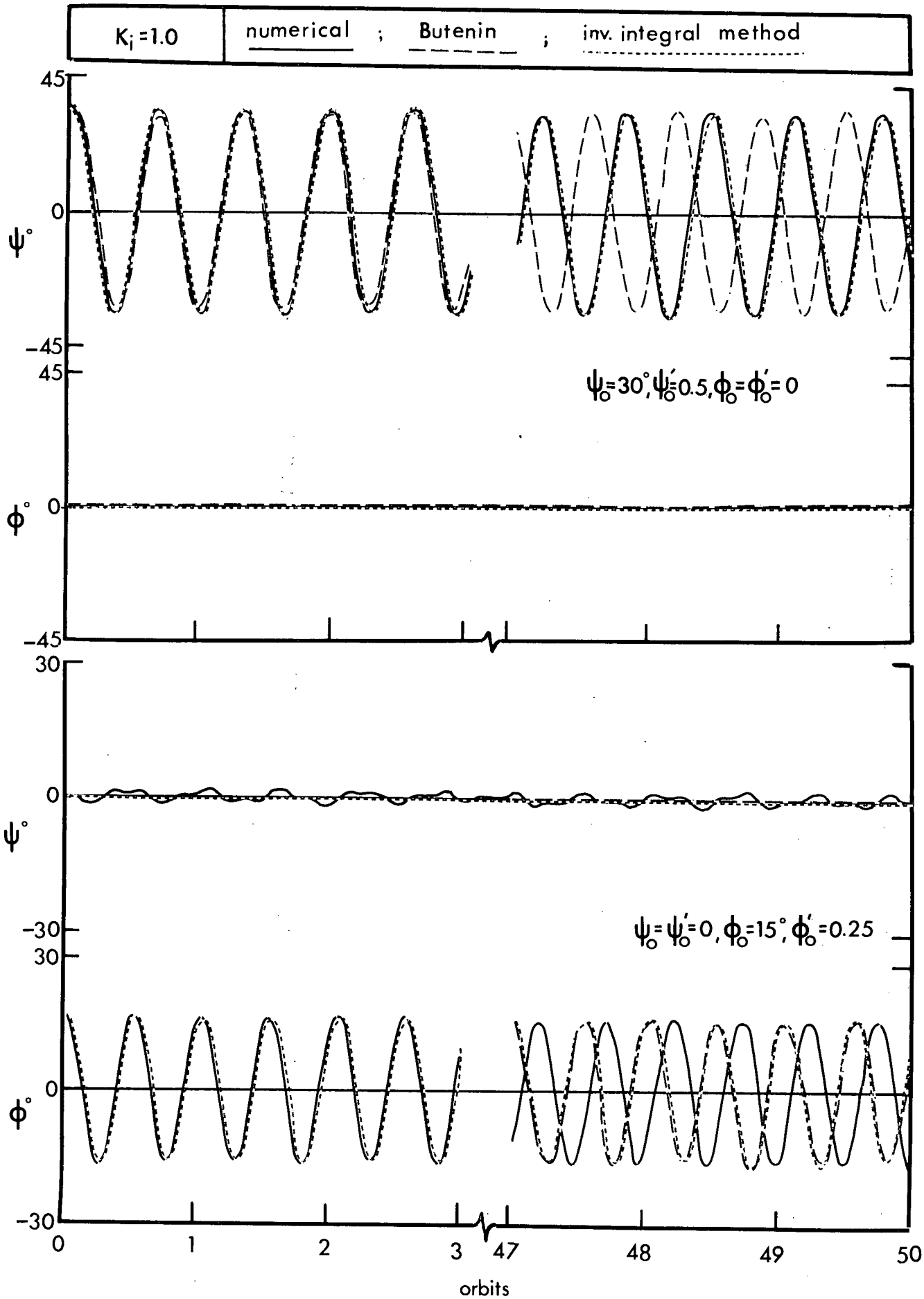

Figure 2-6 Accuracy of approximate solution: (a) response to large disturbance along one of the degrees of freedom

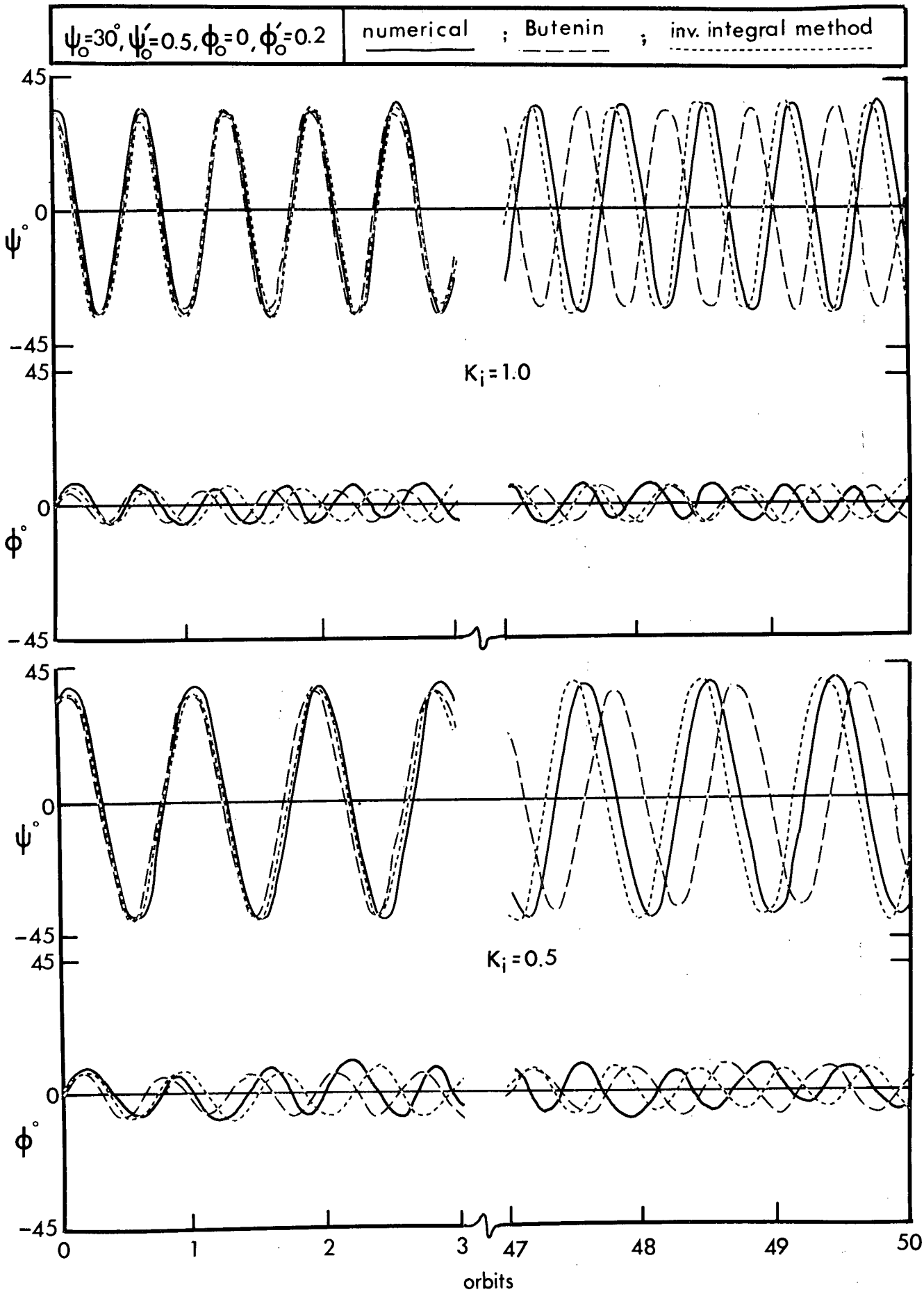

Figure 2-6 Accuracy of approximate solution: (b) response to predominantly planar disturbance

The method, in general, represents a better approximation compared to Butenin's approach, particularly when the disturbances across the orbit are relatively small (Figure 2-6(b)). The correlation improves with increasing inertia, especially in the ψ direction.

Thus, while the widely used linearization techniques may be acceptable for small disturbances (5-6 deg. amplitude of libration), the variation of parameter approach gives a good approximation for relatively large disturbances (20-25 deg.). The invariant integral method appears to extend this range considerably (30-40 deg.), particularly if cross-motion is small. However, for very large disturbances, when the amplitude modulations due to coupling become substantial, a numerical integration is unavoidable for response and stability analysis. Figure 2-7 shows over six orbits, the effect of satellite inertia on the exact response to a large arbitrary disturbance. Decrease in K_i tends to make a satellite more sensitive to a given disturbance with a marked reduction in the librational frequency. The effect appears to be greater in the ψ direction compared to that in the ϕ direction. The modulation of the amplitude due to a coupling between the two degrees of freedom, more pronounced in the ϕ degree of freedom, increases with decreasing K_i. The influence of harmonics may be expected to increase with disturbances.

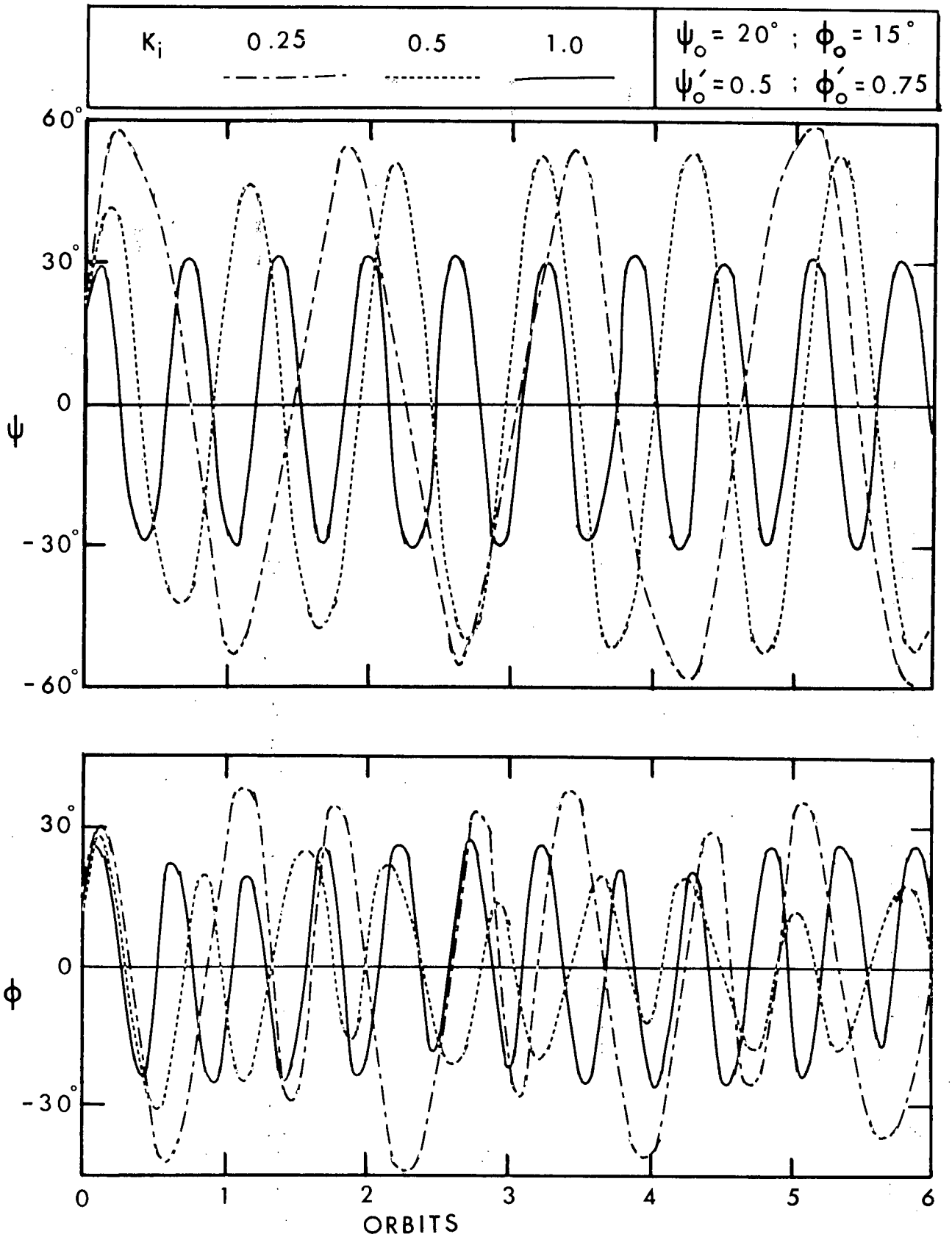

Figure 2-7 Numerically generated response to a large arbitrary disturbance showing effects of satellite inertia

2.5 Nature of the Stable Solutions:

The application of the concept of integral manifolds or invariant surfaces in a three-dimensional phase-space for studying librational stability of a gravity-oriented system has been discussed in some detail by Brereton and Modi[7,10,53]. The method provides a clear picture as to the entire spectrum of disturbances to which a satellite can be subjected at any point in its orbit without causing it to be unstable. Although the system under consideration involves four state elements (ψ,ψ',ϕ,ϕ'), the method is still applicable due to a constant value of the Hamiltonian.However, elimination of an element using equation (2.7) leads to an ambiguity concerning its sign, as pointed out by Hénon and Heiles[60]. It is, therefore, necessary to delineate between the two possibilities to utilize the invariant surface concept. Hence, two spaces must be used to describe the state of the system, one for positive values of the eliminated state element and the other for its negative values. Here the two spaces used for presenting the solution are ψ,ψ',ϕ with $\phi' \gtrless 0$.

To obtain cross-sections of the invariant surface in ϕ' space it was necessary to develop an interpolation scheme so that the state of the system could be ascertained for any given value of the stretching coordinate. This was achieved by Adams-Bashforth predictor-corrector method in conjunction with a polynomial fit to the past history of the state coordinates and their derivatives. Having fitted

the polynomials in θ to the numerical solution the state of the system is readily determined using Newton-Raphson iteration[16].

Figures 2-8 and 2-9 show the cross-sections of the invariant surfaces, at $\phi=0$, obtained using this procedure. The cross-sections of motion envelopes, represented by $\phi'=0$, are also included to fascilitate comparison with the region of possible motion. Due to the coupling effects and relative frequency of motion in the two degrees of freedom the system exhibits three distinct types of stable solutions. For a given Hamiltonian a systematic variation in the initial conditions leads to 'regular', 'ergodic' and 'island' (Figure 2-8) type trajectories.

For certain initial condition, integration of the equations of motion over a large number of orbits leads to the phase space trajectory intersecting $\phi=0$ plane at a series of points defining a smooth curve (0) as shown in Figure 2-8. The selection of any initial condition within the enclosed region leads to a nested surface and hence, a cross-section lying completely within the former. In the limit, the integral manifold degenerates to a line, i.e., cross-section in the ψ-ψ' plane reduces to a point, thus representing a periodic solution.

On the other hand, it may be emphasized that although the stability of the motion is assured for $C_H \leq -1.0$, the

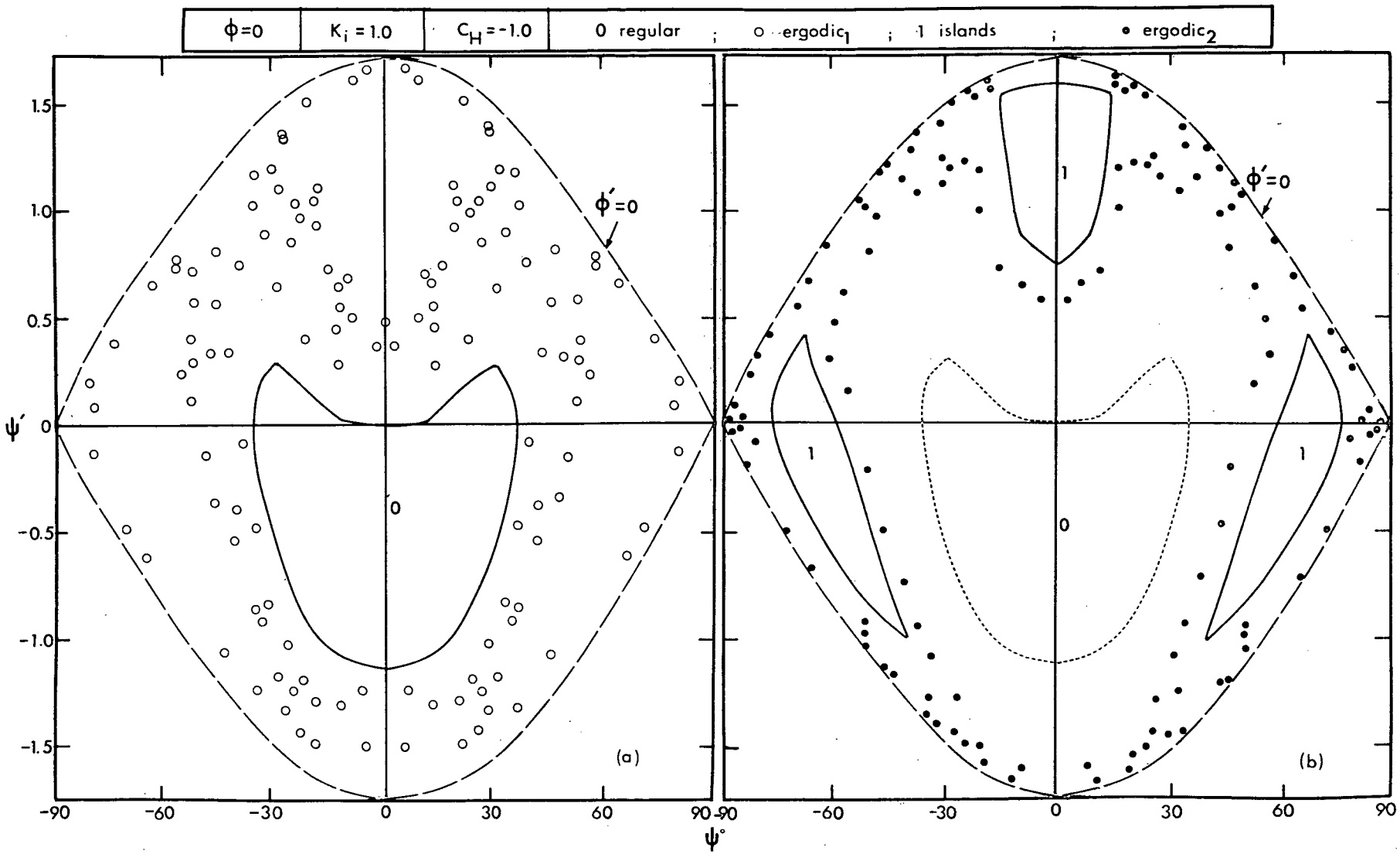

Figure 2-8 The cross-section $\phi=0$ in phase space indicating types of stable solution generated by different initial conditions for a given Hamiltonian: (a) regular and ergodic; (b) islands and their breakdown into ergodic

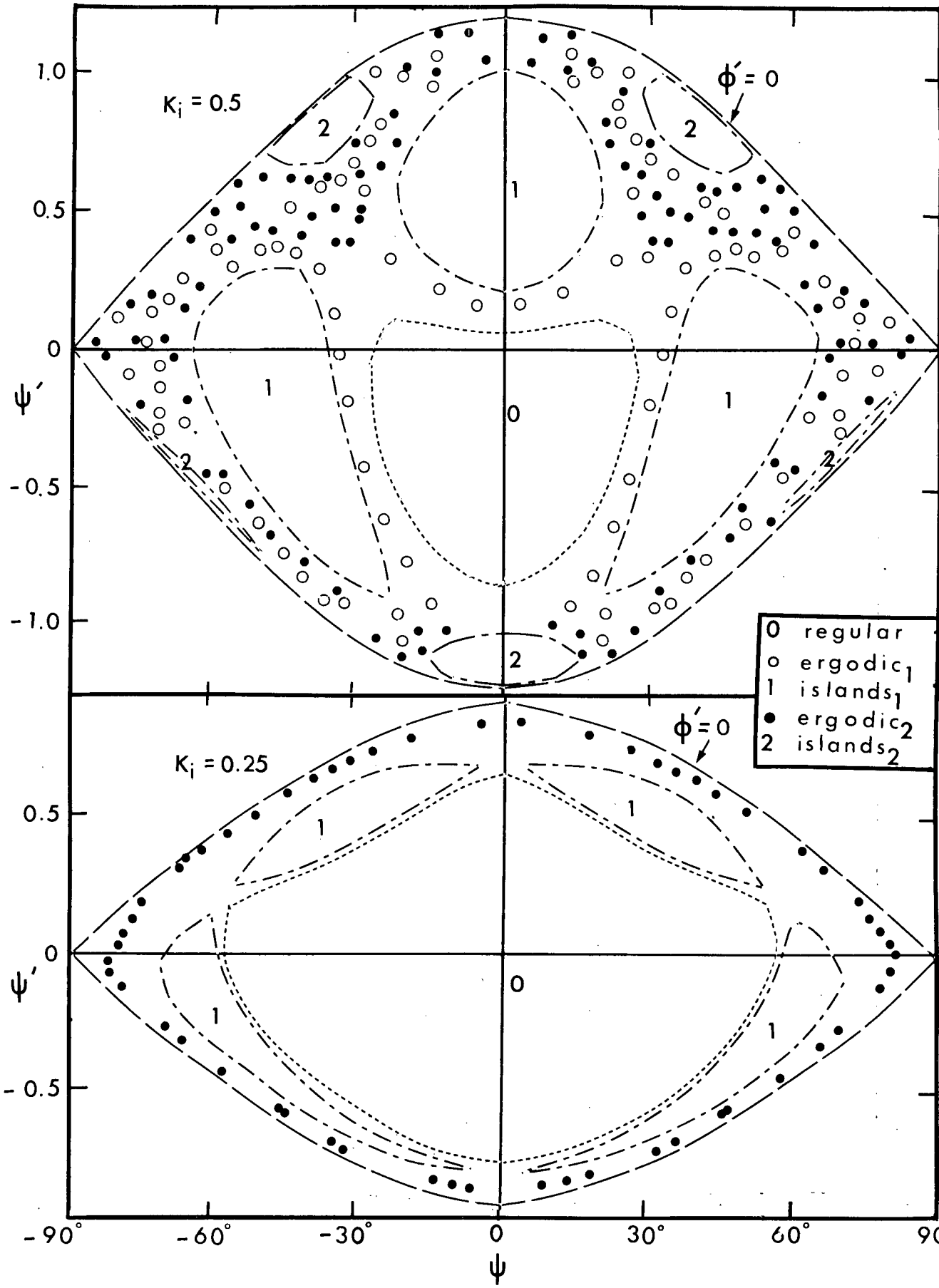

Figure 2-9 Effect of satellite inertia on nature of stable solution; $\phi=0$, $C_H=-1.0$

existance of a well defined integral manifold is not guaranteed as indicated by the figure. It is possible that an ergodic trajectory may exhibit periodicity over a large number of orbits and hence can be thought of as generating small tubular stability surfaces. However, any effort at determining these surfaces would involve an enormous amount of numerical computation, which can hardly be justified due to the academic nature of their usefulness.

Further change in the initial condition leads to a regrouping of the erogodic intersections in a well defined chain of islands (Figure 2-8(b)), which, in this case, represent two cycles of the planar libration for every three oscillations across the orbital plane. Although the stability is assured here, proximity of the islands to the stability bound makes operation of a satellite in this region undesirable. Thus, for all practical purposes, the regular 'mainland' represents the only stable region for safe operation of a satellite.

Subjecting the system to any further variation in the external disturbances results in the breakdown of the islands into the ergodic behaviour. The process of regeneration of islands and their degeneration into ergodic behaviour appears to progress indefinitely approaching the boundary of possible motion, where the margin of stability vanishes.

A comment concerning the effect of the inertia parameter on the character of the solution would be appropriate here. For a given Hamiltonian, the systematic reduction of K_i, from 1.0 (Figures 2-8) to 0.5 and 0.25 diminishes the possibility of ergodicity (Figure 2-9). Thus, decreasing the slenderness of a satellite appears to confine the region of ergodicity closer to the bound of possible motion.

For a given C_H several integral manifolds, representing the region of stable motion, are possible depending on the initial conditions. The largest of these may be called the limiting integral manifold. Figures 2-10(a) and 2-10(b) indicate the limiting regular manifold and that corresponding to the island type solution, respectively. In general, the latter winds around the regular manifold and is associated with a different periodic solution. The increase in Hamiltonian causes a marked reduction in the stability region (Figure 2-10c) suggesting the possibility of a critical value, $C_{H_{cr}}$, beyond which the manifolds cease to exist. Thus, for a value of the Hamiltonian greater than the critical (≈ 0.8) gravity-gradient stabilization of a satellite is not possible.

It should be noted that during the integration of the equations no attempt is made to reduce the order of the system using the Hamiltonian. Rather, the Hamiltonian, a constant of the motion, is computed along with the cross-section data and is used as a check on the overall accuracy of the method.

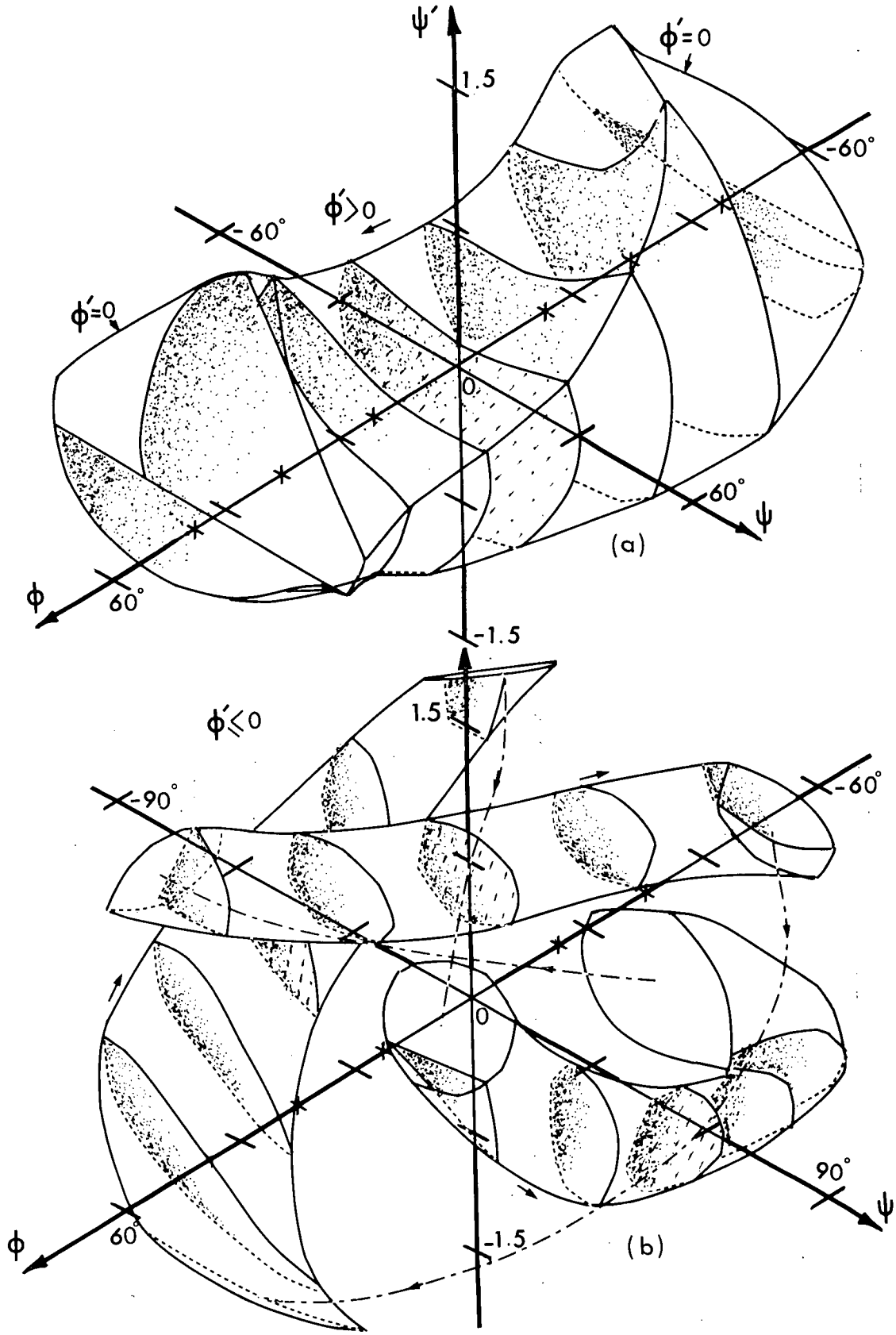

Figure 2-10 Effect of initial conditions and Hamitonian on the limiting integral manifolds (K_i=0.5): (a) regular, C_H=-1.0 ; (b) island type, C_H= -1.0

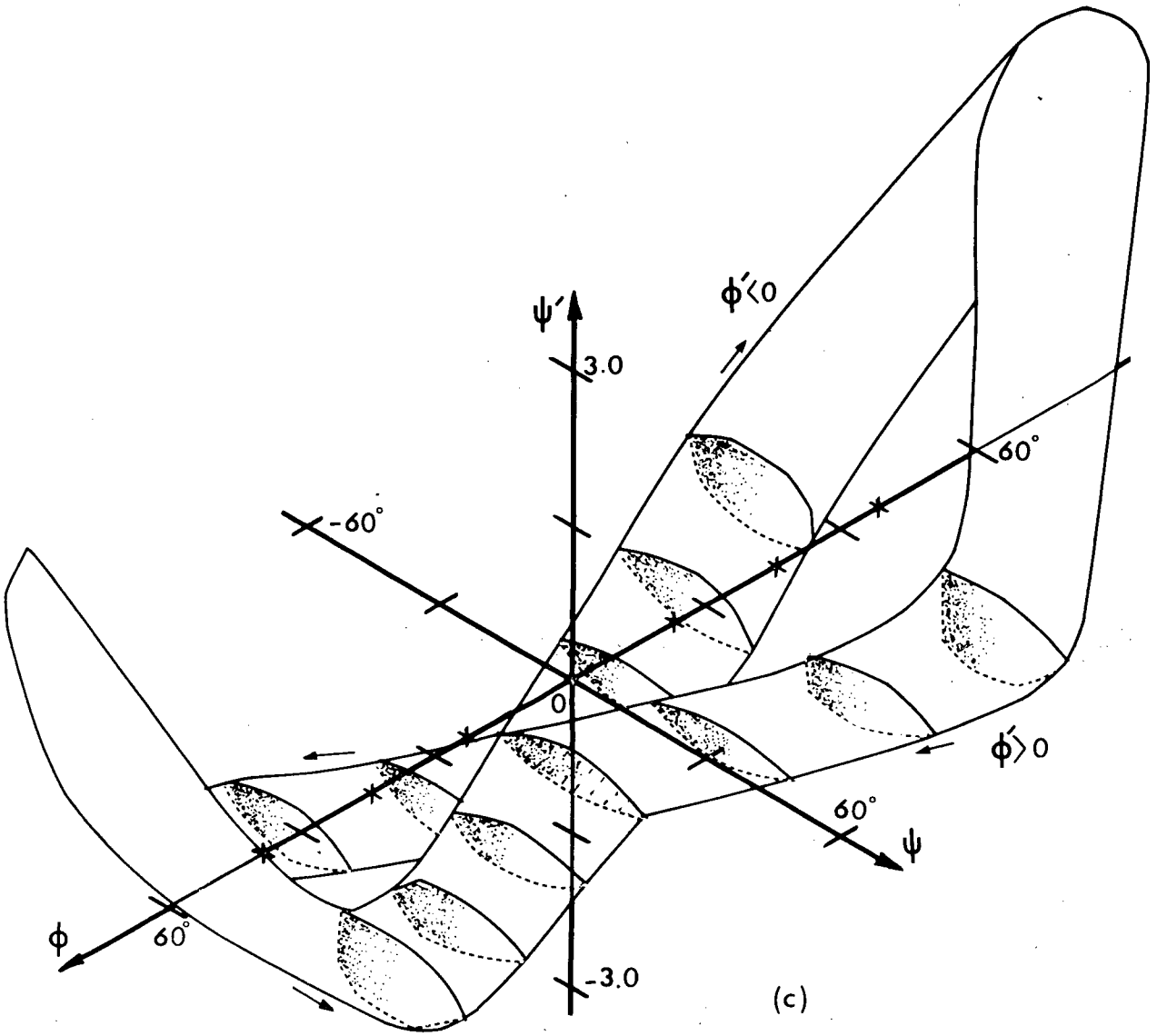

Figure 2-10 Effect of initial conditions and Hamiltonian on the limiting integral manifolds (K_i=0.5): (c) regular, C_H=0.4

2.6 Stability Plots

The results displayed in Figure 2-10 may be presented in a more informative manner, particularly, for design purposes. If ψ and ϕ are held fixed, a constant value of C_H describes, in ψ'-ϕ' plane, an ellipse, which degenerates into a circle for $\phi=0$. For $C_H \leq -1$, i.e., when the stability is guaranteed, the solution is stable over the entire ellipse. However, beyond this, a bounded motion is possible only over varying arcs of constant C_H ellipses, corresponding to the limiting invariant surfaces. Figures 2-11 and 2-12 show the allowable impulsive disturbances for non-tumbling motion for several values of inertia parameters and angular disturbances. The computational effort involved in obtaining these plots is enormous. Fortunately the symmetry properties discussed earlier, which also make the plots of the system with $\psi_o x\ \phi_o=0$ symmetrical about $\phi'=0$ axis, keep the analysis manageable.

The figures, which also include for comparison the results for dumbbell satellites obtained by Brereton[53], show better stability characteristics for slender satellites. It is observed that most satellites can stand larger disturbance across the orbital plane compared to that in the plane of the orbit. Furthermore, the ability of a satellite to withstand larger negative ψ' disturbance for given ψ_o, ϕ_o, ϕ_o' is of interest. In general, the stability bound diminishes with increasing angular disturbances. The peculiar shape

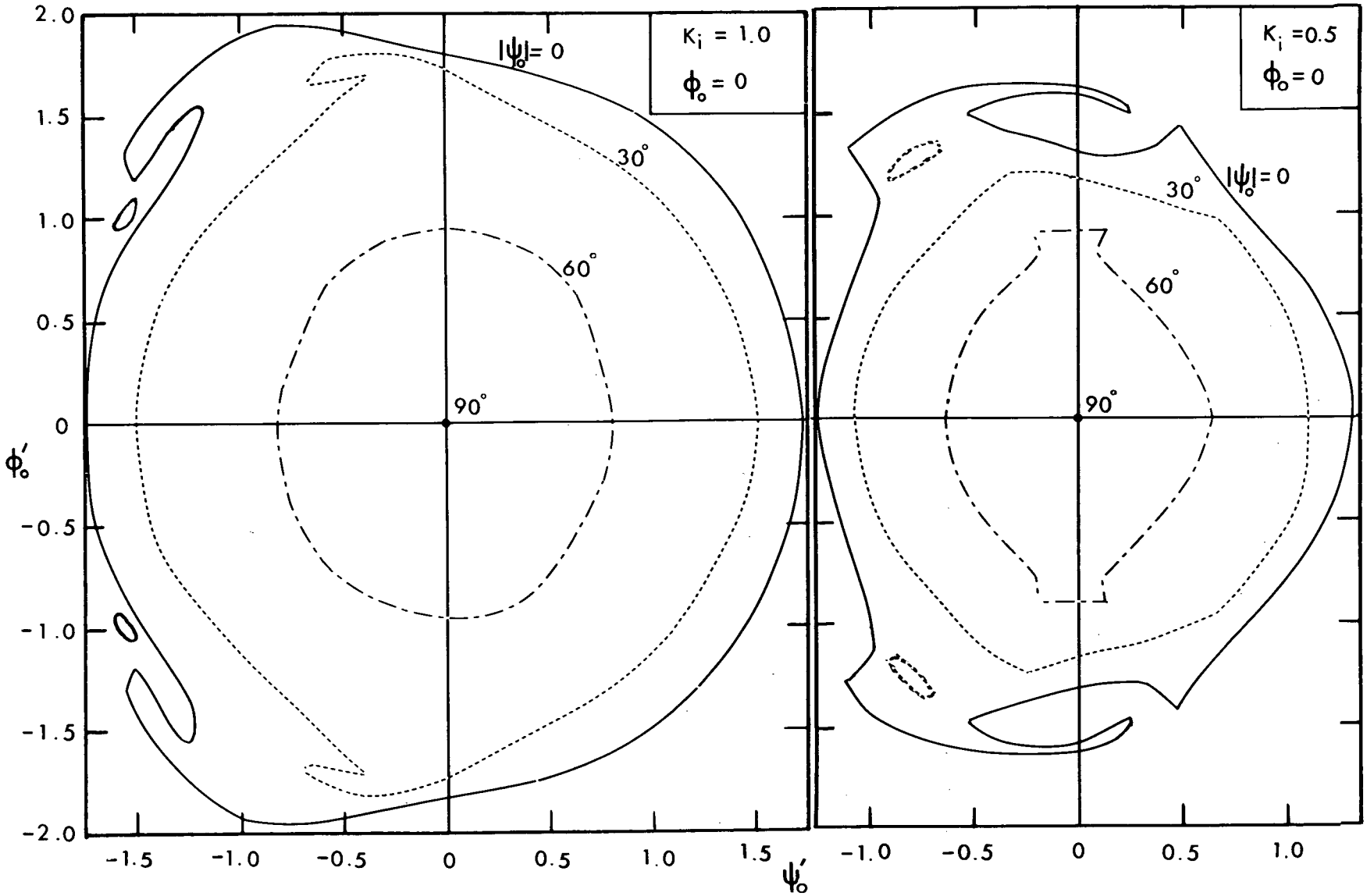

Figure 2-11 Design plots showing allowable impulsive disturbance for stable motion: (a) ϕ=0

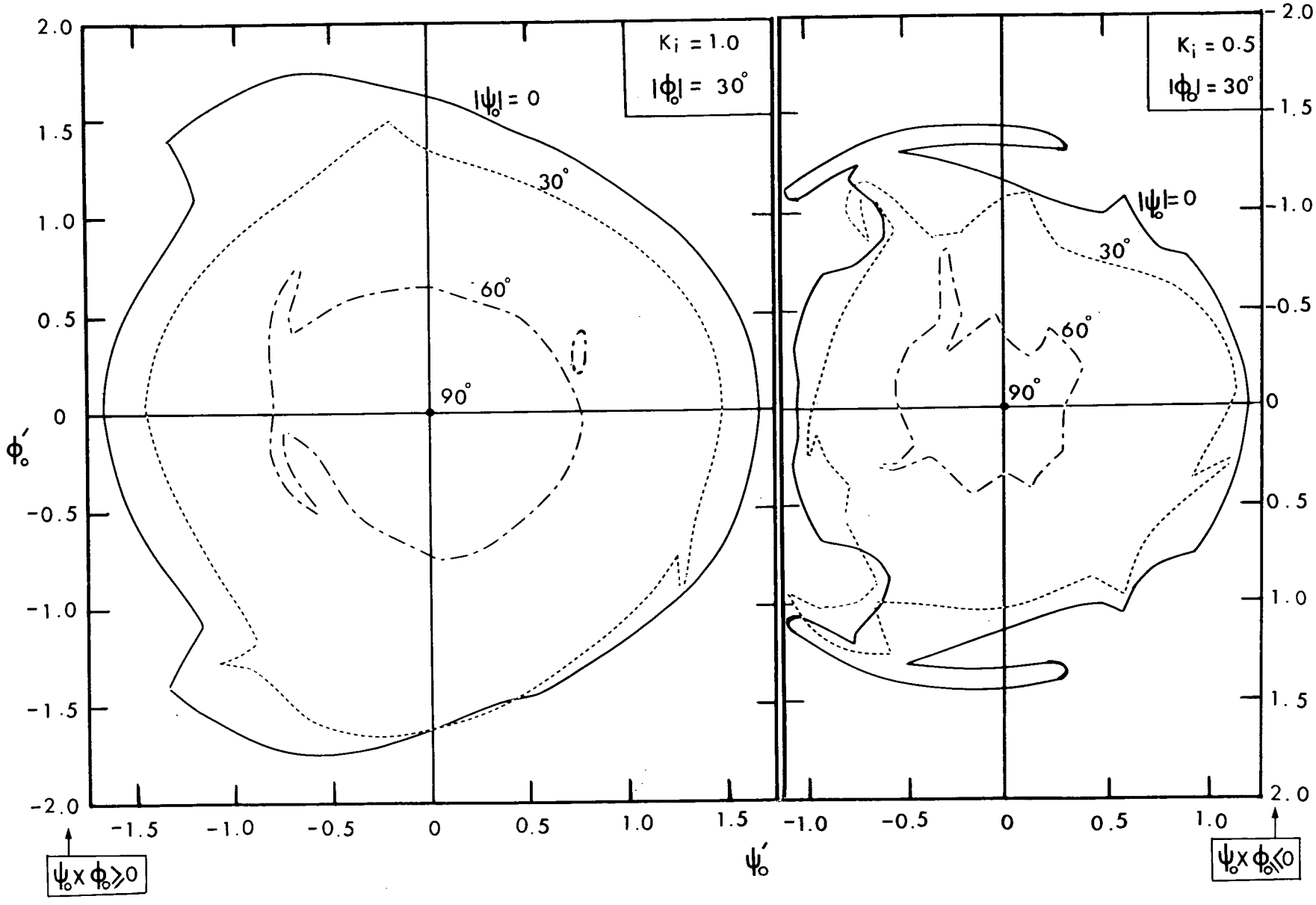

Figure 2-11 Design plots showing allowable impulsive disturbance for stable motion: (b) $|\phi| = 30°$

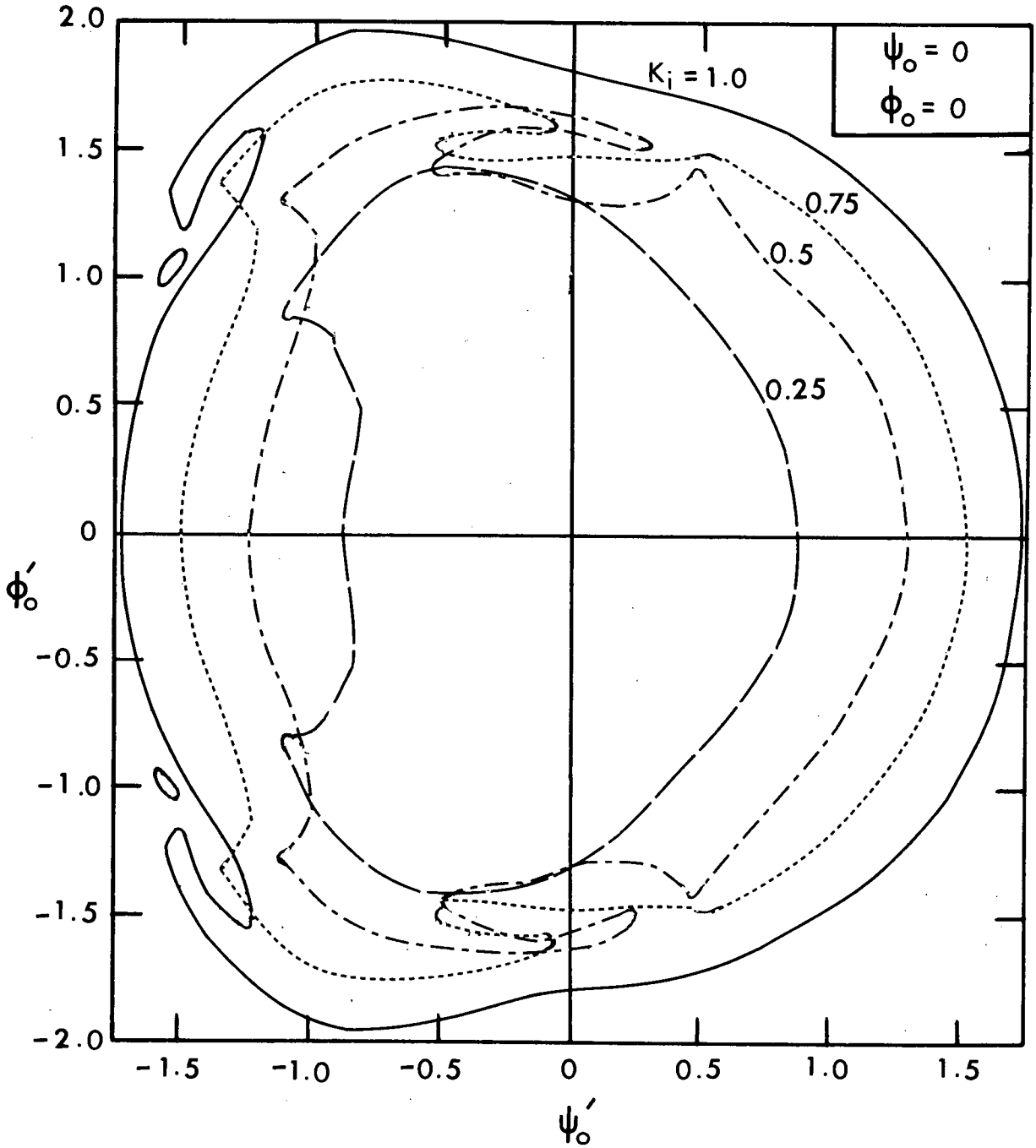

Figure 2-12 Effect of satellite inertia on allowable impulsive disturbance for stable motion

of these curves may be attributed to the coupled non-linear nature of governing equations which also give rise to a few exceptions to the findings mentioned above.

2.7 Concluding Remarks

The significant aspects of the analysis may be summarized as follows:

(i) Inertia parameter plays an important role in the response and stability characteristics of a satellite. Slender satellites (large K_i) are likely to exhibit better stability.

(ii) Zero-velocity curves and motion envelopes can be utilized profitably to identify regions of possible motion. They also provide information concerning conditional and guaranteed stability. For initial conditions leading to the Hamiltonian satisfying the inequality $-(1+3K_i) \leq C_H \leq -1$, the stability of resulting librational motion is assured.

(iii) The analysis suggests conditional stability for $-1 < C_H \leq C_{H_{cr}} \simeq 0.8$. The system is likely to show better performance in ϕ degree of freedom. The actual character of the motion is governed by the initial conditions.

(iv) The approximate closed form solution through the Butenin's approach can determine the librational

frequency and amplitude quite accurately, especially for slender satellites, even with disturbances of appreciable magnitude. A small phase discrepancy, cumulative in time, causes only a circumferential shift in the stroboscopic phase-plane. The method can provide considerable insight into the system behaviour and gives results suitable for preliminary design purposes.

(v) The constant Hamiltonian can be used to reduce the order of the system and leads to yet another analytical solution, which, in general, gives better approximation, particularly when the motion across the orbit is small.

(vi) Both the solutions fail to predict the coupling effects, which increase with increasing disturbances and decreasing K_i

(vii) The librational and orbital frequencies are of the same order of magnitude. An identical disturbance in ψ and ϕ excites higher frequency, smaller amplitude motion in the orbital plane than that across it.

(viii) The system exhibits three distinctly different solutions: regular, island type and ergodic. However, from practical considerations only the regular solution provides usable bounds for stable motion. The concept of integral manifold used

here for stability study gives, for given inertia parameter and Hamiltonian, all possible combinations of external disturbances, to which a satellite can be subjected, without causing it to tumble.

(ix) For a given Hamiltonian the stability bound is represented by the limiting integral manifold. On the other hand, degeneration of the invariant surface to a line corresponds to a periodic solution of the problem. Thus periodic solutions may be thought of as spines around which integral manifolds are built.

(x) The plots of allowable impulsive disturbances should prove useful during satellite design. The symmetry properties considerably extend their range of application.

3. EFFECT OF AERODYNAMIC TORQUE ON SYSTEM RESPONSE AND STABILITY

3.1 Preliminary Remarks

Presence of various perturbing forces necessarily complicates the problem under study. More significant of these, for close-earth satellites, are the aerodynamic forces[20], which may be effective even at four to five hundred miles altitude.

This chapter investigates the effect of aerodynamic moment on the coupled librational motion of the cylindrical satellite negotiating a circular trajectory. In the beginning the stable equilibrium configurations are established through Routh's criteria as well as Liapunov's direct method. The regions of guaranteed and conditionally stable motion are given as functions of inertia parameter, Hamiltonian and aerodynamic torque. The numerically determined response to a variety of disturbances helps in establishing the influence of system parameters. The concept of integral manifolds again proves useful in analyzing the character of stable trajectories and to obtain the stability bounds. The design plots, indicating allowable impulsive disturbances for stability, reveal the adverse effect of atmosphere.

In view of the computational cost involved, an alternate economical approach using analog simulation,

normally used in real-time studies, is attempted. A comparison of the response and stability data with the numerical results establishes the suitability of the method.

3.2 Formulation of the Problem

3.2.1 Aerodynamic Torque

Consider a rigid, axi-symmetric satellite, with mass-centre at S, executing coupled librational motion while moving in a circular orbit about the centre of attraction O (Figure 3-1). As before, x, y, z are principal body axes of the satellite, whose orientation is specified by modified Eulerian rotations: ψ in the orbital plane; ϕ across the orbital plane; and λ about the axis of symmetry. The satellite is subjected to gravitational and aerodynamic torques, which are evaluated using the following simplifying but realistic assumptions:

(i) gravitational potential can very closely be approximated by a truncated series;

(ii) air density ρ and gravity field are functions of height only. Variations of ρ over satellite dimensions are ignored;

(iii) relative velocity of the satellite with respect to the surrounding atmosphere is taken to be the same as satellite's orbital velocity, i.e., its variation due to the satellite's librational motion and atmospheric rotation are neglected;

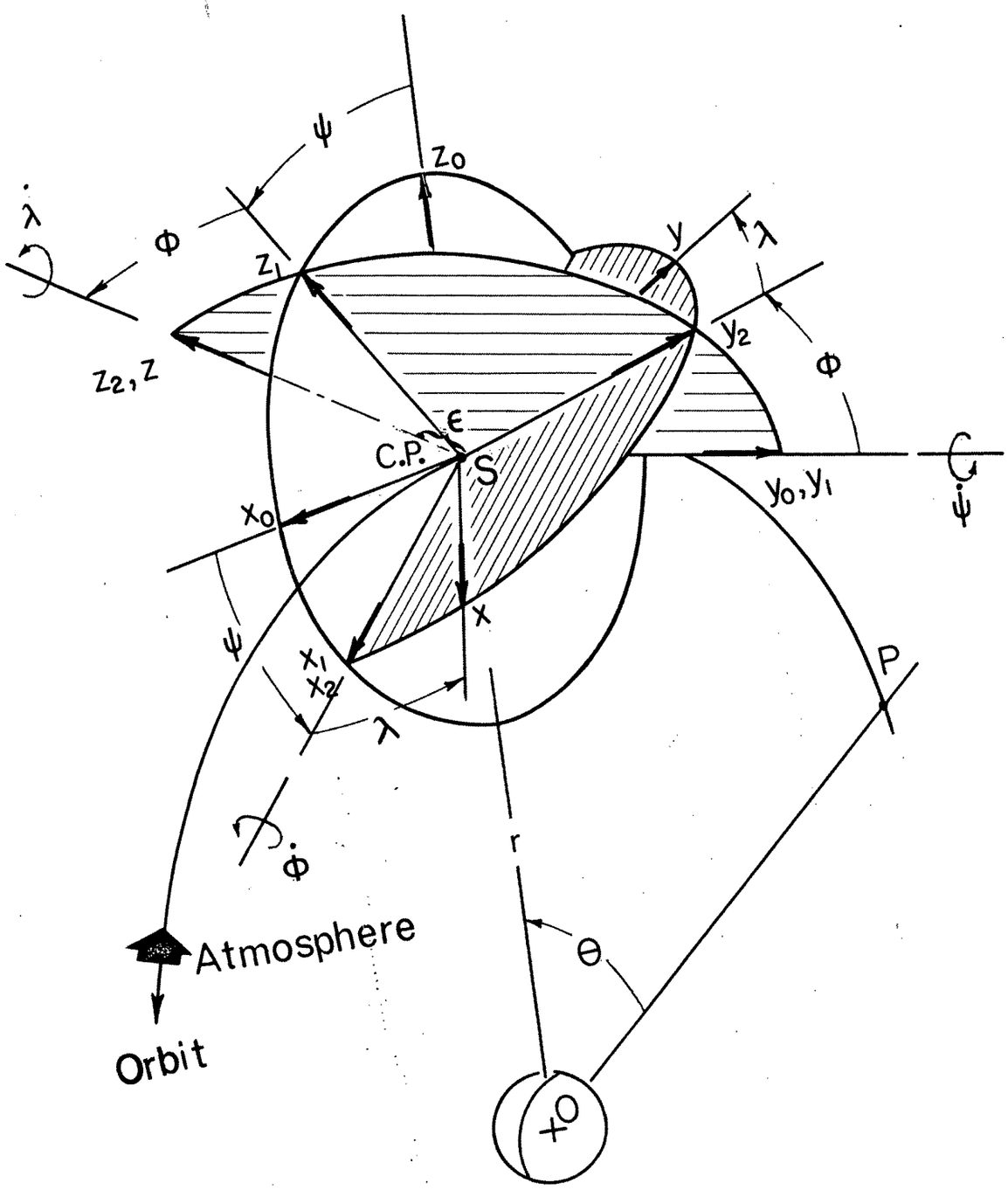

Figure 3-1 Geometry of satellite motion in presence of atmosphere

(iv) ambient condition is represented by free molecular flow;

(v) C_D, based on projected area and usually a very complex function, is taken to be a constant;

(vi) centre of pressure is assumed to be coincident with the geometrical centre of the satellite and small changes in its position due to librational motion are ignored.

At altitudes of about 100 miles and over, the mean free path of molecular motion is large in relation to typical satellite dimensions, and the flow regime is classified as free molecular flow. Surface forces in this regime are due to molecular impingement on its surface and their subsequent re-emission. For convex bodies, the aerodynamic force at a point on the surface of a satellite at specified conditions is a function only of the angle between the impinging stream of molecules and the surface. Consequently, it is possible to integrate the surface force over the frontal area of the satellite, yielding the net lift, drag and moment on the satellite in terms of attitude angles ψ, ϕ, λ. For librational motion only the aerodynamic moment is of interest, slow decay of the orbit because of drag being neglected.

Using the methods of Schaaf and Chambré[66] the normal pressure and shear stress on a satellite surface exposed to free molecular flow can be expressed as

$$P = (\rho v^2/2S_0^2)\left[\left\{(2-\sigma')\, S_0'/\sqrt{\pi} + \sigma' (T_w/T_a)^{1/2}/2\right\} e^{-S_0'^2} + \left\{(2-\sigma')(1/2 + S_0'^2) + \sigma' S_0' (\pi T_w/T_a)^{1/2}/2\right\}(1+\mathrm{erf}(S_0'))\right] \quad \ldots\ldots (3.1)$$

$$\tau = -(\rho v^2 \sigma \cos\xi/2S_0\sqrt{\pi})\left[e^{-S_0'^2} + \sqrt{\pi}\, S_0'(1+\mathrm{erf}(S_0'))\right] \quad \ldots\ldots (3.2)$$

The moment on the body is given by

$$\bar{M}_a = \int_{\bar{A}} \bar{l} \times (\bar{P} + \bar{\tau})\, d\bar{A} \quad \ldots\ldots (3.3a)$$

which, using symmetry properties of the satellite and intermediate body coordinates $x_2y_2z_2$, can be written as

$$\bar{M}_a = \bar{u}_{x_2} \int_{\bar{A}} \left[y_2(P_{z_2} + \tau_{z_2}) - z_2(P_{y_2} + \tau_{y_2})\right] d\bar{A} \quad (3.3b)$$

Here $\bar{u}_{x_2}$ represents a unit vector along x_2 axis. The evaluation of the integral, which, in general, can be achieved only numerically, involves substantial computational efforts. However, for cylindrical satellites, it can be approximated, quite accurately, in a closed form by the expression[36,67]

$$M_a = -0.5\, \rho v^2 C_D \epsilon \cos\psi \left[D_o L_o |\cos\psi| + \pi D_o^2 \sin\psi/4\right] \quad \ldots\ldots (3.3c)$$

The absolute sign ensures applicability of the expression for all values of ψ. Variations in $\rho, v, C_D, \varepsilon$ being usually small,[32,34,67,68,et al.] they are assumed to remain constant for a given satellite in a circular orbit. The analysis, however,

can be extended to accommodate their variations without too much difficulty.

Thus aerodynamic moment is a function of librational angle ψ and not of angular velocities. Consequently, a potential function can be derived that is equal to the negative of the work required to move the satellite from a reference orientation (0,0,0) to the orientation given by ψ,ϕ,λ. For a symmetric satellite it is

$$U_a = -\int_0^{\psi} M_a \, d\psi$$

$$= 1/4 \; \rho \, v^2 \, C_D \, \epsilon \, D_o L_o [\psi + \sin\psi \{\cos\psi + (\pi D_o/4L_o)\sin\psi\}]$$

$$= (I\dot{\theta}^2 B_f/2)[\psi + \sin\psi(\cos\psi + C_1 \sin\psi)] \quad (\text{for } |\psi| \leq \pi/2)$$

. . . . (3.4)

where the dimensionless aerodynamic coefficient, B_f, is represented by

$$B_f = C_D \, \rho \, v^2 \, D_o \, L_o \, \epsilon / 2I\dot{\theta}^2 \qquad \text{. . . . (3.5)}$$

and

$$C_1 = \pi D_o/4L_o = \pi \{(1-K_i)/3(1+K_i)\}^{1/2}/2 \qquad \text{. . (3.6)}$$

3.2.2 Lagrangian and Equations of Motion

As the expressions of kinetic and potential energies due to gravity-gradient (equations 2.2) remain unchanged, the Lagrangian becomes

$$
\begin{aligned}
L &= T - (U_g + U_a) \\
&= m(\dot{r}^2 + r^2\dot{\theta}^2)/2 + I[\dot{\phi}^2 + (\dot{\theta} + \dot{\psi})^2 \cos^2\phi]/2 \\
&\quad - \mu(I - I_{zz})(1 - 3\cos^2\psi \cos^2\phi)/2r^3 \\
&\quad + \int_0^{\psi} M_a \, d\psi
\end{aligned}
\qquad \ldots\ldots (3.7)
$$

As before, ignoring the orbital perturbations due to librational motion and using θ as the independent variable, the equations of motion become:

$$
\begin{aligned}
&\psi'' - 2\phi'(\psi' + 1)\tan\phi + 3K_i \sin\psi \cos\psi \\
&\quad + B_f(|\cos\psi| + C_1 \sin\psi)\cos\psi/\cos^2\phi = 0 \\
&\phi'' + \{(\psi' + 1)^2 + 3K_i \cos^2\psi\} \sin\phi \cos\phi = 0
\end{aligned}
\qquad \ldots\ldots (3.8)
$$

it should be noted that the equations governing the ϕ as well as λ (relation 2.1c) degrees of freedom are unaffected by the presence of aerodynamic moment.

Even for this simplified situation the second order, non-linear, coupled equations of motion have no known closed form solution. A numerical technique under this condition can again be used to advantage. However, considerable useful information concerning equilibrium positions, regions of possible motion, zones of conditional and guaranteed

stability, etc., can be obtained without even solving the equations. This provides some insight into the behaviour of the system without involving appreciable computational time and effort.

3.2.3 Hamiltonian

Since the librational motion is still conservative and as the Lagrangian of the system does not involve time explicitly the Hamiltonian represents a constant of the system, i.e.,

$$
\begin{aligned}
H &= p_\psi \dot{\psi} + p_\phi \dot{\phi} + p_\lambda \dot{\lambda} - L \\
&= I\{\dot{\phi}^2 + (\dot{\psi}^2 - \dot{\theta}^2)\cos^2\phi\}/2 - 3\mu(I \\
&\quad - I_{zz})\cos^2\psi\cos^2\phi/2r^3 + I\dot{\theta}^2 B_f\{\psi + \sin\psi(\cos\psi \\
&\quad + C_1 \sin\psi)\}/2 = \text{constant} \qquad (\text{for } |\psi| \leq \pi/2)
\end{aligned}
\qquad \ldots\ldots (3.9)
$$

or, in a non-dimensional form:

$$
\begin{aligned}
C_H &= 2H/I\dot{\theta}^2 \\
&= \phi'^2 + \cos^2\phi(\psi'^2 - 1 - 3K_i\cos^2\psi) + B_f\{\psi \\
&\quad + \sin\psi(\cos\psi + C_1\sin\psi)\} \\
&= \text{constant} \qquad (\text{for } |\psi| \leq \pi/2)
\end{aligned}
\qquad \ldots\ldots (3.10)
$$

3.3 Dynamic Equilibria and Stability in the Small

3.3.1 Equilibrium Positions

At equilibrium position, the potential is an extremum, hence

$$\partial U/\partial q_i \big|_e = 0$$

$$\therefore \quad \cos\psi\left[3K_i\cos^2\phi\,\sin\psi + B_f|\cos\psi| + B_f C_1 \sin\psi\right] = 0$$

$$\sin 2\phi\left[1 + 3K_i\cos^2\psi\right] = 0 \qquad \ldots\ldots (3.11)$$

In infinite number of solutions are possible. However, if the stability of librational motion is defined such that the librational angles remain within $\pm\pi/2$ from the local vertical (non-tumbling motion), only the following nine equilibrium positions are of interest:

$$\begin{aligned}
\psi_e &= \pm\pi/2 \quad , & \phi_e &= 0 \quad ; \\
\psi_e &= \pm\pi/2 \quad , & \phi_e &= \pm\pi/2 \, ; \\
\psi_e &= \tan^{-1}(-1/C_1), & \phi_e &= \pm\pi/2 \, ; \\
\psi_e &= \tan^{-1}(-B_f/(3K_i + B_f C_1)), & \phi_e &= 0 \, .
\end{aligned} \qquad \ldots\ldots (3.12)$$

Stability of these equilibrium positions can be tested by infinitesimal technique or Liapunov's direct method without having to solve for the perturbed motion about an equilibrium position.

3.3.2 Infinitesimal Technique (Routh)

Linearized perturbation equations for motion about an equilibrium configuration can be written as

$$\delta\psi'' - \delta\psi'\,(2\phi_e' \tan\phi_e) + \delta\psi[3K_i \cos 2\psi_e - \{\sin 2\psi_e - C_1 \cos 2\psi_e\} B_f/\cos^2\phi_e] - \delta\phi'\{2\tan\phi_e(\psi_e'+1)\} - \delta\phi(2\phi_e'\psi_e') = 0 \quad \ldots\ldots (3.13a)$$

$$\delta\phi'' + \delta\phi\{\cos 2\phi_e((\psi_e'+1) + 3K_i \cos^2\psi_e)\} + \delta\psi'\{\sin 2\phi_e(\psi_e'+1)\} + \delta\psi\{-3\sin 2\psi_e \sin 2\phi_e/2\} = 0 \quad \ldots\ldots (3.13b)$$

For the solution of the form

$$\delta\psi = \delta\psi_a e^{\lambda_1 t} \quad , \quad \delta\phi = \delta\phi_a e^{\lambda_1 t}$$

the equations give

$$\begin{bmatrix} [\lambda_1^2 - 2\lambda_1\phi_e' \tan\phi_e + 3K_i \cos 2\psi_e - B_f\{\sin 2\psi_e - C_1 \cos 2\psi_e\}/\cos^2\phi_e] & [-2\lambda_1(\psi_e'+1)\tan\phi_e - 2\phi_e'\psi_e'] \\ [\lambda_1(\psi_e'+1)\sin 2\phi_e - 3K_i \sin 2\psi_e \sin 2\phi_e/2] & [\lambda_1^2 + \cos 2\phi_e\{(\psi_e'+1)^2 + 3K_i \cos^2\psi_e\}] \end{bmatrix} \begin{Bmatrix} \delta\psi_a \\ \delta\phi_a \end{Bmatrix} = \begin{Bmatrix} 0 \\ 0 \end{Bmatrix} \quad \ldots (3.14)$$

leading to the characteristic equation

$$A\lambda_1^4 + B\lambda_1^3 + C\lambda_1^2 + D\lambda_1 + E = 0 \quad \ldots . \quad (3.15)$$

where

$$A = 1$$

$$B = -2\phi_e' \tan\phi_e$$

$$C = 3K_i \cos 2\psi_e - B_f\{\sin 2\psi_e - C_1 \cos 2\psi_e\}/\cos^2\phi_e$$
$$+ \cos 2\phi_e\{(\psi_e'+1)^2 + 3K_i \cos^2\psi_e\} + 4(\psi_e'+1)^2 \sin^2\phi_e$$

$$D = -2\phi_e' \tan\phi_e \cos 2\phi_e \{(\psi_e'+1)^2 + 3K_i \cos^2\psi_e\}$$
$$- 3K_i \sin 2\psi_e \sin 2\phi_e \tan\phi_e (\psi_e'+1)$$
$$+ 2\phi_e'\psi_e'(\psi_e'+1)\sin 2\phi_e$$

$$E = \cos 2\phi_e\{(\psi_e'+1)^2 + 3K_i \cos^2\psi_e\}\{3K_i \cos 2\psi_e$$
$$- B_f(\sin 2\psi_e - C_1 \cos 2\psi_e)/\cos^2\phi_e\}$$
$$- 3K_i \phi_e' \psi_e' \sin 2\psi_e \sin 2\phi_e$$

The application of the stability conditions

$$A, B, C, D, E \geqslant 0$$

$$(BC - AD)D - B^2 E \geqslant 0$$

showed all the equilibrium positions to be unstable except the last one, i.e.,

$$\psi_e = \tan^{-1}\{-B_f/(3K_i + B_f C_1)\} \quad , \quad \phi_e = 0 \qquad (3.16)$$

3.3.3 Liapunov's Direct Method

A simpler and more useful approach to the stability study of an equilibrium position is by Liapunov's second or direct method.

Using Hamiltonian as a Liapunov's function

$$\begin{aligned} V_L &= C_H - C_{H_e} \\ &= \phi'^2 + \cos^2\phi\,(\psi'^2 - 1 - 3K_i\cos^2\psi) \\ &\quad + B_f\{\psi + \sin\psi(\cos\psi + C_1\sin\psi) + \cos^2\phi_e(1 \\ &\quad + 3K_i\cos^2\psi_e)\} - B_f\{\psi_e + \sin\psi_e(\cos\psi_e + C_1\sin\psi_e)\} \end{aligned} \qquad \ldots\ldots (3.17)$$

Therefore, from equation (3.8)

$$\dot{V}_L = \dot{\theta}\{\partial V_L/\partial\psi\ \psi' + \partial V_L/\partial\phi\ \phi' + \partial V_L/\partial\psi'\ \psi'' + \partial V_L/\partial\phi'\ \phi''\} = 0 \qquad \ldots\ldots (3.18)$$

Thus the system is plain stable if $V_L \geq 0$. It can be shown that for $V_L \geq 0$,

$$\left[\partial^2 V_L/\partial q_i \partial q_j\right]_e \geqslant 0$$

i.e.,

$$\begin{bmatrix} \partial^2 V_L/\partial\psi^2 & \partial^2 V_L/\partial\psi\partial\phi \\ \partial^2 V_L/\partial\phi\partial\psi & \partial^2 V_L/\partial\phi^2 \end{bmatrix} \geq 0 \quad \ldots \quad (3.19)$$

This implies a minimum value for potential energy at the equilibrium position. For the matrix to be positive definite

$$2\cos 2\psi_e\,(3K_i\cos^2\phi_e + B_f C_1) - 2B_f \sin 2\psi_e \geq 0$$

$$2\cos 2\phi_e\,(1 + 3K_i\cos^2\psi_e) \geq 0$$

$$-3K_i \sin 2\phi_e \sin 2\psi_e \geq 0 \quad \ldots \quad (3.20)$$

Testing the equilibrium positions listed earlier (equation 3.12), confirms the conclusions of the infinitesimal analysis.

The 'plain stable' equilibrium position is a function of inertia parameter as well as aerodynamic coefficient. Figure 3-2 shows the stable equilibrium configuration as a function of aerodynamic coefficient for four representative satellites. It is apparent that the equilibrium position rapidly changes with aerodynamic coefficient, particularly in the range of small B_f and K_i. However, beyond $B_f \simeq 4.75$ the trend reverses and most satellites tend to attain a uniform attitude around 50 - 60 deg.

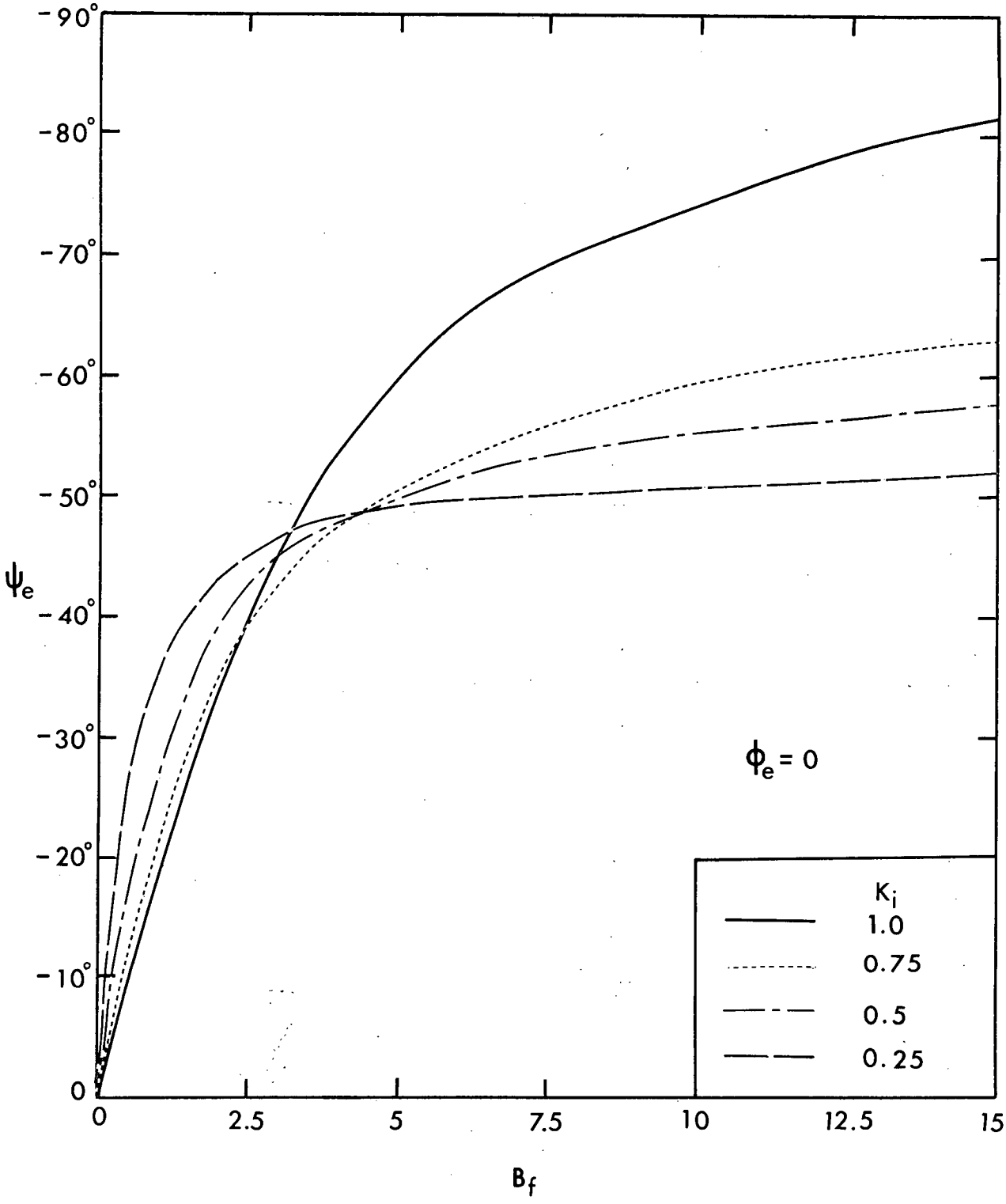

Figure 3-2 Variation of stable equilibrium position due to aerodynamic torque and satellite inertia

3.4 Bounds of Librations

Hamiltonian, being a constant of the motion, can be used quite effectively to study the general behaviour of the system through zero velocity curves defined by

$$C_H = -\cos^2\phi(1+3K_i\cos^2\psi) + B_f\{\psi+\sin\psi(\cos\psi+C_1\sin\psi)\} \quad \ldots\ldots (3.21)$$

Figure 3-3 presents these plots for various values of Hamiltonian, inertia parameter and aerodynamic coefficients. The curves, enclosing the regions of real velocities, represent the bounds of librational motion. It may be observed that for:

(i) $C_{H_e} = -1-3K_i + B_f \tan^{-1}\{-B_f/(3K_i+B_fC_1)\} \geqslant C_H$,

no motion is possible;

(ii) $C_{H_e} < C_H \leqslant -1 - B_f(\pi/2 - C_1)$,

the motion is bounded;

(iii) $-1 - B_f(\pi/2 - C_1) < C_H < -B_f(\pi/2 - C_1)$,

the motion is bounded in ϕ only;

(iv) $C_H \geqslant -B_f(\pi/2 - C_1)$,

unbounded motion is possible in both directions.

$\ldots\ldots (3.22)$

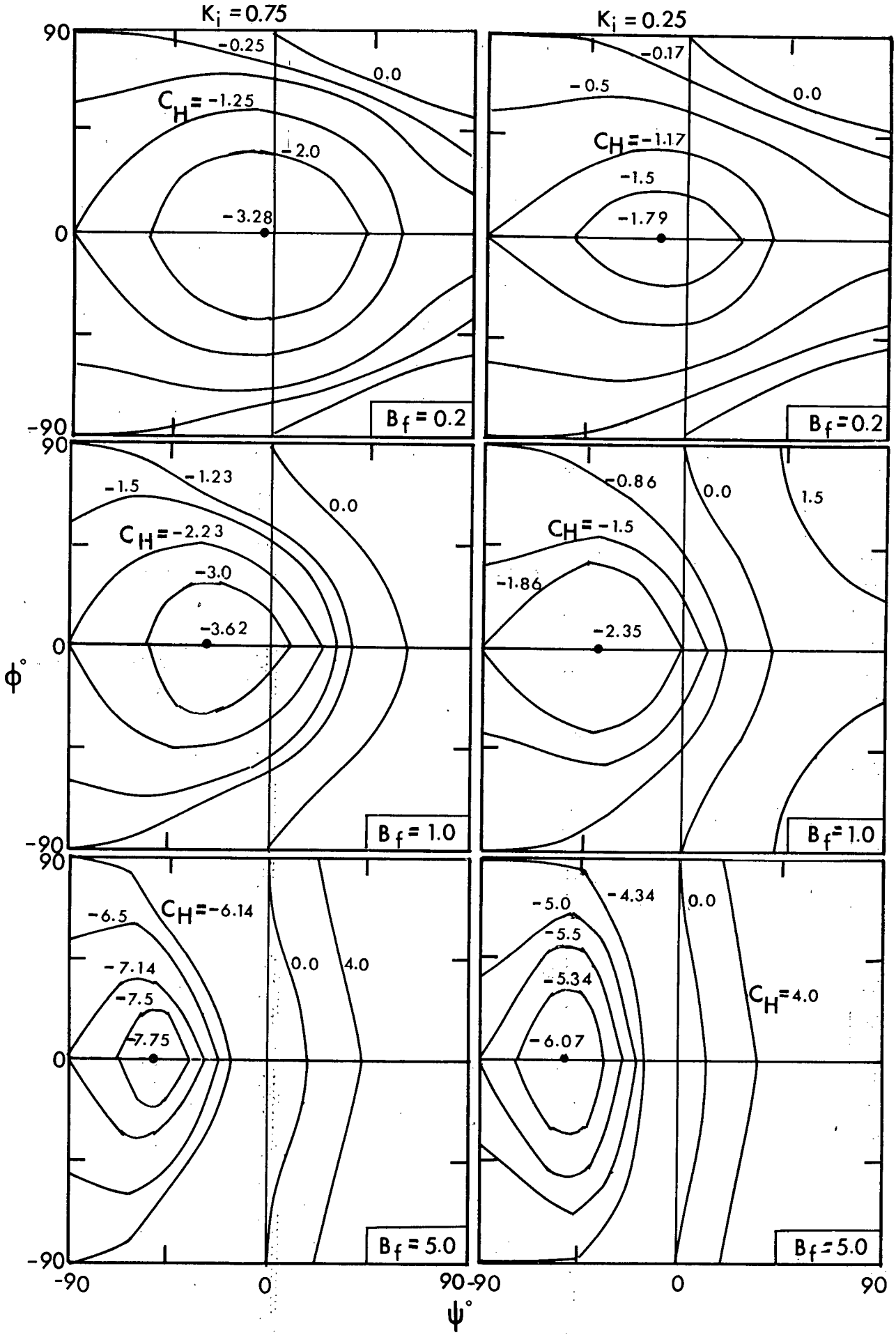

Figure 3-3 Effect of satellite inertia, Hamiltonian and aerodynamic torque on zero-velocity curves

The presence of aerodynamic moment destroys the symmetry of the curves about ϕ axis by shifting them towards $-\psi$ direction. A study of the largest region enclosed by the bounded curves suggests that although the slender satellites, in general, exhibit better stability characteristics, their performance degenerates substantially when subjected to appreciable aerodynamic torque. The plots also indicate the satellite's increased susceptibility to planar disturbances. An increase in aerodynamic coefficient reduces the value of the limiting Hamiltonian for guaranteed stability.

Figure 3-4 shows these regions as functions of Hamiltonian and aerodynamic coefficients for several values of inertia parameter. It is apparent that slender satellites are likely to exhibit better stability characteristics for small aerodynamic moment, however, larger B_f is expected to reverse this trend.

The motion envelope in ψ,ψ,ϕ -space is defined by

$$C_H - \cos^2\phi\,(\psi'^2 - 1 - 3K_1\cos^2\psi) - B_f[\psi + \sin\psi(\cos\psi + C_1\sin\psi)] = 0 \qquad \ldots\ldots (3.23)$$

In Figure 3-5 a typical motion envelope shows that the aerodynamic torque causes a breakdown of the symmetry about $\psi=0$ plane and increases the possibility of instability.

Having established the equilibrium positions, their stability, and the bounds of librations, the next logical

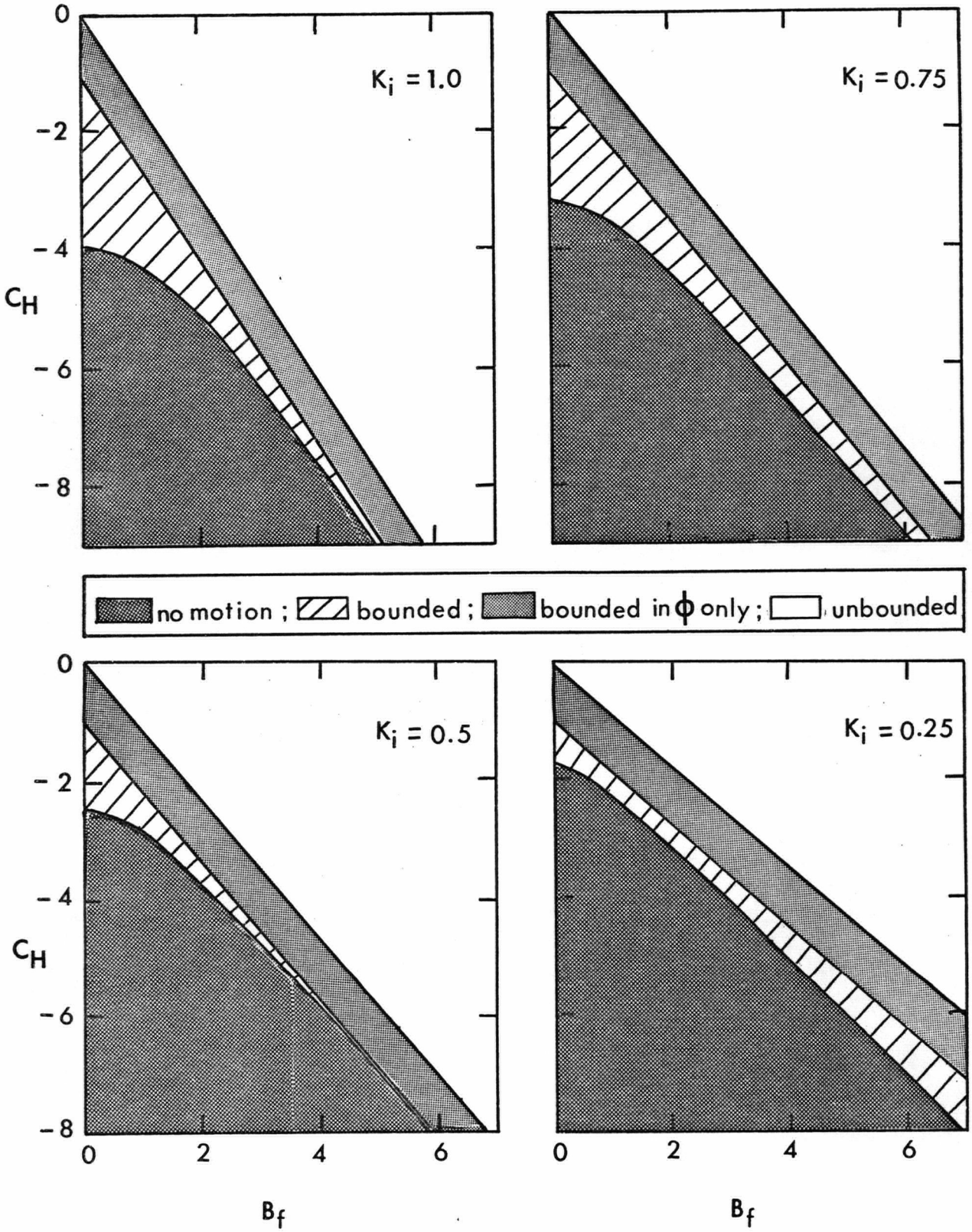

Figure 3-4 Regions of bounded motion

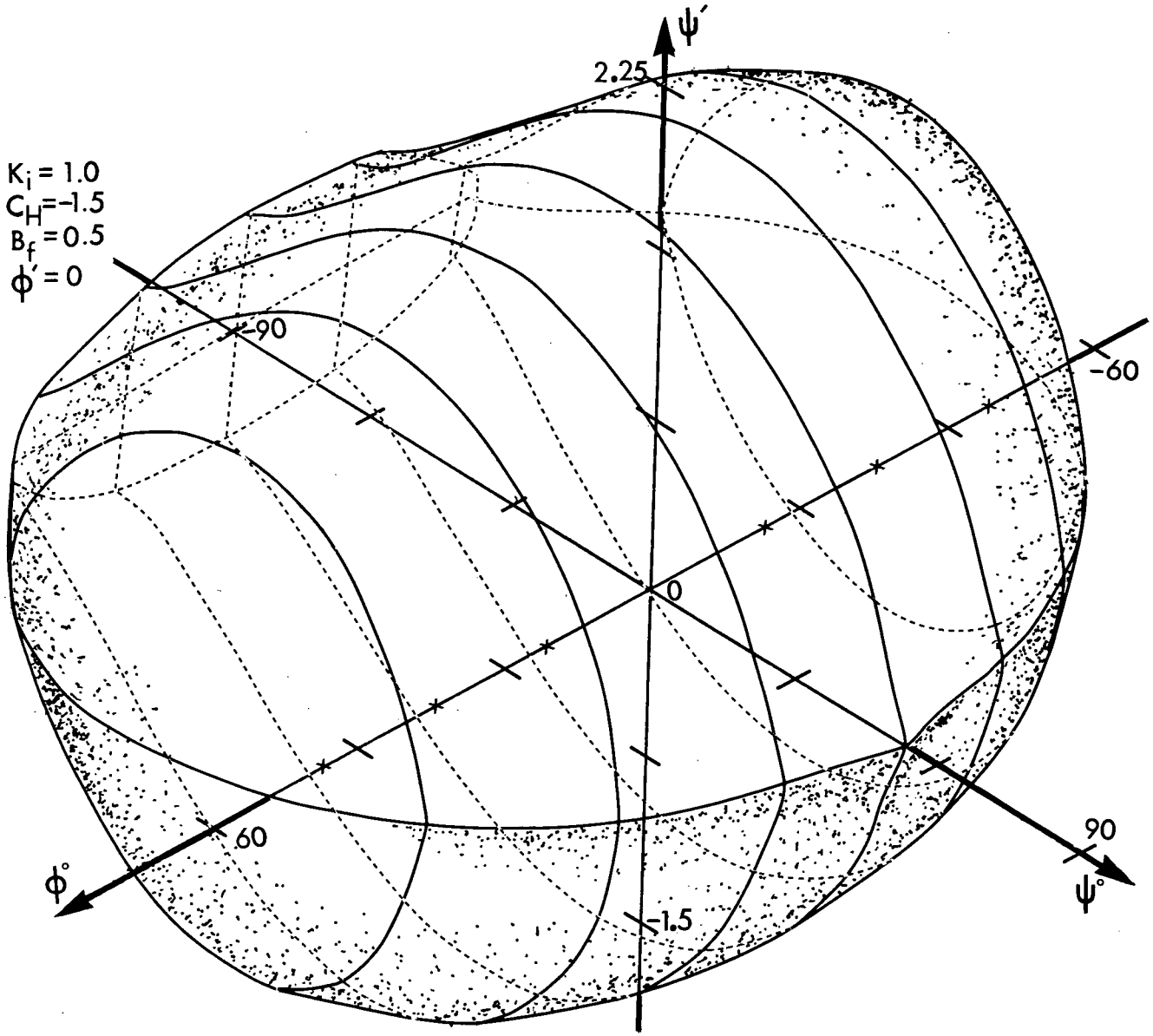

Figure 3-5 Influence of aerodynamic torque on motion envelope

step would be to investigate the system response and stability.

3.5 Numerical Solution

The equations of motion (equation 3.8) can be written as a set of four first order relations:

$$d\psi/d\theta = \psi' \quad ; \quad d\phi/d\theta = \phi'$$

$$d\psi'/d\theta = 2\phi'(\psi'+1)\tan\phi - 3K_i \sin\psi\cos\psi - B_f(\cos\psi + C_\perp \sin\psi)\cos\psi/\cos^2\phi$$

$$d\phi'/d\theta = -\{(\psi'+1)^2 + 3K_i\cos^2\psi\}\cos\phi\sin\phi \qquad \ldots (3.24)$$

Adams-Bashforth predictor-corrector integration procedure was used for numerical solution of these equations. Note that the system exhibits an invariant character only under the transformation (θ,ψ,ϕ) to $(\theta,\psi,-\phi)$. Figures 3-6 and 3-7 show the response charts thus obtained for a set of satellites subjected to systematically varying aerodynamic coefficient and initial disturbances. A step size of 3° was chosen for integration.

The solution involving four dependent variables ψ,ψ', ϕ and ϕ' defines a trajectory in a four-dimensional

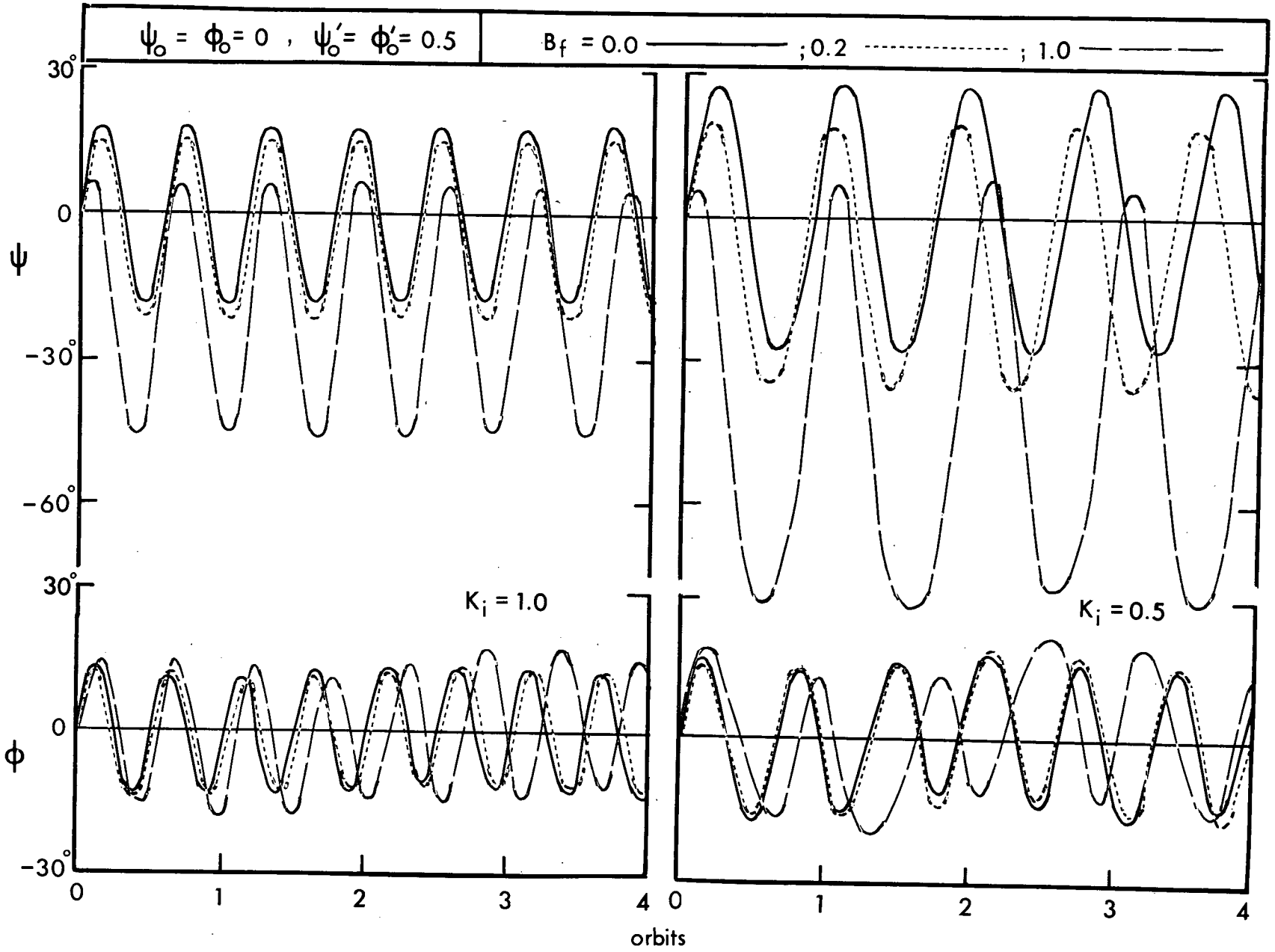

Figure 3-6 Effects of aerodynamic torque and inertia parameter on the response of satellite to an impulsive disturbance

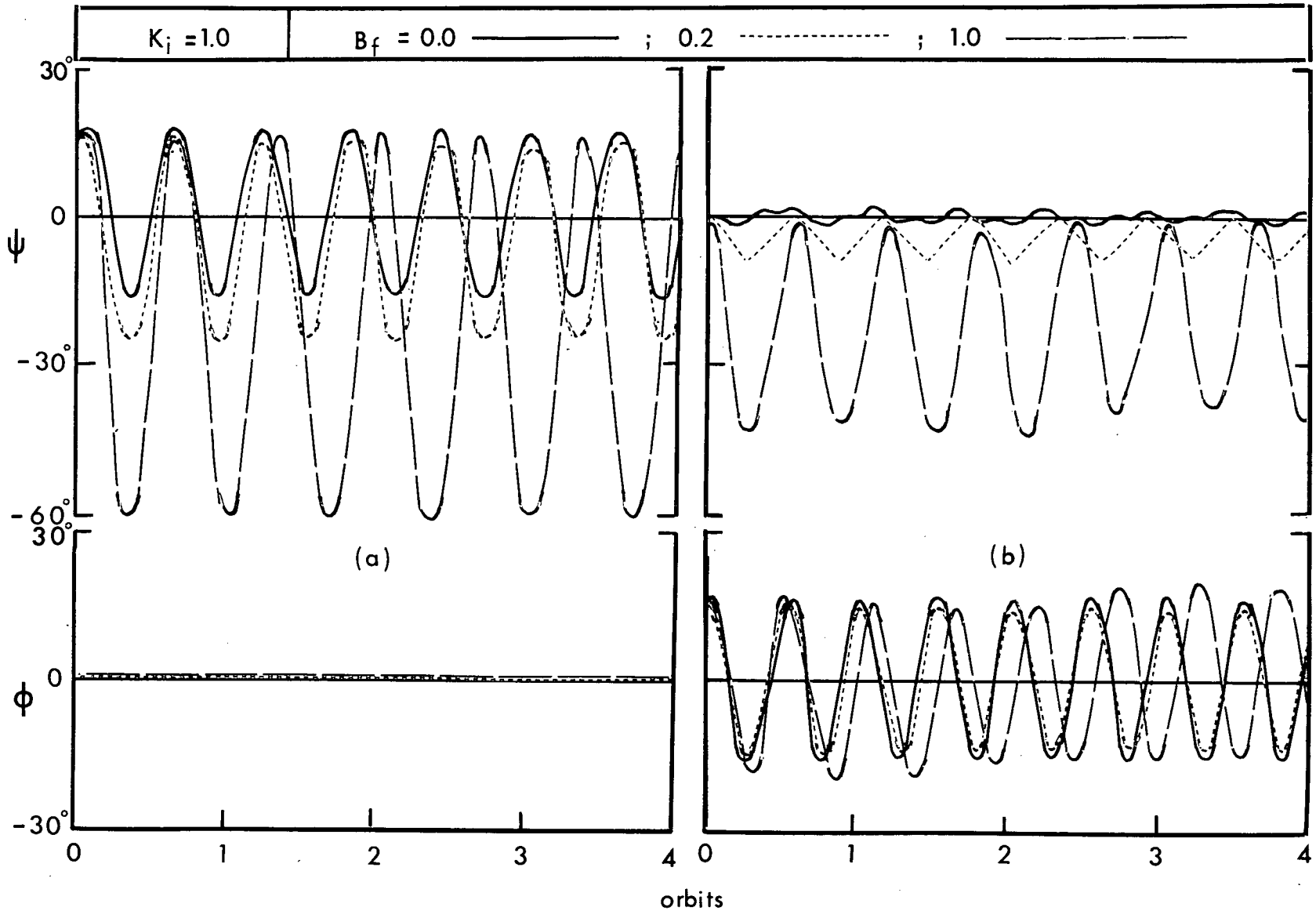

Figure 3-7 Response of a satellite to a disturbance in one degree of freedom in presence of aerodynamic torque: (a) ψ_o=15°, ψ_o'=0.25, ϕ_o=ϕ_o'=0; (b) ψ_o=ψ_o'=0, ϕ_o=15°, ϕ_o'=0.25

phase-space. The invariant Hamiltonian (equation 3-10) permits determination of any one of the variables in terms of the other three. Hence it is possible to present the solution as a trajectory traced by the representative point in a three dimensional phase space. For example the solution is completely defined in ψ, ψ', ϕ - space for $\phi' \gtrless 0$. The procedure for generating an integral manifold was discussed in Chapter 2. Figure 3-8 shows the cross-section of such a limiting surface as affected by the aerodynamic coefficient. The sections of motion envelopes are also included for comparison.

A comment concerning the influence of initial conditions on the nature of the solution and hence on the associated invariant surface would be appropriate here. As before, for $C_H = -1.5$, Figure 3-8 shows regular invariant surface cross-section. However, for the same value of C_H but different initial conditions, Figure 3-9 shows formation of six islands surrounding the main regular region. Further variations in the initial conditions result in complete breakdown of the invariant surface, as shown by ergodic solution, followed by reformation of the second set of islands. Note that, throughout, the librational response of the satellite is bounded and hence stable in accordance with the stated criterion.

Figure 3-10 shows representative sections of limiting invariant surfaces and motion envelopes for a wide

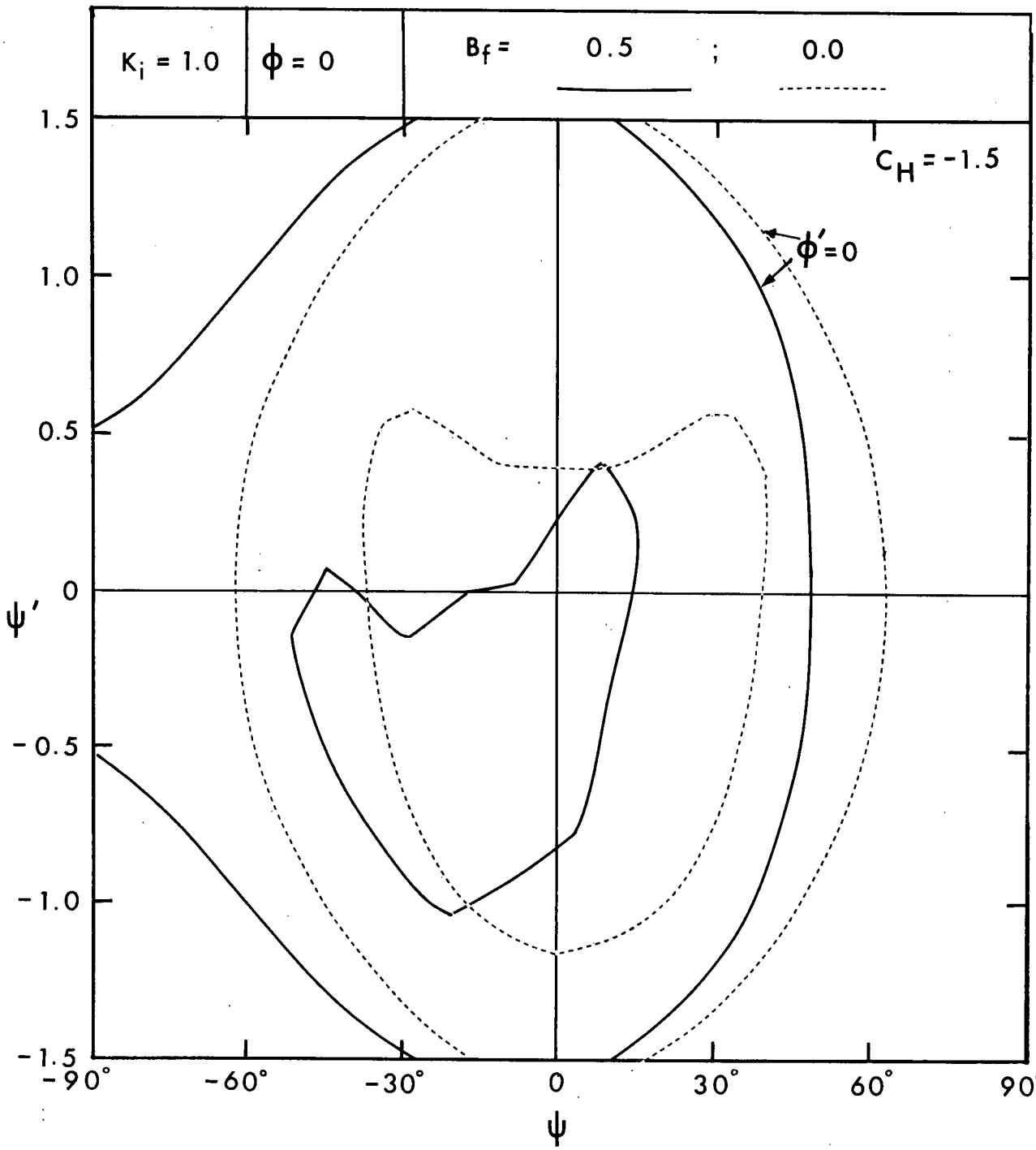

Figure 3-8 Representative cross-sections of motion envelopes and limiting integral manifolds indicating influence of aerodynamic torque

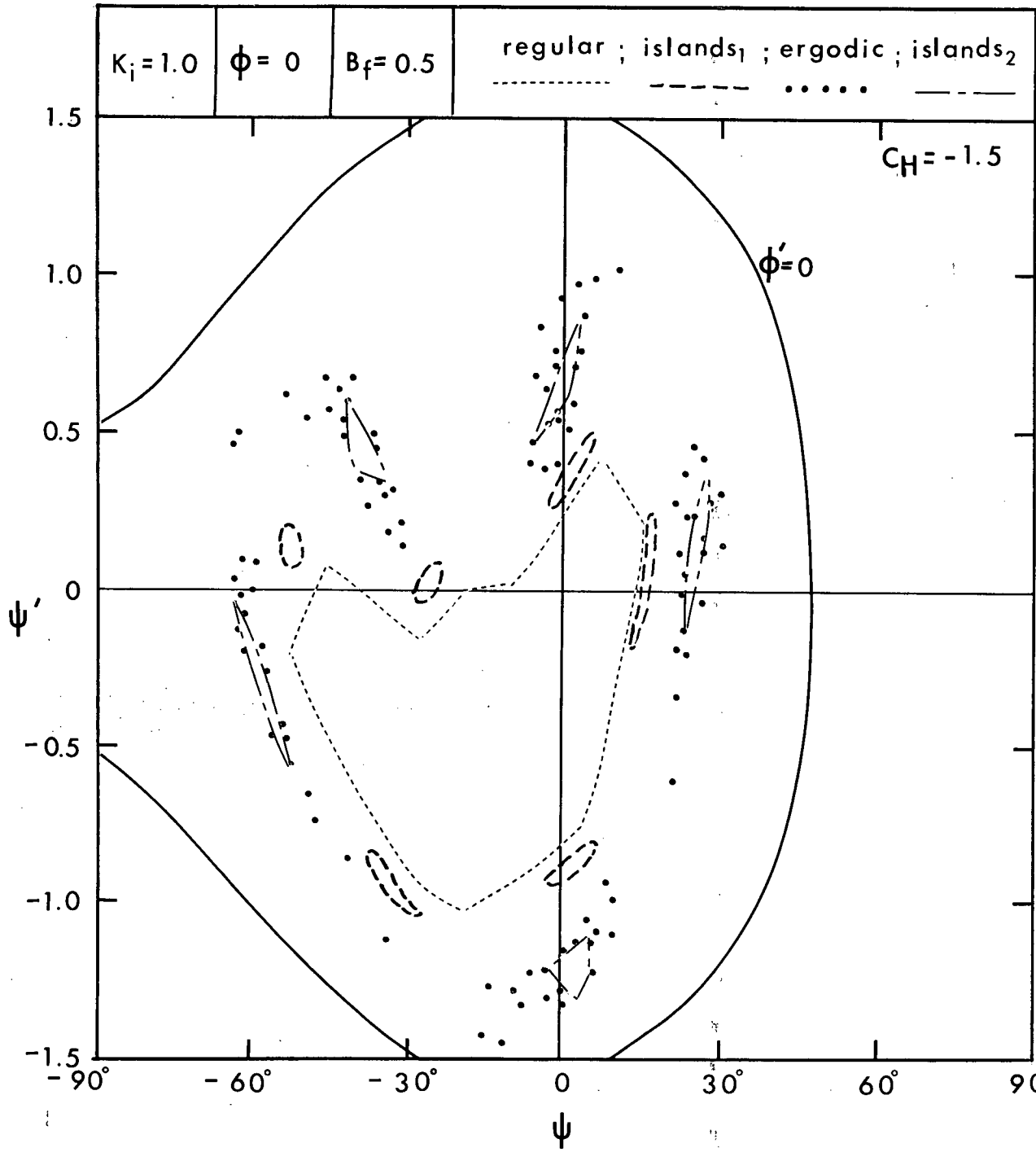

Figure 3-9 The cross-section $\phi=0$ in phase space indicating types of stable solution generated by different initial conditions for given Hamiltonian

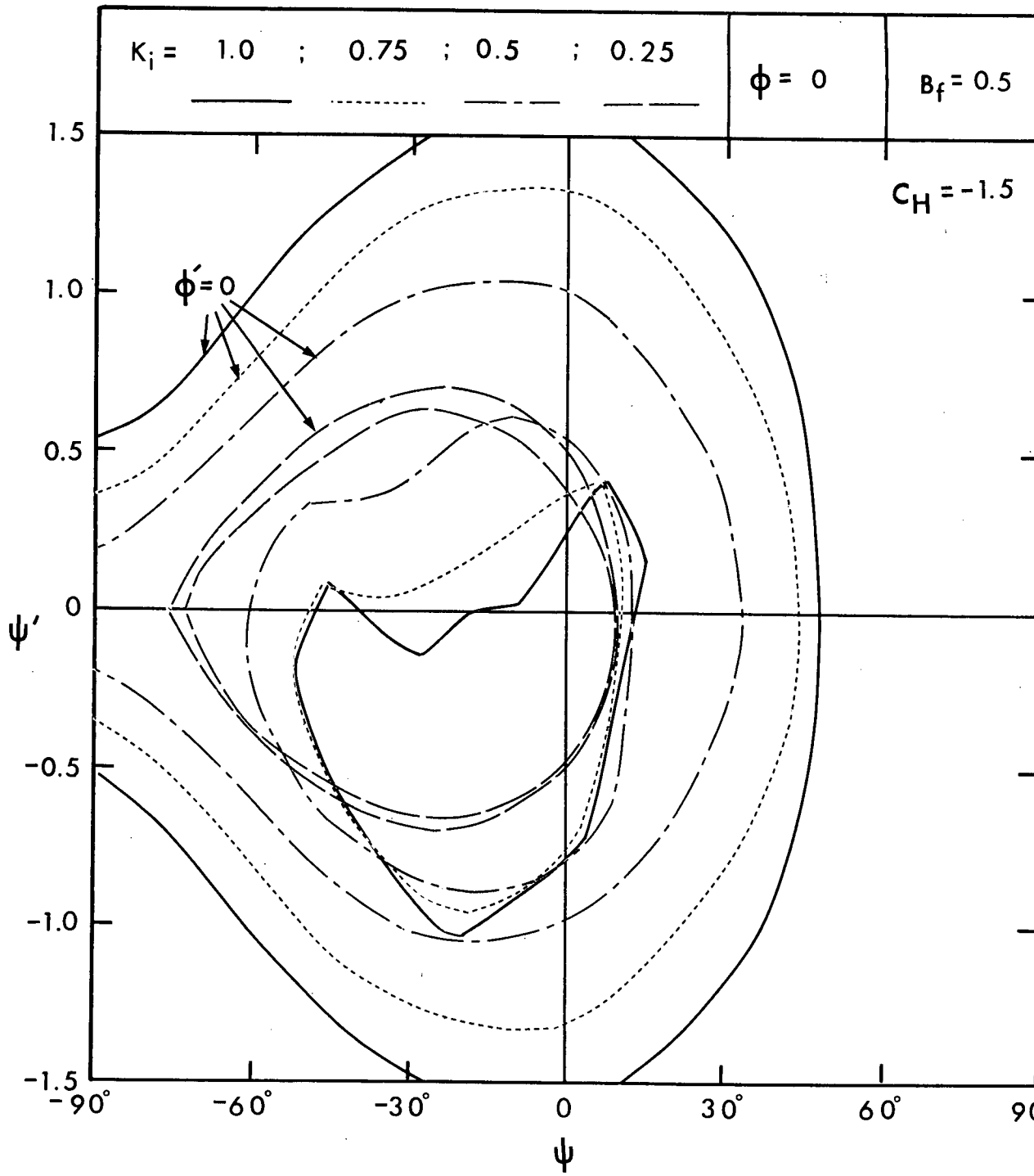

Figure 3-10 Effect of inertia parameter on motion envelope and limiting integral manifolds for given aerodynamic moment and Hamiltonian

range of satellite inertia parameter. The effects of aerodynamic moment and Hamiltonian on limiting integral manifolds themselves are shown in Figures 3-11 and 3-12, respectively. It is apparent that increase in B_f and C_H affect the region of stability adversely.

As explained in Section 2.6, for a given Hamiltonian, the plot of ψ' vs. ϕ' is an ellipse reducing to a circle for $\phi_e=0$. In the region where the stability is assured the solution is bounded over the entire ellipse. However, for $C_H > -1 - B_f(\pi/2-C_1)$ stable motion occurs only over a portion of the constant C_H ellipses. Figure 3-13 shows the influence of inertia parameter and aerodynamic coefficient on the allowable impulse for stability. The symmetry of the plots about $\phi'=0$ axis is retained which helps in reducing rather extensive computations.

3.6 Discussion of Results

In general, response of a satellite depends on its physical properties, aerodynamic moment and disturbances encountered. For the given inertia parameter and disturbance, the amplitude of motion in the orbital plane and sharpness of the peaks in the $+\psi$ direction increases with increasing B_f, however, motion across the orbital plane is relatively unaffected. So far as the effect of inertia is concerned,

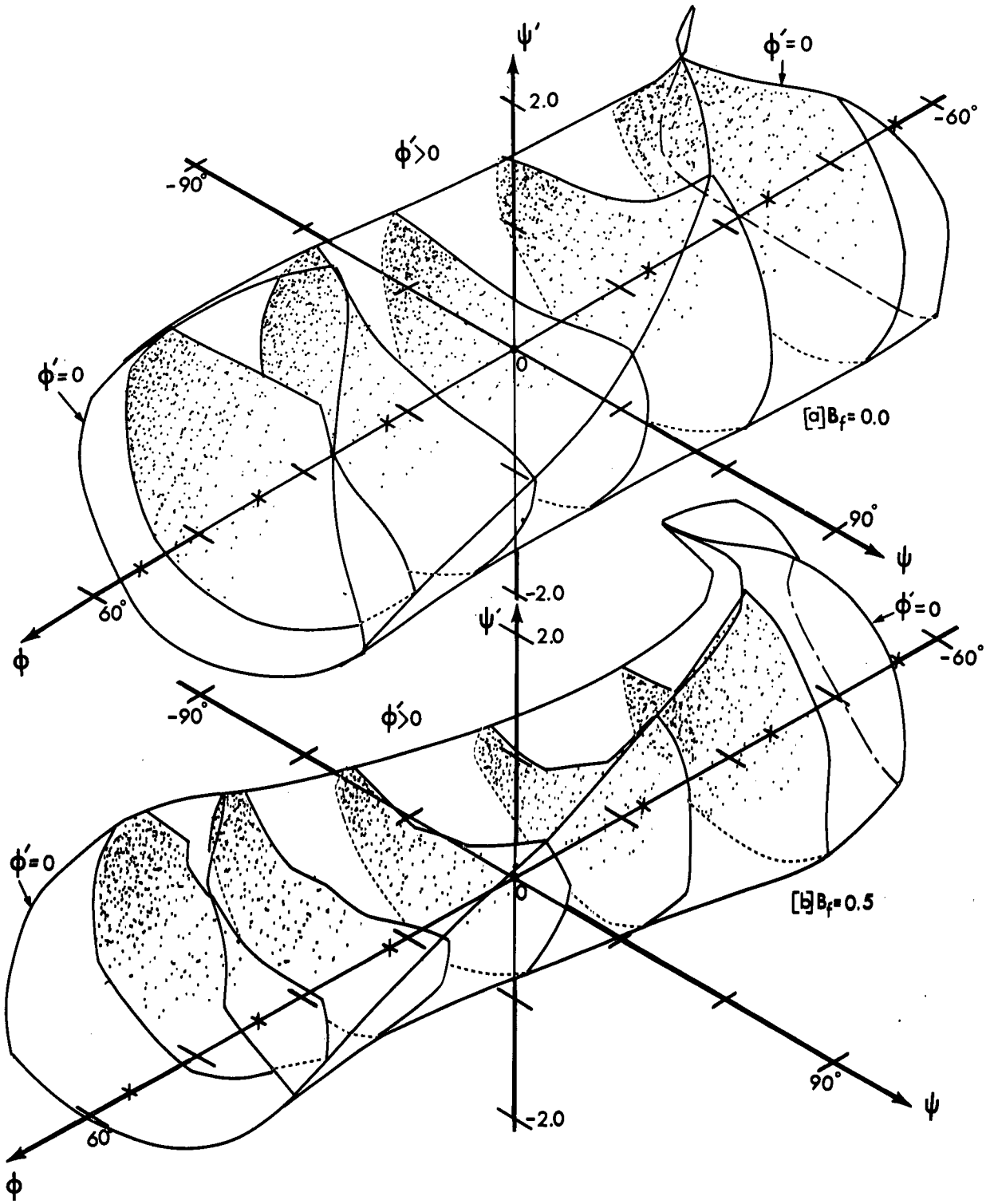

Figure 3-11 Effect of aerodynamic moment on limiting integral manifold; K_i=1.0, C_H=-1.5

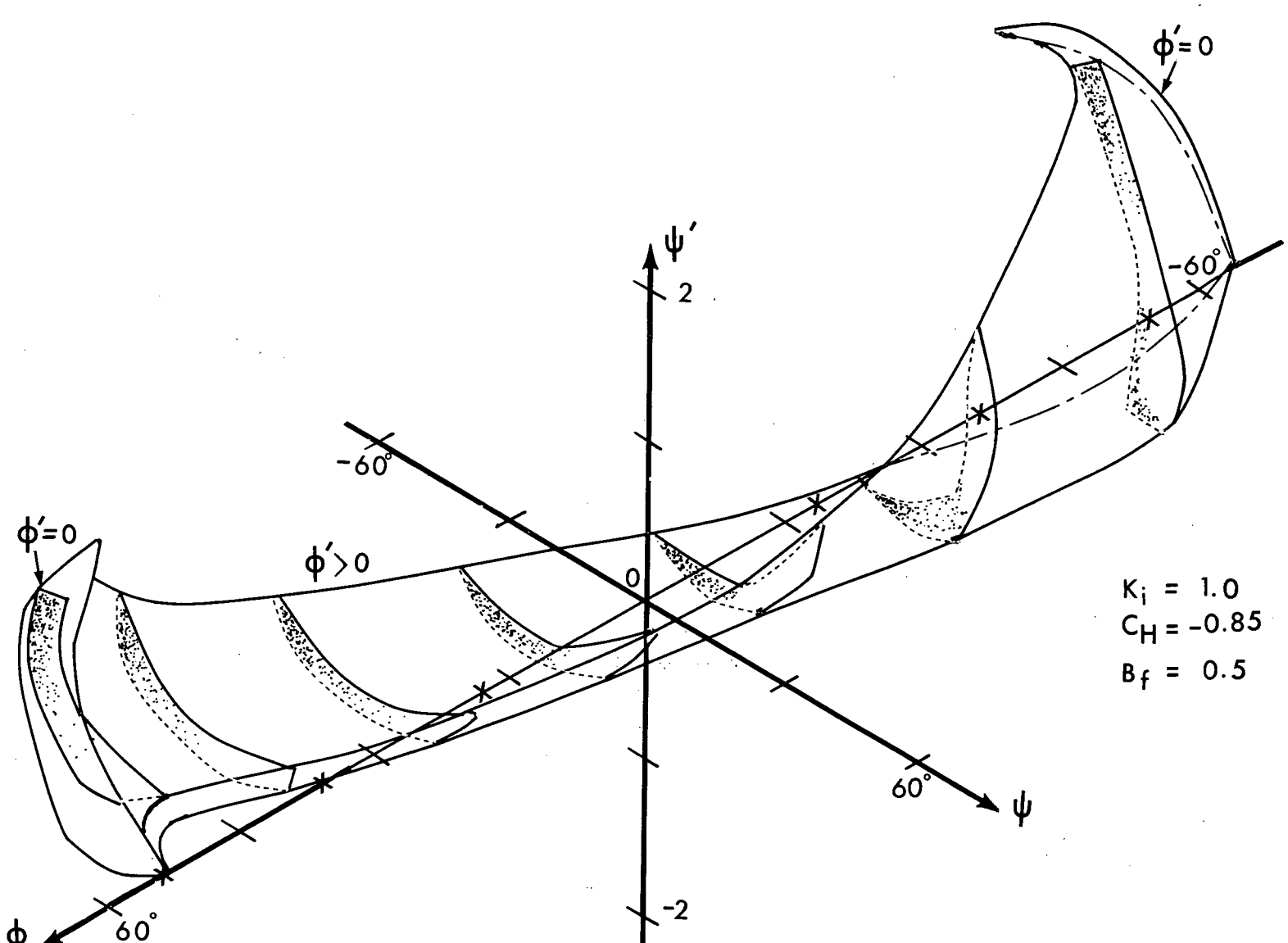

Figure 3-12 Limiting integral manifold for large Hamiltonian

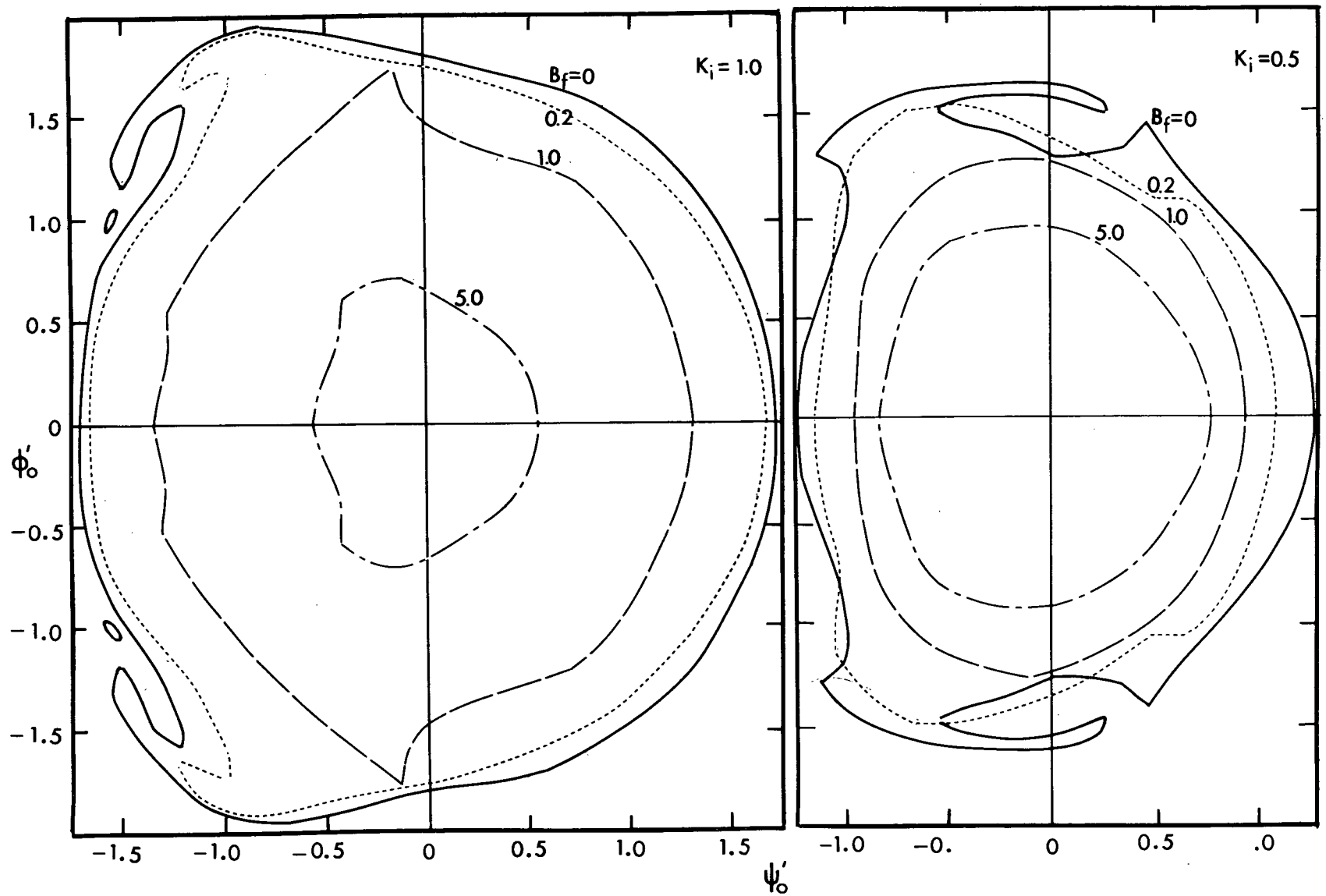

Figure 3-13 Design plots indicating allowable impulsive disturbance at equilibrium positions for stable motion: (a) K_i=1.0, 0.5

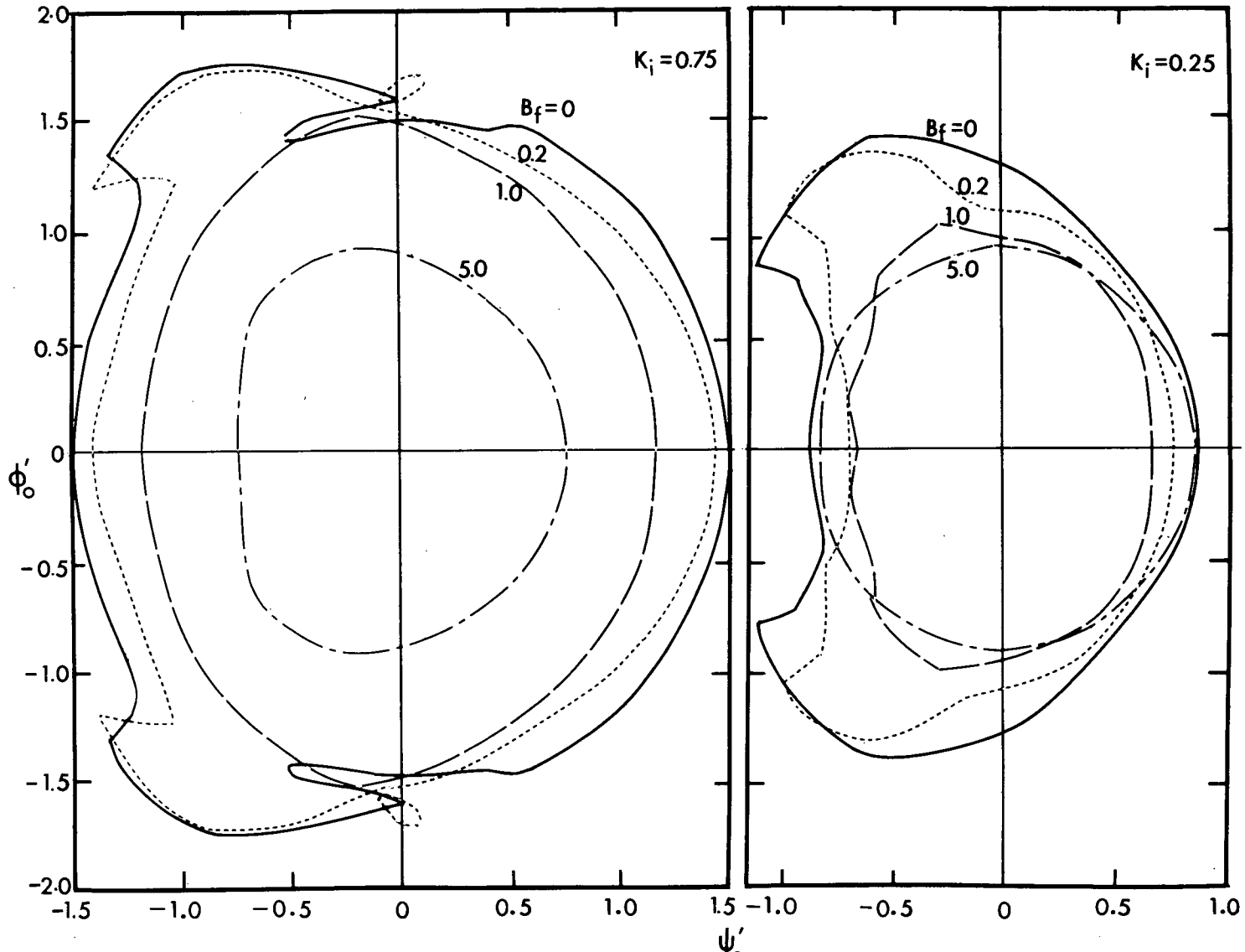

Figure 3-13 Design plots indicating allowable impulsive disturbance at equilibrium positions for stable motion: (b) K_i=0.75, 0.25

decrease in K_i tends to make a satellite more sensitive to a given disturbance and the frequency of response shows marked reduction (Figure 3-6). Figure 3-7(a) shows motion across the orbital plane to be relatively less affected by a transverse disturbance even in presence of an aerodynamic moment. However, a disturbance across the orbital plane excites appreciable in-plane motion, which grows with increasing B_f (Figure 3-7(b)). A larger amplitude, smaller frequency motion is observed in the orbital plane than that across it for an identical disturbance in the two degrees of freedom. The frequencies are of the order of orbital frequency.

As before, the stable solutions of the system may lead to three distinct classes of trajectories in the phase space (Figures 3-8, 3-9) referred to as 'regular', 'island type', or 'ergodic'. However, the aerodynamic moment destroys the symmetry of manifold cross-sections. Although the solution in each case represents stable motion, island and ergodic type of behaviour, being of little use from practical design considerations, lead to substantial reduction in stability.

It is interesting to note that the possibility of ergodicity diminishes with decreasing K_i, as region between integral manifold and motion envelope is reduced (Figure 3-10).

The integral manifolds as well as motion envelopes shrink in size with increasing aerodynamic moment and Hamiltonian. Thus there is a limiting value of C_H, dependent upon

B_f, beyond which stable motion is not possible.

A convenient condensation of the results for design purposes (Figure 3-13) shows bounds of impulsive disturbances at equilibrium position for several different satellites under a set of aerodynamic moments. It is apparent that the presence of B_f, in general, decreases the bound for stable motion, reduction being more pronounced for slender satellites. The satellites with large K_i show better stability characteristics when no or small aerodynamic moment is present. However, for large B_f, shorter satellites (small K_i) are likely to have better performance.

The results presented here are confined only to a few situations. The numerical approach, though informative, tends to be quite expensive. Hence the possibility of using the analog technique, normally preferred for economic, real-time simulation, is explored.

3.7 Analog Simulation

Using trignometric identities the equations of motion (for $|\psi| \leq \pi/2$) can be rewritten as:

$$\psi'' = \left\{2\phi'(\psi'+1)\sin 2\phi - B_f(1+\cos 2\psi + C_1 \sin 2\psi)\right\}/(1 + \cos 2\phi) - 3K_i \sin 2\psi/2$$

$$\phi'' = -\left\{(\psi'+1)^2 + 3K_i(1+\cos 2\psi)/2\right\} \sin 2\phi/2 \qquad \ldots\ldots (3.25)$$

With θ, as the independent variable of the analog computer the equations were programmed by the general method[69]. The trignometric functions of dependent variables were generated explicitly using generalized integration technique, i.e.,

$$d^{n-1}y/dx^{n-1} = \int (d^n y/dx^n)\, dx = \int (d^n y/dx^n)\, x'\, d\theta \quad \ldots\ldots (3.26)$$

Figure 3-14 shows a schematic of the simulation circuit used in conjunction with the analog computer PACE 231-R5. The computer has a reference voltage of ±100 V. Characteristics of the multipliers and the divider suggested the need for suitable amplitude scaling. The relatively large values of ϕ often made the output of the divider grow rapidly. However, it can be shown that, in general, for $|\phi| > 75°$ the satellites become unstable in ψ. Using known maximum values of the variables, the scaling factors K, K_1 and α were adjusted (e.g., $K = K_1 = 25$, $\alpha = 0.25$) to arrive at a balanced, well-scaled circuit.

The simulation was about 1000 times faster than the actual system (1 second $\equiv$ 1 radian). Further improvement in the speed can be accomplished by suitably adjusting the integrators' gains. However, any attempt at speeding-up the process beyond a factor of 5,000 showed results to be unstable through accumulated error.

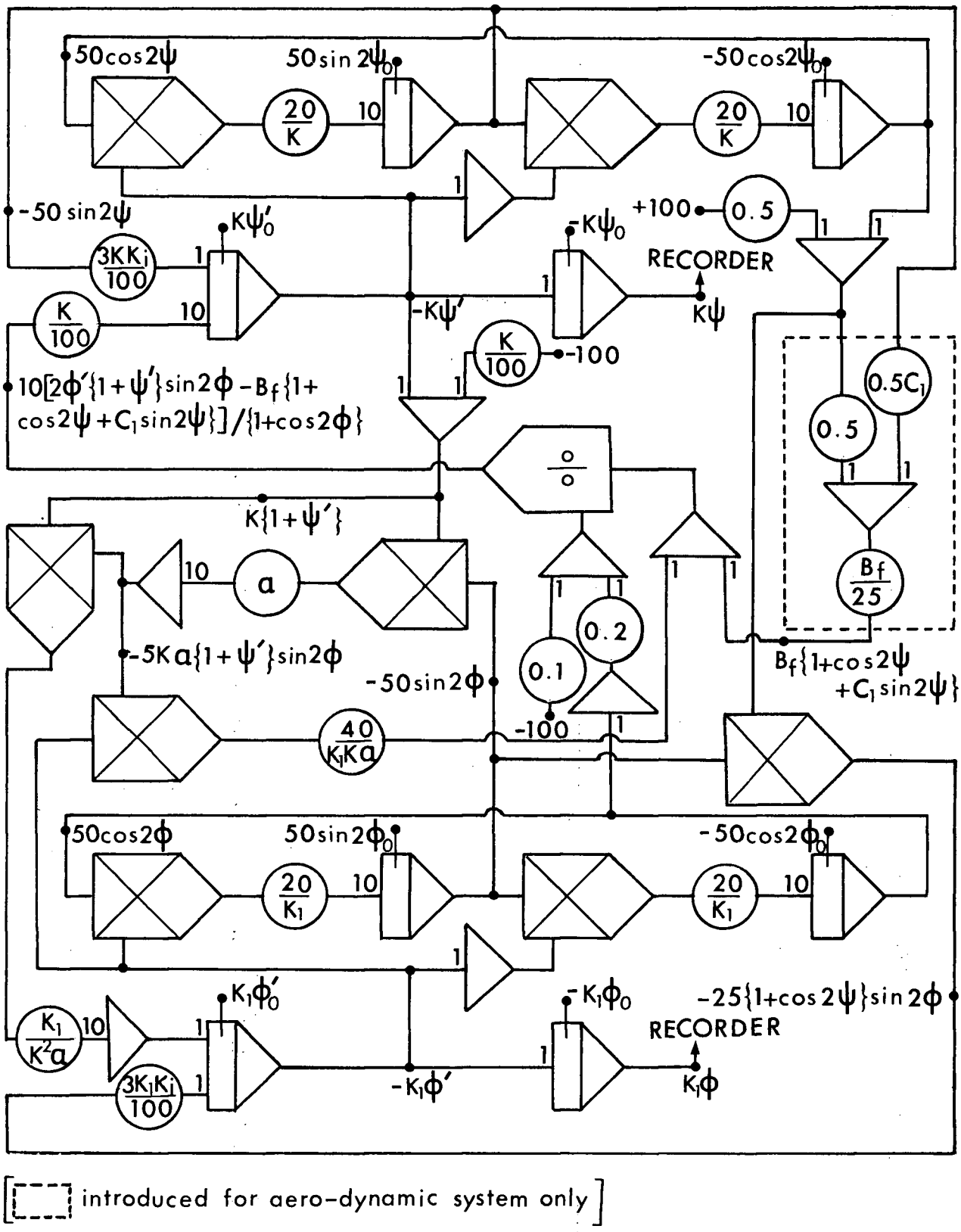

Figure 3-14 Analog simulation circuit using θ as the independent variable

Any combination of disturbances can be provided by setting the initial conditions of the integrators, as indicated. The inertia parameter K_i and aerodynamic coefficient B_f can be varied by changing the corresponding potentiometer setting. In absence of an atmosphere the same circuit may be used by disconnecting the dotted block in Figure 3-14.

3.7.1 Accuracy of Simulation

The librational response of a wide range of satellites under a variety of atmospheric conditions and disturbances was examined by systematically varying the inertia parameter, aerodynamic coefficient and initial conditions. The planar as well as the out of plane librations were recorded as a function of the satellite's orbital position on a x-t plotter.

In all cases studied, the results agreed well with numerical solution. Figure 3-15 shows a typical plot of satellite's response to impulsive disturbance as a function of inertia parameter and aerodynamic coefficient.

The analysis confirms the earlier findings and suggests the suitability of the simulation for quantitative investigation.

To establish the accuracy of the method for stability studies the analog solutions were compared with the digital results. Plots of allowable impulsive disturbances, at equilibrium position, for non-tumbling motion were found

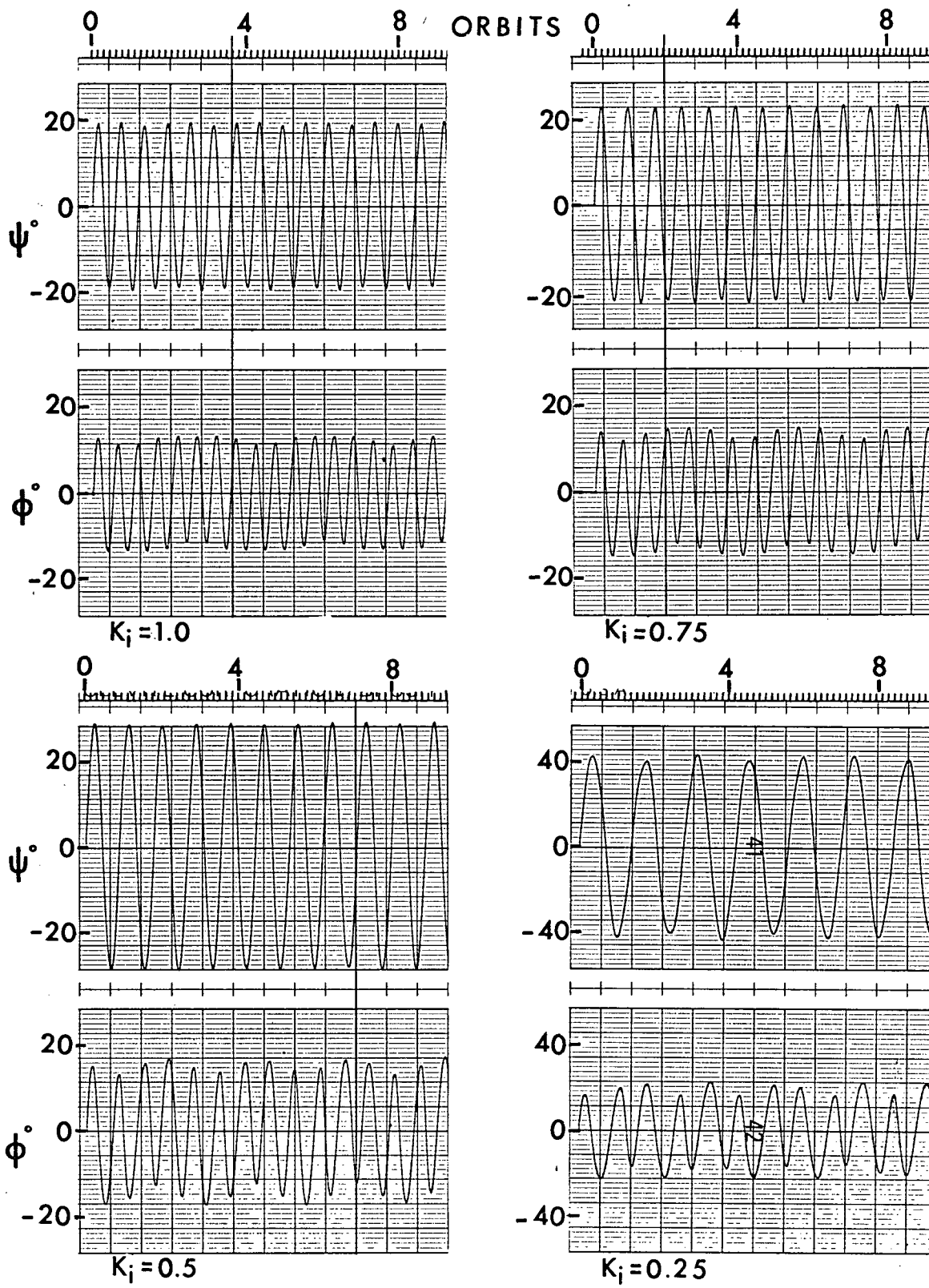

Figure 3-15 Representative response plots obtained using analog simpulation; $\psi_o = \phi_o = 0$, $\psi'_o = \phi'_o = 0.5$: (a) in absence of aerodynamic torque

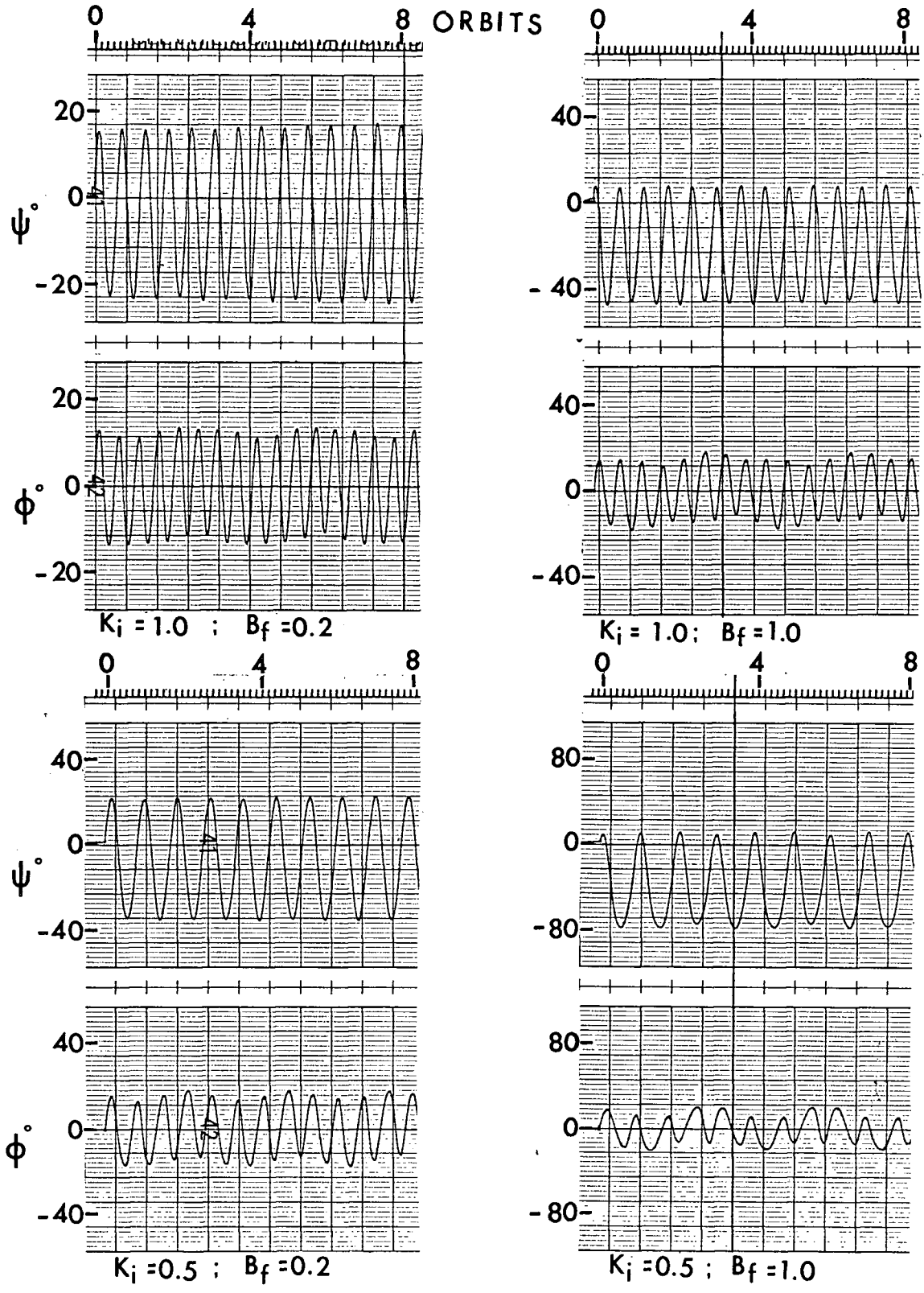

Figure 3-15 Representative response plots obtained using analog simulation; $\psi_o=\phi_o=0$, $\psi'_o=\phi'_o=0.5$: (b) in presence of aerodynamic torque

for several combinations of K_i and B_f. Due to absence of any inherent logic and memory in the analog computer, point by point checking was necessary for generating these plots. Their symmetry about ϕ_o' axis, however, helped in reducing the effort considerably. The impulsive disturbance at equilibrium position was varied systematically and the satellite response was observed over 50 orbits. The computer has a safety characteristic of going into hold mode in case of overload. This feature may be utilized to serve as a logic unit. The outputs ψ and ϕ were scaled in such a manner as to overload the computer as soon as tumbling occurred. The feature also proved useful in limiting the integration to 50 orbits.

Figure 3-16 compares, for several representative situations, the digital and analog simulation results. In general, the agreement appears to be acceptable except for minor discrepancies in the vicinity of "spikes" and "islands." Fortunately, this does not appear to be critical as their proximity to the stability bound would, in any case, be considered unsuitable for satellite operation.

In spite of the inherent limitations of an analog computer, the simulation presented here is economical and sufficiently accurate for quantitative analysis. Its usefulness in satellite design and real time studies could be enhanced considerably through hybridization with the digital computer to take advantage of latter's memory and logic.

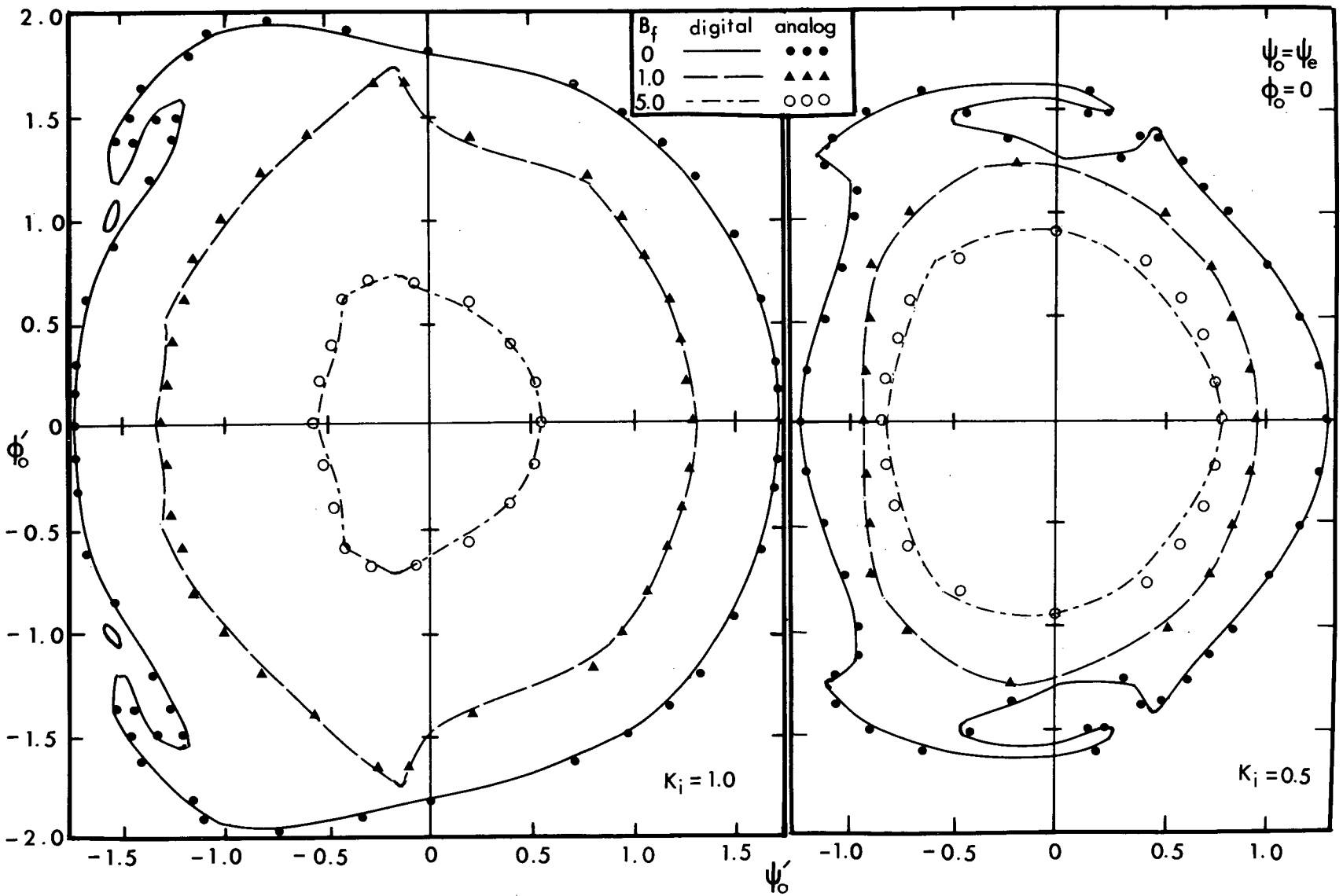

Figure 3-16 Allowable impulsive disturbances at equilibrium positions for stable motion - a comparison between numerical and analog results

3.8 Concluding Remarks

The important aspects of the investigation and relevant conclusions may be summarized as follows:

(i) The analysis presented here, involving several simplifying but realistic assumptions, can be applied readily to actual systems with sufficient accuracy. It gives a complete picture concerning response and stability of satellites under the influence of aerodynamic moment, which cannot be ignored for near earth operation.

(ii) The local vertical is no longer the equilibrium position in the presence of an aerodynamic moment. The stable equilibrium orientations, found using infinitesimal technique as well as Liapunov's direct method, and bounds of librations obtained through the Hamiltonian of the system, are strongly affected by inertia characteristics and aerodynamic moments.

(iii) The amplitude of motion, especially in the orbital plane, increases considerably with increasing B_f. The effect of disturbance to transverse motion is more pronounced for the generalized co-ordinate in the plane of the orbit.

(iv) The system exhibits three, distinctly different, stable trajectories: regular, islands, and ergodic. However, from practical considerations,

only the regular solution provides bounds for stable motion.

(v) The reduction in size of integral manifolds with increasing B_f and C_H suggests a critical value of Hamiltonian for stable motion.

(vi) Plots of allowable impulsive disturbances, which a satellite at equilibrium can sustain without tumbling, show satellites with large inertia to be relatively more stable at higher altitudes (small B_f). However, shorter satellites exhibit better stability characteristics in the presence of a large aerodynamic moment.

(vii) The analog real-time simulation of the problem gives results of sufficient accuracy. The discrepancies with digital results are confined to the regions which are of little importance from design considerations.

The analysis and results presented here should prove useful in stability and design considerations of near-earth satellites.

4. REGULAR STABILITY AND PERIODIC SOLUTIONS

4.1 Preliminary Remarks

For the axi-symmetric satellites executing coupled librations in circular orbit, it was found that the stable conditions may not, in all cases, lead to a well defined 'regular' surface in phase space. In the region of guaranteed stability, as indicated by closed zero-velocity curves, it was also possible to obtain, a chain of 'islands' or 'ergodic' solutions in the transition region. The same behaviour persisted in the presence of aerodynamic torque. The study of the librational motion, governed by the nonlinear, coupled, autonomous equation (3.8) suggested that the largest regular surface represents the only usable stable region from design considerations.

Modi and Brereton[8,9] studied periodic solutions associated with the planar gravity oriented systems. They emphasized the importance of the solutions by pointing out the fact that, at the largest eccentricity for stability, the only possible motion is a periodic one. A significant relationship between integral manifold and periodic solution becomes apparent. A succession of initial conditions may be chosen to determine progressively smaller manifolds, which degenerate, in the limit, to a line. Because of the periodic nature of the invariant surface, this line must, then, rep-

resent a periodic solution. Hence the periodic trajectories must act as spines around which the manifolds are built.

Modi and Neilson[17] extended the concept to an axi-symmetric spinning satellite librating in presence of gravity gradient torques. Initial conditions for periodic solutions were presented over a range of system parameters for motion in circular and elliptic orbits. Variational stability of periodic solution was examined using extension of Floquet's criterion[70] to the fourth order system.

The coupled librational motion of an axi-symmetric satellite in the presence of aerodynamic torque is investigated here with particular emphasis on the bound between regular and ergodic type of stability. Transition of the periodic solution P_{21}, associated with the regular stability region, to P_{45} and P_{23}, corresponding to the chains of islands, is studied through cross sections of the integral manifolds with a systematic variation of disturbances. Initial conditions for regular, stable, periodic motion are obtained over a range of inertia and aerodynamic parameters and the limiting stability conditions are established, precisely, using the Floquet analysis. Representative response data are also included to show the variation of the associated period. Finally, a set of design plots, indicating region of regular stability as a function of system parameters, are presented.

4.2 Analysis

As pointed out before (Sections 2.5 and 3.5), the constant Hamiltonian (equations 2.7 and 3.10) makes it possible to represent the stable motion concisely by an integral manifold in ψ,ψ',ϕ- space. Consider, for example, its cross-section at $\phi=0$ revealing three distinct classes of stable solutions (Figure 4-1). It is apparent that the most predominant of these is the well defined, nested, regular solution. Its degeneration to a point, achieved through appropriate choice of initial conditions, would represent a periodic solution P_{21}, which acts as a spine of the manifold.

On the other hand, an alternate set of disturbance, though lying within the region of guaranteed stability as suggested by the closed motion envelopes, may give rise to a chain of five 'islands' surrounding the limiting regular region. In the three dimensional phase-space they would appear as a helical tubular surface around the largest regular manifold. Its degeneration to a helix obviously represents another periodic solution P_{45}.

The third type of stable solution, represented by apparently 'ergodic' character of the trajectory filling the transition zone between the regular stability region and islands, may also involve periodicity over a large number of orbits.

Subjecting the system to further variation in the external disturbances may result in the formation of new islands, corresponding to a different periodic solution

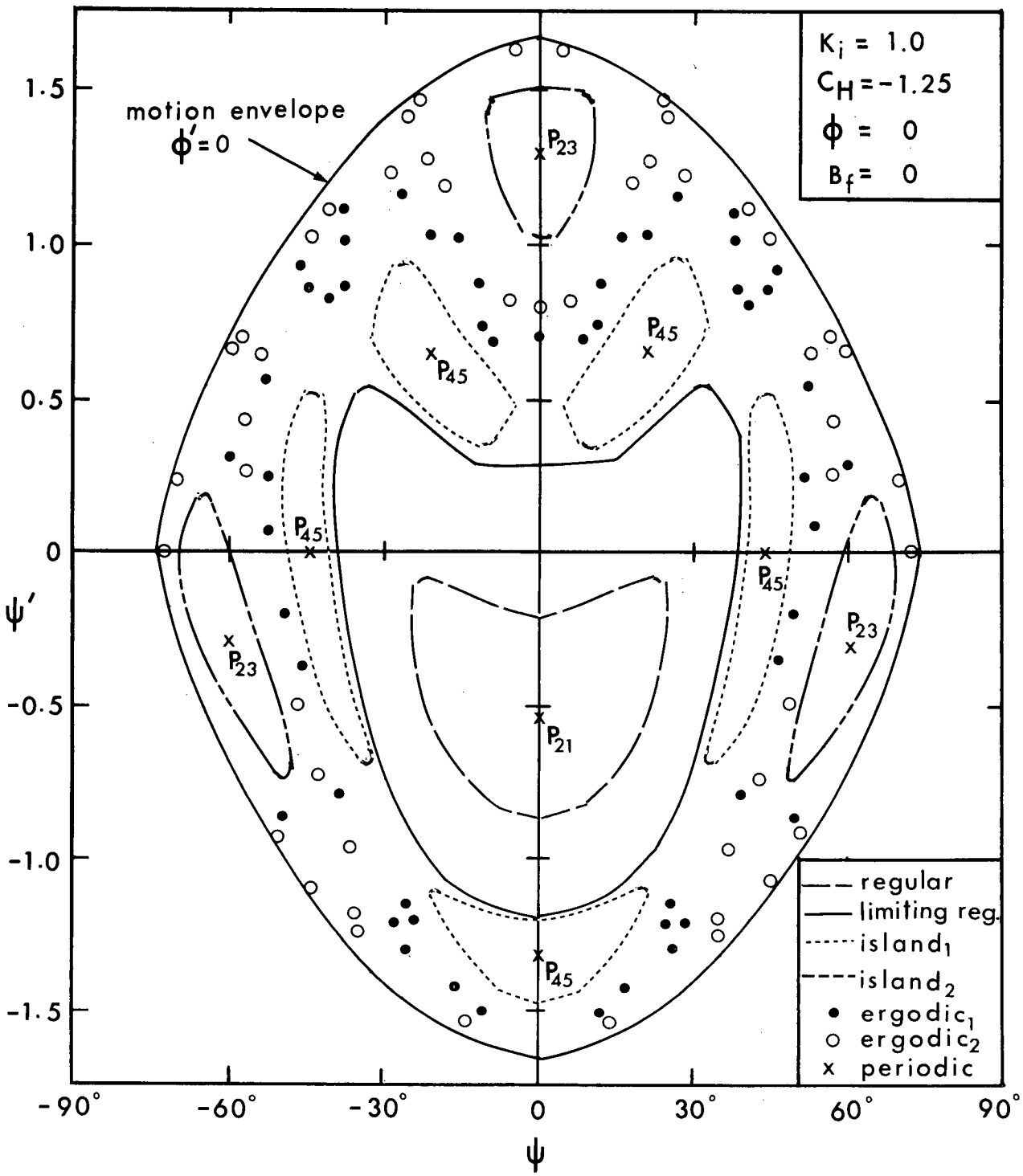

Figure 4-1 Stroboscopic phase plane at ϕ=0 indicating types of stable solutions generated by various initial conditions at given Hamiltonian: (a) in absence of aerodynamic torque

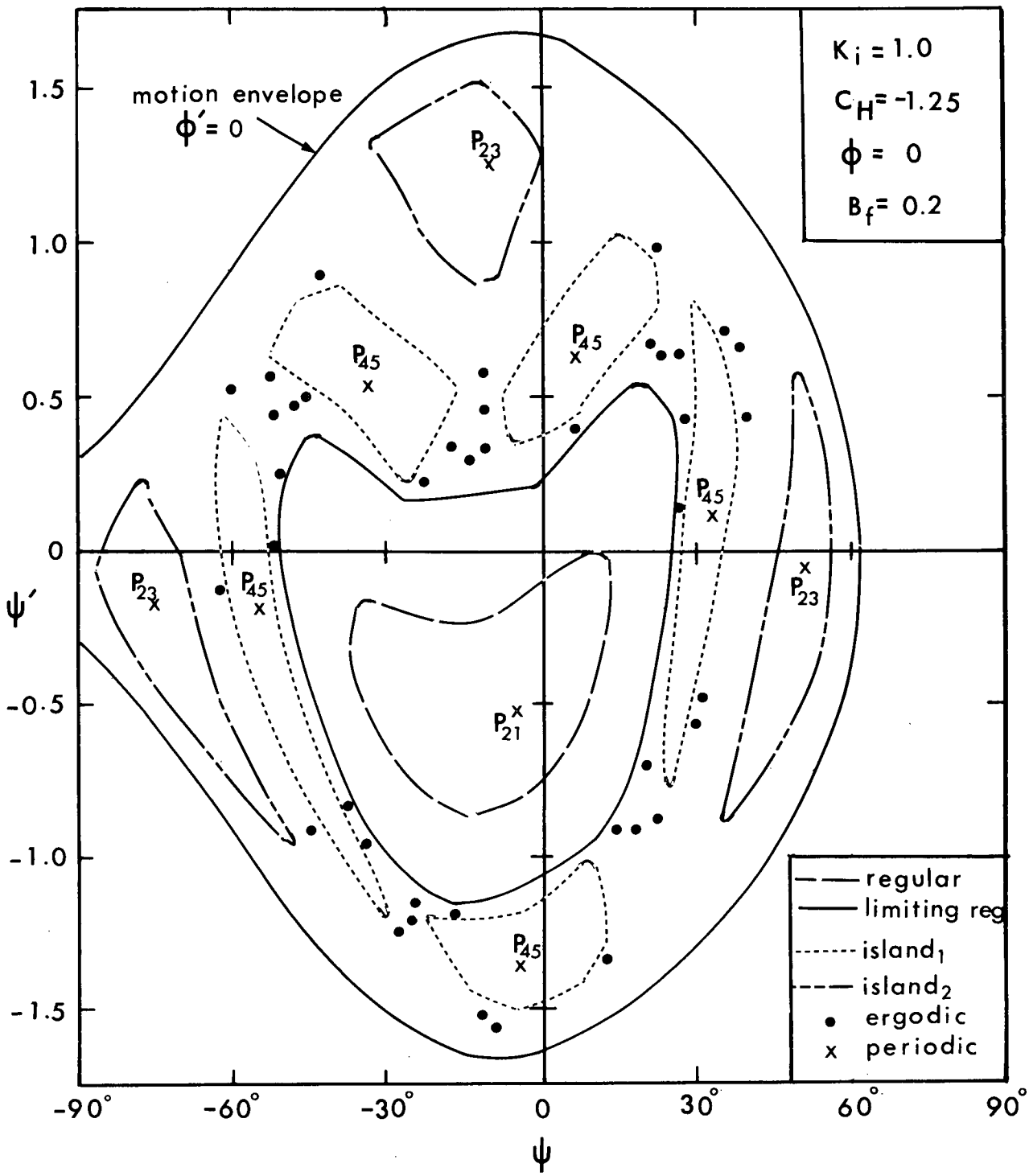

Figure 4-1 Stroboscopic phase plane at ϕ=0 indicating types of stable solutions generated by various initial conditions at given Hamiltonian: (b) in presence of aerodynamic torque

(e.g., P_{23}). This process of formation of islands and their degeneration is limited only by the approach of the motion envelope.

Although stable, proximity of islands to the motion envelope and the irregular nature of the ergodic solutions render them of questionable value. Thus, the limiting regular region remains the only practically usable stability bound. Rest of the discussion is, therefore, confined to this region.

4.2.1 Limiting Stability and Periodic Solutions

The determination of regular integral manifold was accomplished numerically. In general, the equation (3.8) was integrated over 40-50 orbits for a few representative disturbances within the motion envelope. For the case of regular stability this leads to a well defined cross-section in the stroboscopic phase plane at $\phi=0$. The limiting region of stability was established by choosing a condition corresponding to the mid-point of the smallest intercept on $\psi=\psi_e$ between the regular and other trajectories. The process was repeated until the intercept approached zero. Usually 4-5 iterations were found to be sufficient.

So far as the periodic solution associated with the regular region is concerned, it was necessary to establish its degeneration to a point. This was accomplished by selecting, successively, initial conditions corresponding to

the mid-point of the intercept by the regular region on $\psi=\psi_e$. This variable secant iteration process converged quite rapidly, leading to the desired periodic solution in 2-3 cycles.

The same technique can be applied to determine the limiting stability for island type trajectories and associated periodic solution. The period of the solutions was established through response analysis (Figure 4-2).

4.2.2 Variational Stability of Periodic Solutions

As periodic solutions play an important role in the librational dynamics of a satellite, it was thought appropriate to explore the conditions for their stability. However, it should be emphasized that, although the cross-sectioning concept is relatively simple and yields considerable insight into the nature of the motion in the large, the numerical character of this approach involves a substantial amount of computer time. This is particularly true for a precise determination of the critical disturbance beyond which even the periodic solutions show instability (i.e., the integral manifolds cease to exist). A need for variational stability analysis of periodic solutions is, therefore, quite apparent.

Substituting $\psi=\psi_p+\psi_v, \phi=\phi_p+\phi_v$ in equation (3.8) and linearizing with respect to ψ_v and ϕ_v yields:

$$\begin{aligned} \psi_v'' &= A_1\psi_v' + A_2\phi_v' + A_3\psi_v + A_4\phi_v \\ \phi_v'' &= B_1\psi_v' + B_2\phi_v' + B_3\psi_v + B_4\phi_v \end{aligned} \qquad \ldots\ldots (4.1)$$

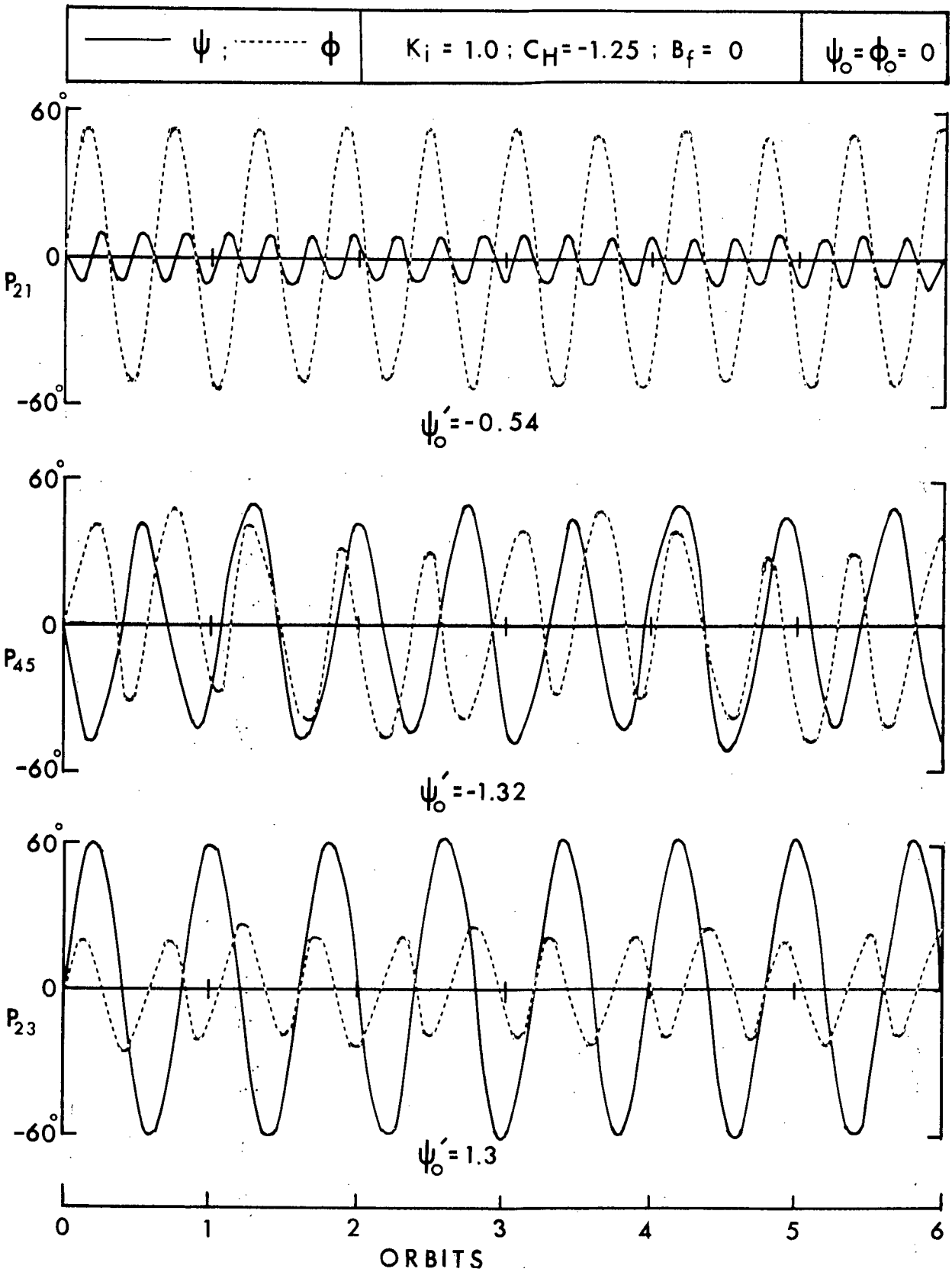

Figure 4-2 Periodic response: (a) in absence of aerodynamic torque

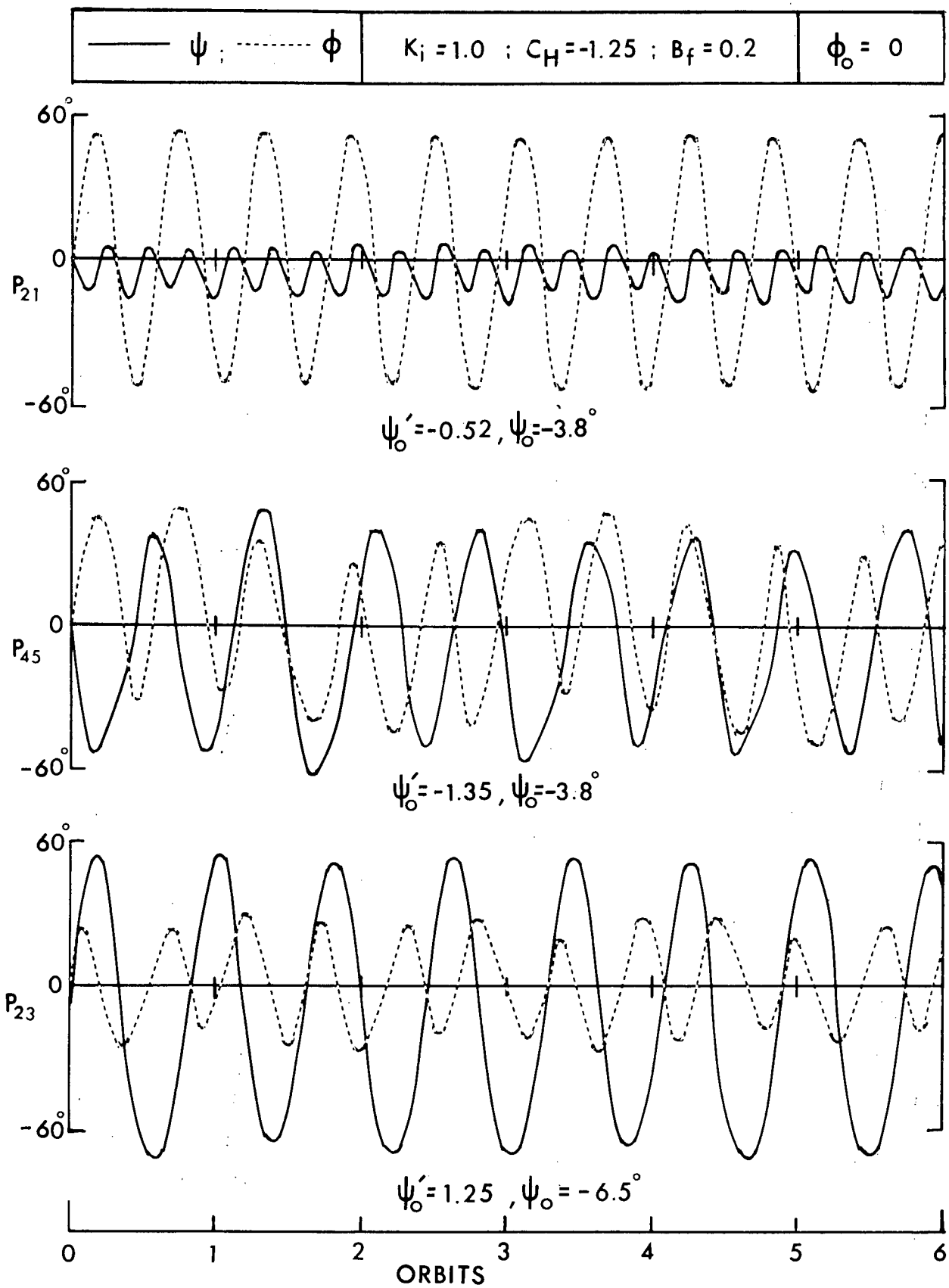

Figure 4-2 Periodic response: (b) in presence of aerodynamic torque

where

$$A_1 = 2\phi_p' \tan \phi_p$$

$$A_2 = 2(\psi_p' + 1) \tan \phi_p$$

$$A_3 = -3K_i \cos 2\psi_p + B_f (\sin 2\psi_p - C_1 \cos 2\psi_p)/\cos^2\phi_p$$

$$A_4 = [2\phi_p'(\psi_p' + 1) - B_f \tan \phi_p (1 + \cos 2\psi_p + C_1 \sin 2\psi_p)]/\cos^2\phi_p$$

$$B_1 = -(\psi_p' + 1) \sin 2\phi_p$$

$$B_2 = 0$$

$$B_3 = 3K_i \sin 2\psi_p \sin 2\phi_p/2$$

$$B_4 = -[(\psi_p' + 1)^2 + 3K_i \cos^2\psi_p] \cos 2\phi_p$$

This fourth order linear system has periodically varying coefficients of a common period, say T_p. Thus, Floquet theory is applicable. The stability criterion can be expressed as:

$$|\lambda_i| \begin{cases} \leqslant 1, & i = 1,2,3,4; \text{ stable} \\ > 1, & i = 1,2,3,4; \text{ unstable} \end{cases} \quad \ldots (4.2)$$

The system being autonomous, one of the characteristic multipliers is unity as the derivative of the periodic solution satisfies the variational equation. Existence of constant Hamiltonian, a first integral of motion, makes another multiplier unity. For the system having these properties along with the invariant nature of phase space representation, it can be shown that $\pi\lambda_i = 1$. If $\lambda_1 = \lambda_2 = 1$, then $\lambda_3\lambda_4 = 1$.

Hence the two free exponents λ_3 and λ_4, which determine the stability of the solution, must lie on the unit circle or the real axis in the complex plane. Thus the stability criterion becomes

$$\sum_{i=1}^{4} \lambda_i \begin{cases} >4 \text{ or } <0 \; ; & \text{unstable} \\ \leqslant 4 \text{ or } \geqslant 0 \; ; & \text{stable} \end{cases} \qquad \ldots .(4.3)$$

A final condition matrix $\Theta(T_p)$ is computed from $\Theta(0)$ equal to identity matrix. As $Tr[\Theta(T_p)] = \sum_{i=1}^{4} \lambda_i$, the stability of the periodic solution is determined by

$$\left| Tr[\Theta(T_p)] - 2 \right| \begin{cases} > 2 \; ; & \text{unstable} \\ \leqslant 2 \; ; & \text{stable} \end{cases} \qquad \ldots .(4.4)$$

4.3 Discussion of Results

The closed motion envelope in Figure 4-1(a) guarantees a non-tumbling motion leading to three distinctly different characters of phase-space representations regular, ergodic and island type each associated with a periodic solution. The presence of aerodynamic moment destroys the symmetry of the motion envelope as well as the integral manifold cross-section at $\phi=0$ (Figure 4-1(b)). Both the regular and island type stability regions are distorted even for small B_f. This makes the determination of stability bound as well as the periodic solutions somewhat difficult.

Figure 4-2 shows the periodic response plotted over six orbits during which at least two cycles are completed.

In absence of aerodynamic torque the fundamental periodic solution associated with the regular region executes two planar oscillations for one transverse cycle. On the other hand, island stability regions are associated with the periodic solutions P_{45} and P_{23} (Figure 4-2(a)). Although the presence of atmosphere shifts the response towards the $-\psi$ direction the basic characteristics, indicated above, remain essentially unaffected (Figure 4-2(b)). In all the cases investigated, the smaller frequency response was associated with larger amplitudes.

The determination of a complete set of periodic solutions would involve a careful scanning of the region of possible motion. However, the invariant nature of the integral manifold and predominance of the fundamental periodic solution render it sufficient, from the point of view of usefulness, to give only a set of initial conditions generating P_{21}.

Figure 4-3 shows the effects of satellite inertia and aerodynamic torque on the impulsive disturbances to excite a stable, fundamental periodic motion. The limits of their stability, as obtained from the Floquet theory, are also indicated. Besides being symmetrical about $\phi'=0$, the plots suggest relatively larger demand on transverse disturbance. In all cases P_{21} requires a negative planar impulse $-\psi_o'$, the magnitude of which reduces, in general, with increasing B_f and K_i. For comparison, generating conditions corresponding

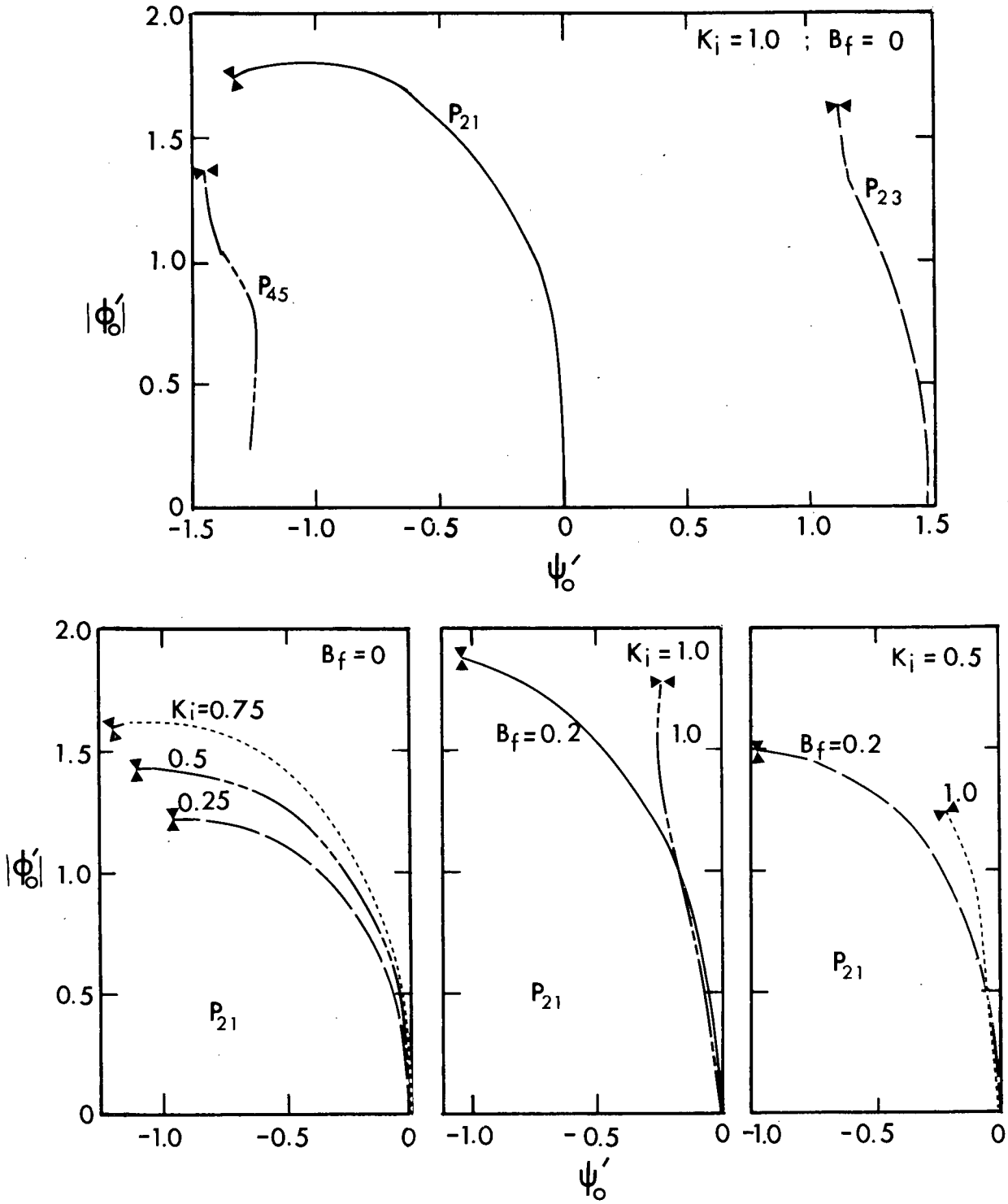

Figure 4-3 Effect of inertia and atmosphere on the impulsive disturbances for stable periodic motion; $\psi_o = \psi_e$, $\phi_e = 0$

to some of the other periodic solutions are also included for the particular case of a dumbbell satellite operating in absence of atmosphere. Relatively (compared to that for P_{21}) large positive planar impulses excite P_{23} while the large negative ones lead to P_{45}.

The system, being dependent upon a number of variables, would involve an enormous amount of computation for any comprehensive analysis. Furthermore, massive information so generated has to be presented in a concise form for ease of application. One way would be to represent an integral manifold by its intercept, with a convenient axis, as a measure of stability. The variation of ψ' intercept with the limiting regular manifold as a function of Hamiltonian is shown in Figure 4-4. The fundamental periodic solutions and the critical conditions for their stability are also indicated. The plots clearly emphasize the influence of satellite inertia and aerodynamic moment. It may be observed that appreciable reduction in stability would result for satellites with smaller K_i, particularly in the presence of an atmosphere. The spinal character of the periodic solutions is quite apparent. The plot indicates that, at critical Hamiltonian ($C_{H_{cr}}$) for stable motion, the only available solution is a periodic one.

In conjunction with the earlier results concerning the limiting motion envelope, equation (3.22), the plots provide better insight into the nature of the solutions as affected by the Hamiltonian.

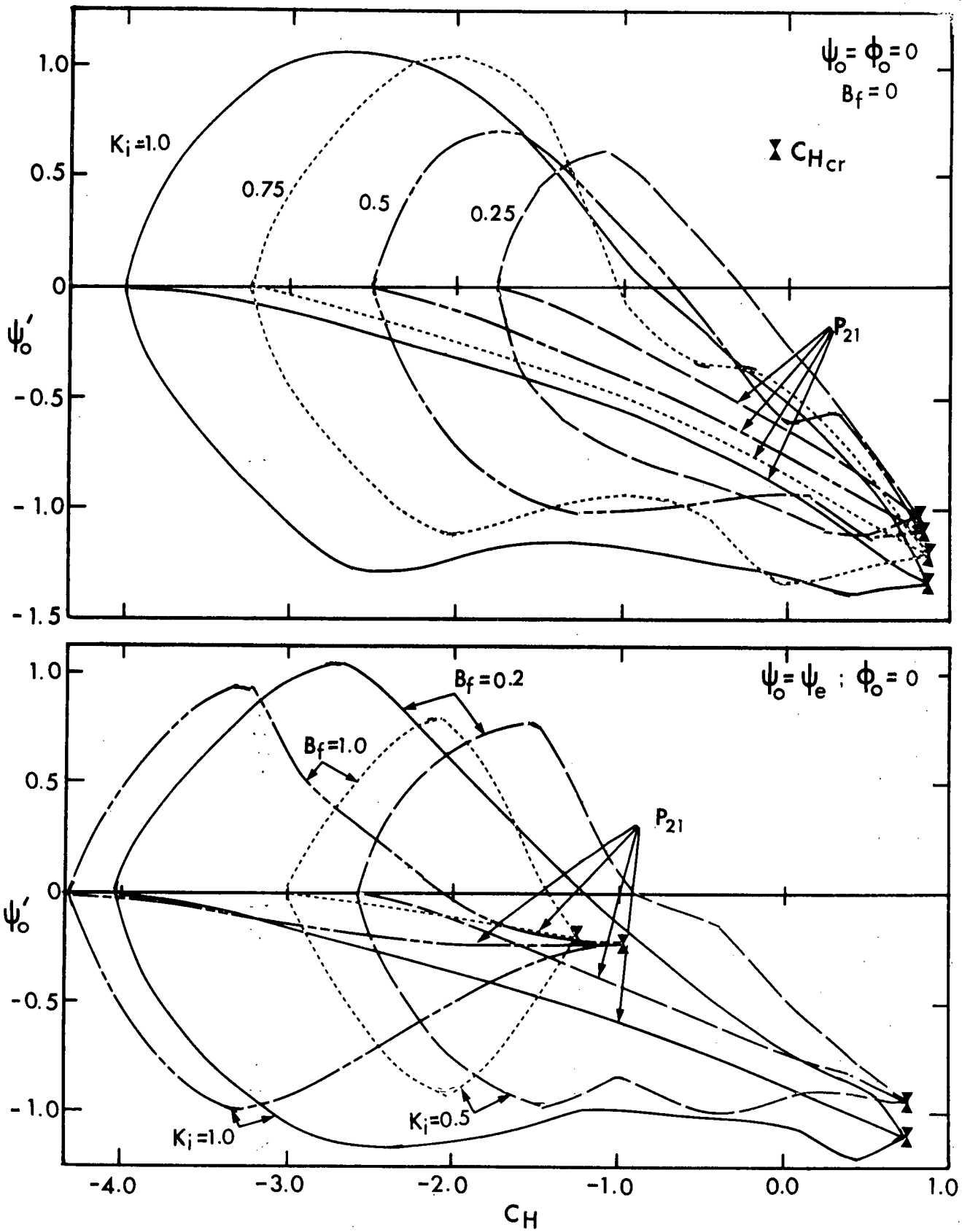

Figure 4-4 Effect of system parameters on the region of regular stability and fundamental periodic solution P_{21}

For small values of C_H the system behaviour is regular. This continues until C_{H_R}, representing the bound beyond which the island type and ergodic solutions also appear, is attained. As the condition for guaranteed bounded motion (3.22) is approached, the trajectories show increasing tendency towards non-regular behaviour, particularly for positive planar impulses. For larger values of Hamiltonian, however, the stable solutions appear, only as regular trajectories. At $C_{H_{cr}}$ the manifolds cease to exist, leaving the fundamental periodic solution to be the only stable condition. The following table shows the impulsive disturbances at equilibrium configuration required to excite P_{21} at $C_{H_{cr}}$, determined using Floquet's variational analysis. The corresponding librational period $T_{P_{cr}}$ is shown as a fraction of orbital period. From the consideration of practical application, the values C_{H_R} are also included, which emphasize the reduced stability condition.

Table 4-1 Critical conditions as affected by satellite inertia and aerodynamic torque

K_i	B_f	C_{H_R}	$C_{H_{cr}}$	$\psi'_{o_{cr}}$	$T_{P_{cr}}$
1.0	0.0	-2.56	0.827	-1.337	0.7157
1.0	0.2	-2.80	0.766	-1.155	0.7365
1.0	1.0	-3.32	-1.055	-0.252	0.6362
0.75	0.0	-2.04	0.812	-1.235	0.7611
0.5	0.0	-1.92	0.796	-1.126	0.8161
0.5	0.2	-2.05	0.802	-0.957	0.8133
0.5	1.0	-2.36	-1.288	-0.181	0.7560
0.25	0.0	-1.71	0.787	-0.995	0.8823

For stable, fundamental, periodic motion T_p increases with C_H and B_f. Increase in K_i, however, causes its reduction (Figure 4-5). The trace of the final condition matrix $\Theta(T_p)$, appearing as Floquet's stability criterion, also varies substantially with the system parameters.

For preliminary design of a satellite, it would be more pertinent to have, from stability considerations, information about the satellite's ability to withstand impulsive disturbances for regular behaviour. This could be accomplished quite readily recognizing the fact that, at equilibrium position, the plot ψ' vs. ϕ', for a given Hamiltonian, is a circle. When C_H is small all conditions on this circle lead to regular trajectories. However, for $C_{H_R} < C_H < C_{H_{cr}}$, i.e., when island, ergodic type or unstable solutions are possible, regular behaviour can occur only over the arc corresponding to a limiting intercept (Figures 4-1, 4-4).

Figure 4-6 compares, for a dumbbell satellite, the allowable impulsive disturbance for regular behaviour with critical conditions for stability as obtained by Brereton.[10] The plots are symmetrical about ψ_o' -axis. The reduction ($\simeq$ 27.5% in area) in the bound due to the ergodic and island type behaviour is particularly significant in ψ degree of freedom. The presence of atmosphere further deteriorates the situation. The physical parameters indicated in the diagram approximately correspond to the gravity-gradient stabilized satellite GEOS-A, launched on November 6, 1965

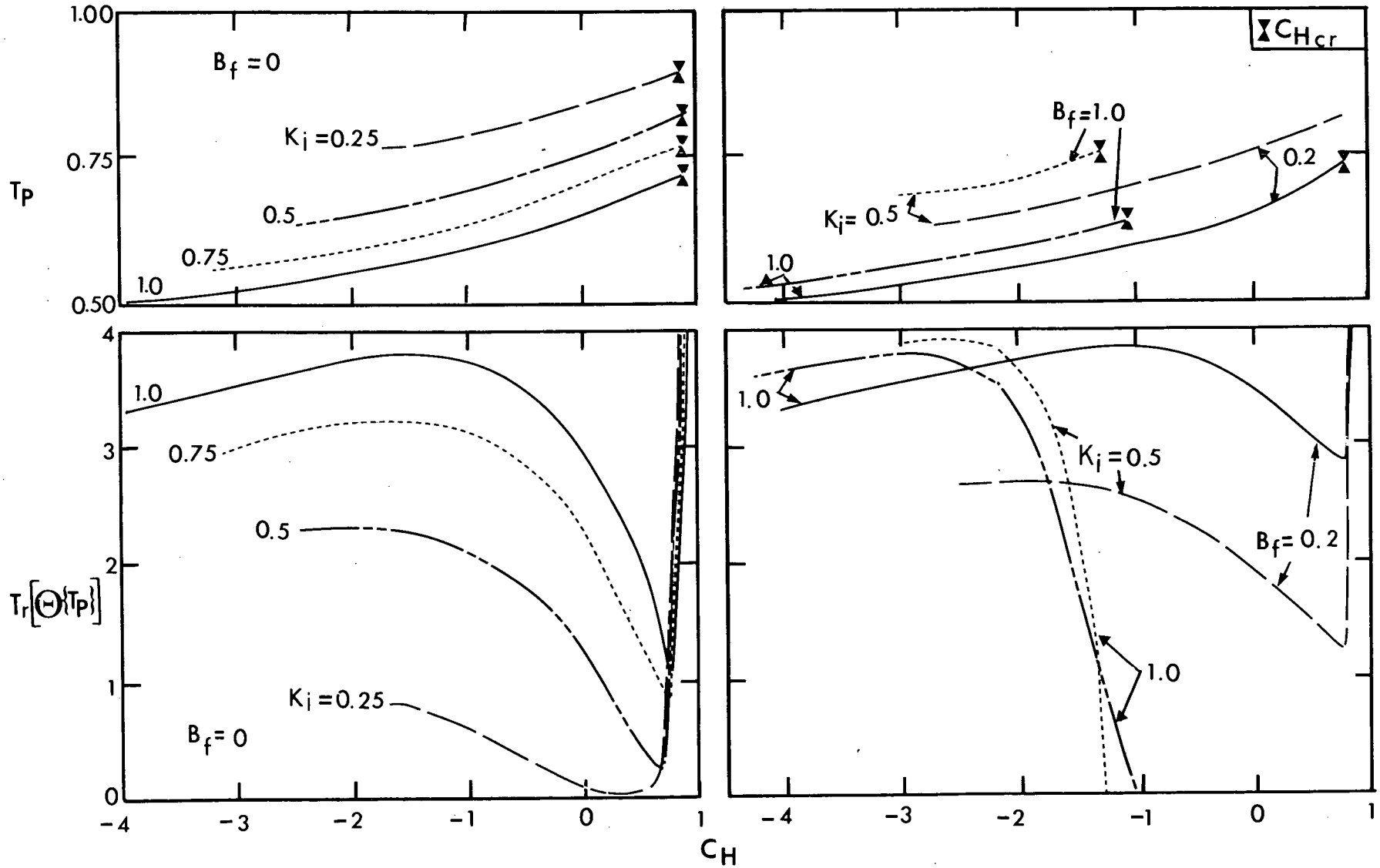

Figure 4-5 Variation of the period and the trace of final condition matrix with Hamiltonian for the stable periodic solution P_{21}

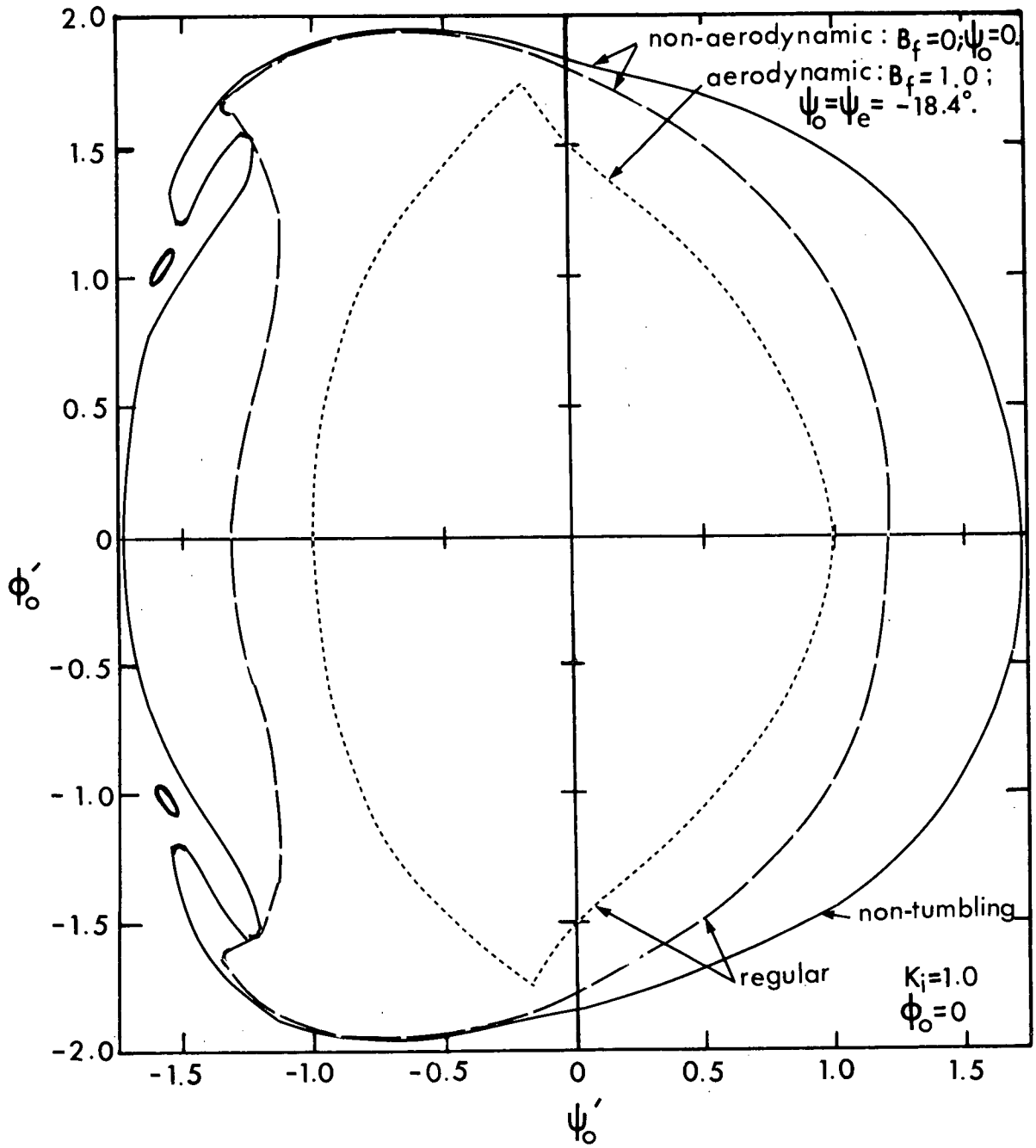

Figure 4-6 Reduction of the allowable impulsive disturbance for stable motion due to non-regular solution and atmosphere

(data: semi-major axis ≃ 5,000 miles; $e=0.07$; $I_{xx}=615.3$ slug. ft^2; $I_{yy}=716.0$ slug. ft^2; $I_{zz}=20.8$ slug. ft^2; $D_oL_o=$ 13.1 ft^2; $\varepsilon=5.75$ ft)[54]. It is apparent that the satellite would have its regular stability reduced by ≃ 45% at 250 miles altitude, where $B_f \simeq 1$.

The effect of inertia and atmosphere on the regular stability region is shown in Figure 4-7. Although the reduction in available stability bound due to ergodic and island type solutions is significant for satellites with larger K_i, they still show better stability characteristics particularly when B_f is small.

4.4 Concluding Remarks

The important conclusions based on the analysis may be summarized as follows:

(i) The investigation emphasizes the usefulness of the concept of integral manifolds by pointing out the fact that, beside providing the bound of stability, their degeneration leads to periodic solutions. Thus the periodic solutions act as spines around which the stability regions are built.

(ii) The system exhibits three distinctly different solutions even when the bounded motion is guaranteed. The regular behaviour corresponds to the periodic solution P_{21}, while the island type representation in the phase plane is associated with

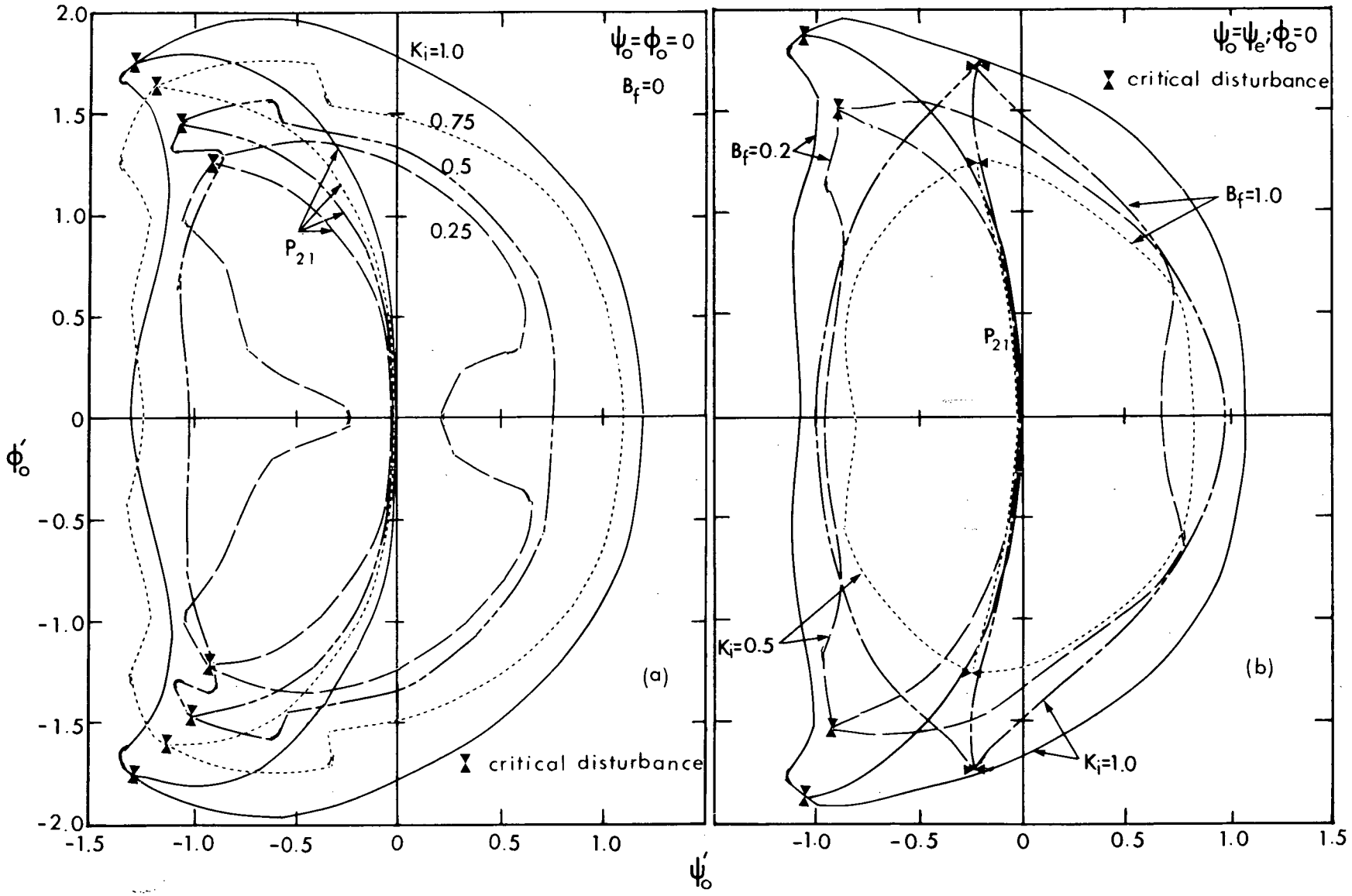

Figure 4-7 Allowable impulsive disturbance at equilibrium position for regular motion and corresponding periodic solutions: (a) effect of inertia; (b) effect of atmosphere

other periodic solutions, e.g., P_{23}, P_{45}, etc. The ergodic behaviour in the transition region is probably indicative of long period librations.

(iii) Proximity of the islands to the motion envelope and the unpredictable nature of the ergodic solutions render the limiting regular region to be the only useful stability bound for satellite design.

(iv) The fundamental period corresponding to the solution P_{21} is close to the orbital rate. It increases with decreasing K_i and increasing C_H or B_f.

(v) In general, the critical Hamiltonian for stable motion decreases with decreasing K_i. The reduction is enhanced during the presence of aerodynamic torque. As the only available solution is a periodic one for $C_{H_{cr}}$, it can be determined quite readily and accurately using extension of Floquet's stability criterion to the fourth order system.

5. LIBRATIONAL RESPONSE AND STABILITY IN ELLIPTIC ORBITS

5.1 Preliminary Remarks

The librational analysis, so far, was restricted to the satellites negotiating circular trajectories. The simplification was necessary because of the complex character of the governing equations which then became autonomous. The next logical step would be the consideration of a more general situation involving motion in an elliptic trajectory. It may be pointed out that the analysis of the resulting non-autonomous, gravity oriented system, even in absence of environmental forces, remains unexplored. On the other hand, the importance of such a study becomes apparent when one recognizes the fact that meteorological, earth resources, military reconnaissance, etc., satellites using close earth orbits for better resolutions, can have their life span increased through use of elliptic trajectories.

This chapter investigates coupled librational dynamics of such non-autonomous systems. In the beginning an approximate closed form analytical solution is obtained for the system in absence of aerodynamic moment using modification of Butenin's[57] approach. This is followed by numerical response and stability analysis in the large over a wide range of inertia parameter. Next, the effect of aerodynamic moment on the equilibrium configuration, system response, and stability

are studied in detail. As the concept of integral manifold breaks down due to the non-autonomous character of the system, the amount of computational effort involved is enormous. A convenient condensation of the response data, effected through plots showing allowable impulsive disturbances over a set of eccentricities, represents an attempt at providing information of particular use during preliminary design of a satellite.

5.2 Formulation of the Problem

In absence of atmosphere (Figure 2-1), equations (2.1c) and (2.3) represented the general motion of the system. Using the Keplerian relations and noting that

$$
\begin{aligned}
d/dt &= \dot{\theta}\, d/d\theta = (h_\theta/r^2)\, d/d\theta \\
d^2/dt^2 &= \dot{\theta}^2 d^2/d\theta^2 + \ddot{\theta}\, d/d\theta \\
&= (h_\theta^2/r^4)\, d^2/d\theta^2 - 2(h_\theta^2/r^5)(dr/d\theta)\, d/d\theta
\end{aligned}
\qquad \ldots\ldots (5.1)
$$

the equations in the librational degrees of freedom transform to:

$$
\psi''(1+e\cos\theta) - 2e\sin\theta(\psi'+1) - 2\phi'(\psi'+1)(1+e\cos\theta)\tan\phi + 3K_i \sin\psi\cos\psi = 0 \qquad \ldots\ldots (5.2a)
$$

$$
\phi''(1+e\cos\theta) - 2e\sin\theta\,\phi' + [(1+\psi')^2(1+e\cos\theta) + 3K_i\cos^2\psi]\sin\phi\cos\phi = 0 \qquad \ldots\ldots (5.2b)
$$

These second order, coupled, non-linear, non-autonomous equations of motion remain invariant under the transformation (θ,ψ,ϕ) to $(\theta,\psi,-\phi)$, $(-\theta,-\psi,\phi)$ or $(-\theta,-\psi,-\phi)$.

5.3 Approximate Solution and System Response

5.3.1 Variation of Parameter Method (Butenin)

In absence of known, exact, closed form solution, it was decided to analyze the problem approximately using modification of Butenin's variation of parameter technique. The method was described earlier in Section 2.4.1.

Replacing the trignometric functions of the dependent variables by their series, ignoring fifth and higher degree terms in ψ, ϕ, and their derivatives, and collecting non-linear terms and forcing function on the right side, equation (5.2) takes the form:

$$\psi'' + 3K_i\psi \simeq 2e\sin\theta + 2\left[e\sin\theta\,\psi'/(1+e\cos\theta) + \phi'\phi(\psi'+1) + 2\phi'\phi^3/3 + 3K_i\psi^3\right] \quad \text{(5.3a)}$$

$$\phi'' + (1+3K_i)\phi \simeq \left[2e\sin\theta\,\phi'/(1+e\cos\theta) + 2\phi^3\{1 + 3K_i/(1+e\cos\theta)\}/3 - 2\psi'\phi - \psi'^2\phi - 4\psi'\phi^3/3 + 3K_i\psi^2\phi/(1+e\cos\theta)\right]$$

or

$$\psi'' + n_1^2\psi = 2e\sin\theta + f_1(\psi,\psi',\phi,\phi',\theta) \quad \text{(5.3b)}$$

$$\phi'' + n_2^2\phi = g_1(\psi,\psi',\phi,\phi',\theta) \quad \text{(5.4)}$$

The solution of the corresponding linear system (i.e., $f_1=g_1=0$) is given as:

$$\psi = a\sin(n_1\theta+\beta_1) + 2e\sin\theta/(n_1^2-1) \quad \ldots\ldots (5.5a)$$

$$\phi = b\sin(n_2\theta+\beta_2) \quad \ldots\ldots (5.5b)$$

where a, b, β_1 and β_2 are constants which can be determined from initial conditions. A solution of the similar form is sought for the case under consideration, allowing, however, the amplitude and phase angles to be functions of θ, i.e.,

$$\psi = a(\theta)\sin(n_1\theta + \beta_1(\theta)) + 2e\sin\theta/(n_1^2-1) \quad (5.6a)$$

$$\phi = b(\theta)\sin(n_2\theta + \beta_2(\theta)) \quad \ldots\ldots (5.6b)$$

a, b, β_1 and β_2 can be expressed as functions of θ plus a constant. Thus the solution in the present form involves eight unknowns, four of which can be determined by the initial conditions while the remaining have to be found through the imposition of constraints.

Keeping the first derivative of equations (5.6a) and (5.6b) to be similar to the homogeneous solution gives two of the constraint relations:

$$a'\sin\zeta + a\beta_1'\cos\zeta = 0 \quad \ldots\ldots (5.7a)$$

$$b'\sin\eta + b\beta_2'\cos\eta = 0 \quad \ldots\ldots (5.7b)$$

Other two relations are obtained by substituting (5.6) in equations of motion (5.4) giving

$$a' n_1 \cos\zeta - a n_1 \beta_1' \sin\zeta = f_1^* \quad \ldots . (5.7c)$$

$$b n_2 \cos\eta - b n_2 \beta_2' \sin\eta = g_1^* \quad \ldots . (5.7d)$$

where

$$f_1^* = f_1 [a \sin\zeta + 2e \sin\theta/(n_1^2 - 1) , a n_1 \cos\zeta + 2e \cos\theta/(n_1^2 - 1) , b \sin\eta , b n_2 \cos\eta , \theta]$$

$$g_1^* = g_1 [a \sin\zeta + 2e \sin\theta/(n_1^2 - 1) , a n_1 \cos\zeta + 2e \cos\theta/(n_1^2 - 1) , b \sin\eta , b n_2 \cos\eta , \theta]$$

$$\ldots . (5.8)$$

solving the equations (5.7) yields

$$a' = f_1^* \cos\zeta / n_1$$
$$b' = g_1^* \cos\eta / n_2$$
$$\beta_1' = - f_1^* \sin\zeta / a n_1$$
$$\beta_2' = - g_1^* \sin\eta / b n_2 \quad \ldots . (5.9)$$

f_1^*, g_1^* being small for small disturbances, a, b, β_1 and β_2 are slowly varying parameters. Using their average values over a period gives

$$da/d\theta = (1/8\pi^3 n_1) \int_0^{2\pi} \int_0^{2\pi} \int_0^{2\pi} f_1^* \cos\zeta \, d\zeta \, d\eta \, d\theta$$
$$db/d\theta = (1/8\pi^3 n_2) \int_0^{2\pi} \int_0^{2\pi} \int_0^{2\pi} g_1^* \cos\eta \, d\zeta \, d\eta \, d\theta$$
$$d\beta_1/d\theta = -(1/8\pi^3 n_1 a) \int_0^{2\pi} \int_0^{2\pi} \int_0^{2\pi} f_1^* \sin\zeta \, d\zeta \, d\eta \, d\theta$$
$$d\beta_2/d\theta = -(1/8\pi^3 n_2 b) \int_0^{2\pi} \int_0^{2\pi} \int_0^{2\pi} g_1^* \sin\eta \, d\zeta \, d\eta \, d\theta$$

$$\ldots . (5.10)$$

or,

$$\psi = a \sin\left[(3K_i)^{1/2}\theta + \beta_1\right] + 2e\sin\theta/(3K_i - 1) \quad (5.11a)$$

$$\phi = b \sin\left[(3K_i + 1)^{1/2}\theta + \beta_2\right] \quad \ldots\ldots (5.11b)$$

where

$$a = \left[\psi_o^2 + \{\psi_o' - 2e/(3K_i - 1)\}^2/3K_i\right]^{1/2}$$

$$b = \left[\phi_o^2 + \phi_o'^2/(1 + 3K_i)\right]^{1/2}$$

$$\beta_1 = -(3K_i)^{1/2} a^2\theta/4 + \tan^{-1}\left[(3K_i)^{1/2}\psi_o/\{\psi_o' - 2e/(3K_i - 1)\}\right]$$

$$\beta_2 = -\left[b^2\{1 + 3K_i/(1 - e^2)^{1/2}\} - 3a^2K_i\{1 - 1/(1 - e^2)^{1/2}\}\right.$$
$$\left. + 4e^2/(3K_i - 1)\right]\theta/\{4(1 + 3K_i)^{1/2}\} + \tan^{-1}\left[(1 + 3K_i)^{1/2}\phi_o/\phi_o'\right]$$

$$\ldots\ldots (5.12)$$

5.3.2 Accuracy of the Solution

To establish the accuracy of this analytical technique the equations of motion (5.2) were integrated numerically. The librational response as affected by satellite inertia, orbital eccentricity and external disturbance was obtained over fifty orbits using a step-size of 3°. However, for conciseness, the comparison between the two methods is limited to initial and terminal regions in Figure 5-1.

As in the case of a circular orbit, the solution appears to agree well with the numerical results, particularly for the motion across the orbital plane, even for a disturbance of appreciable magnitude ($\psi_o' = \phi_o' = 0.5$). The effect of eccentricity is reflected through motion modulations. Both methods show that a larger amplitude, smaller frequency motion, with

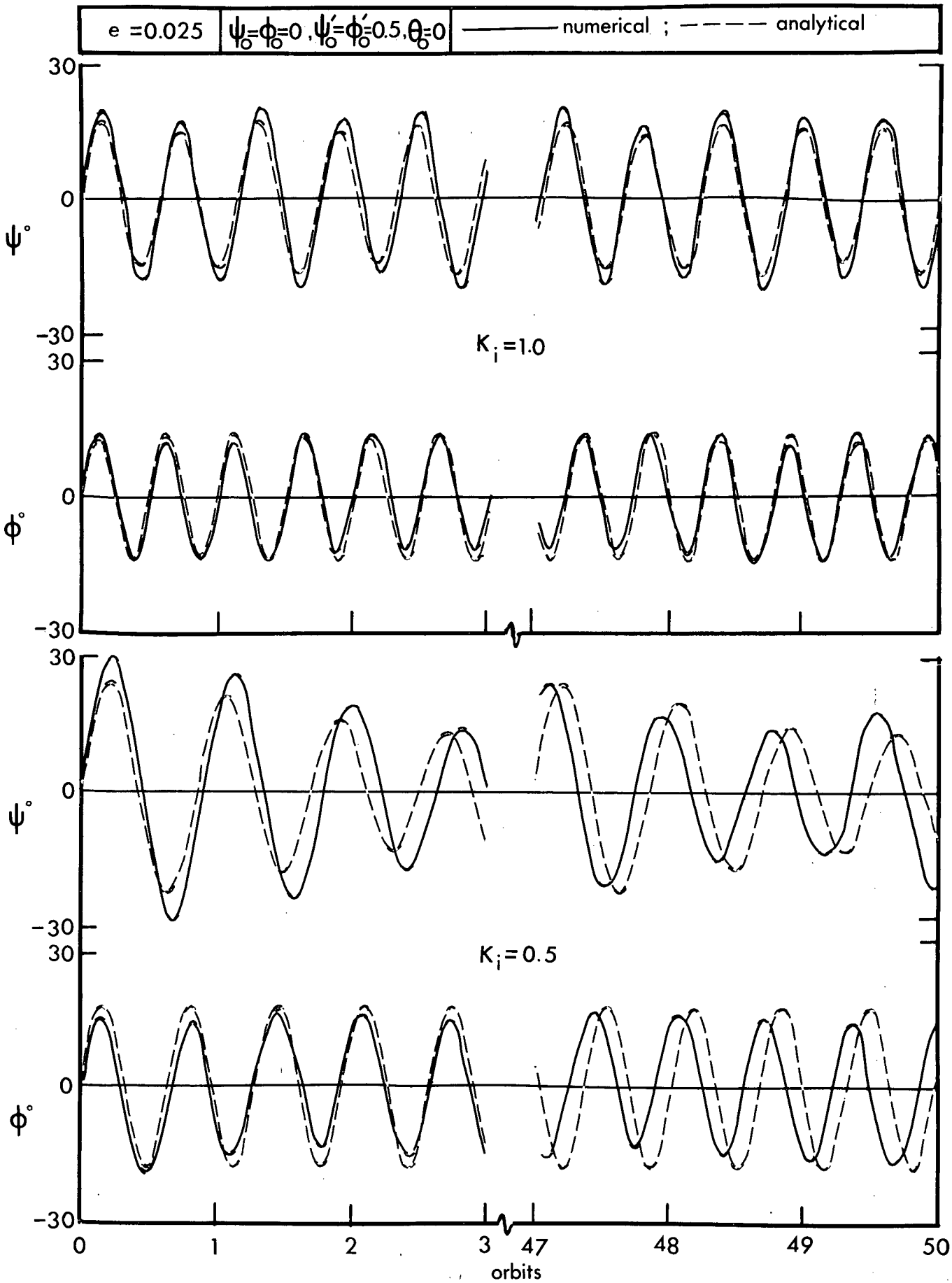

Figure 5-1 Representative comparison of the responses generated using Butenin's approach and numerical method, showing effects of: (a) satellite inertia

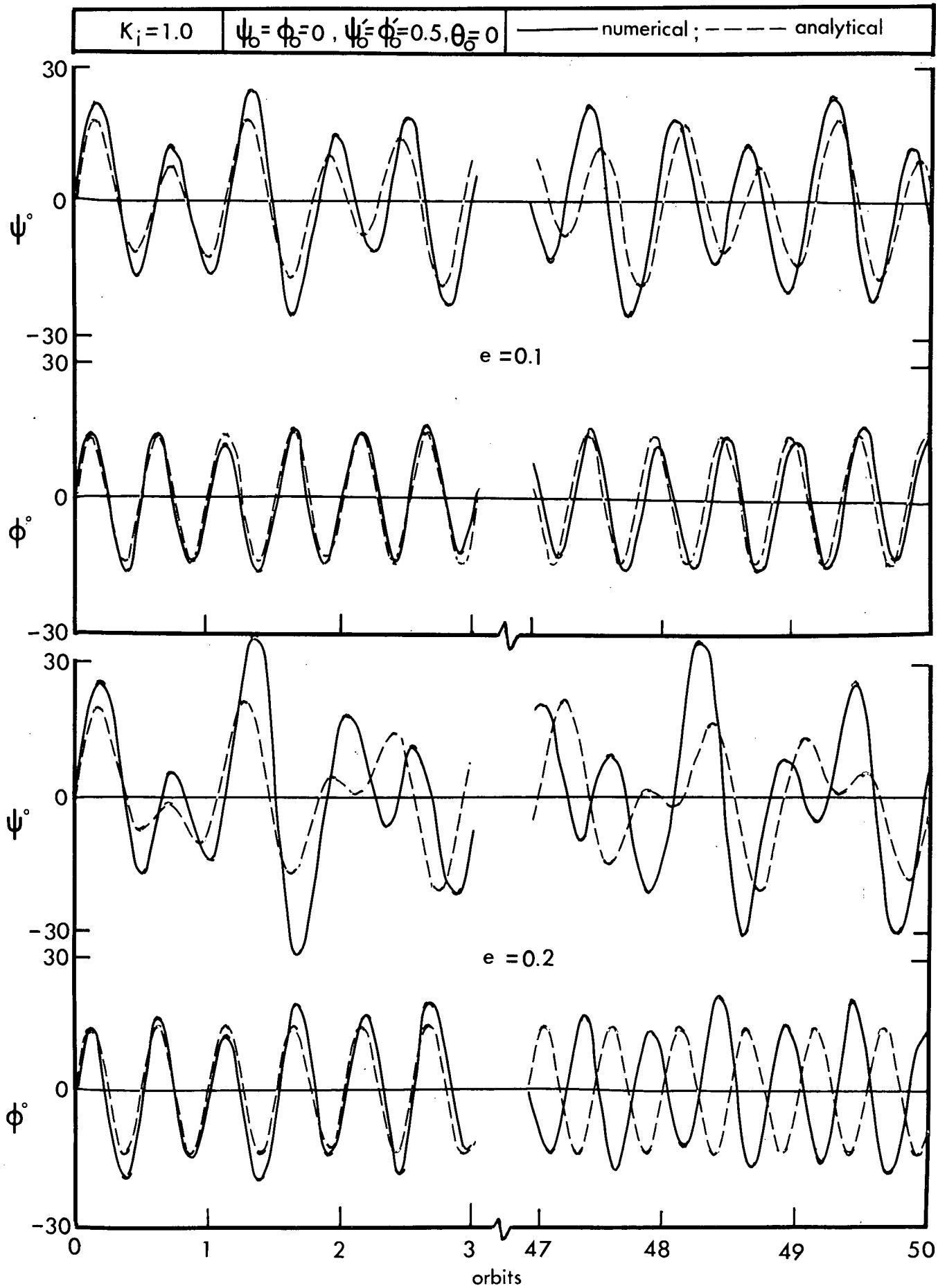

Figure 5-1 Representative comparison of the responses, generated using Butenin's approach and numerical method, showing effects of: (b) orbit eccentricity

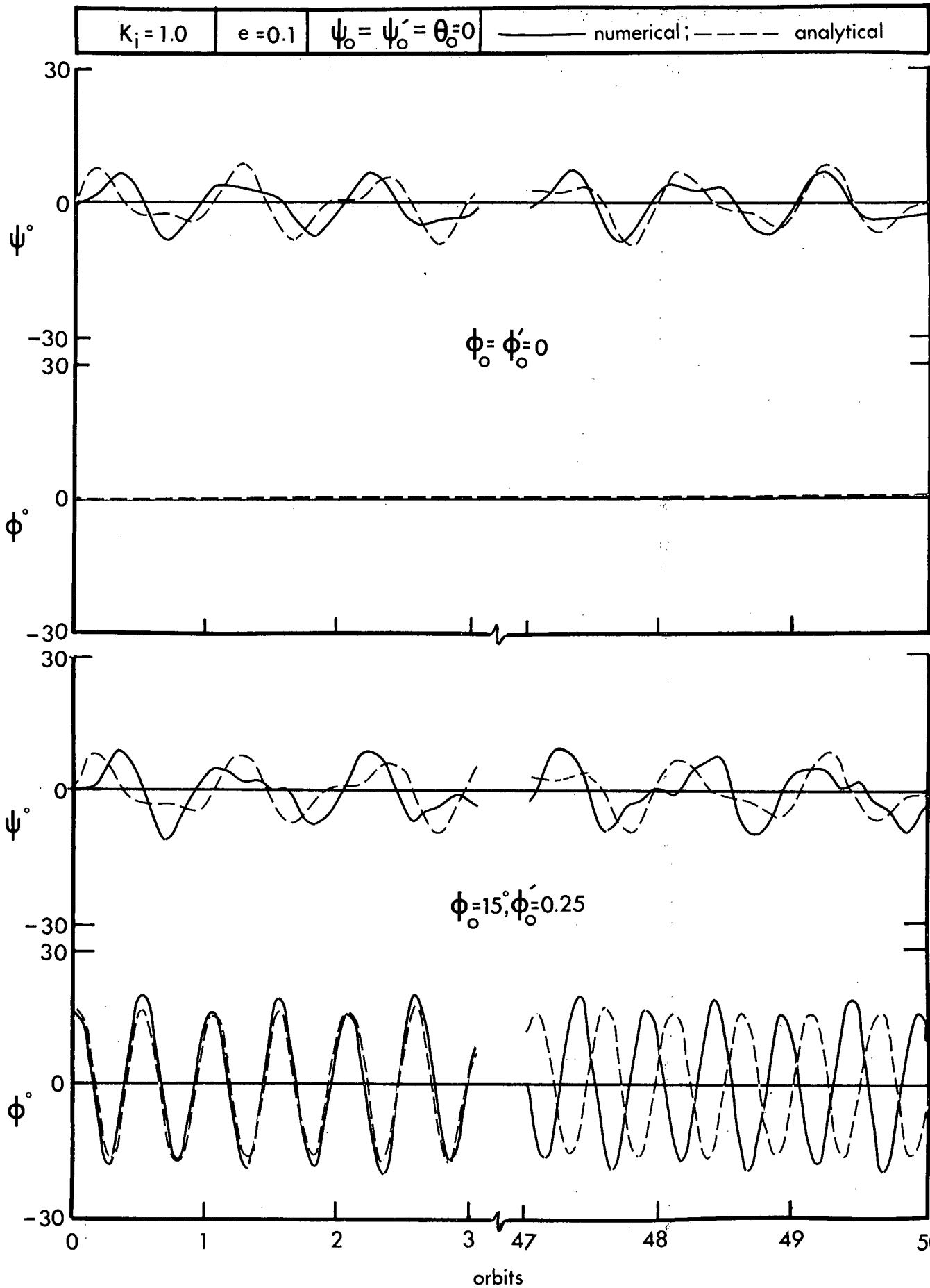

Figure 5-1 Representative comparison of the responses, generated using Butenin's approach and numerical method, showing effects of: (c) initial conditions

a period of the order same as that of the orbit, is excited in the orbital plane when the satellite is subjected to identical disturbances in the two degrees of freedom. The phase discrepancy between the solutions appears to grow with time. The librational amplitude predicted by the approach is, in general, smaller than the actual. Thus the resulting analytical stability bound is likely to be larger.

Although, the agreement deteriorates with decreasing slenderness of the satellite (Figure 5-1(a)) and increasing eccentricity (Figure 5-1(b)), the analysis continues to predict the general behaviour, at least qualitatively. Reduction of K_i or increase in e enhances the amplitude modulation, especially for planar degree of freedom. Both the solutions indicate that in absence of any initial disturbance, appreciable oscillations in the orbital plane are excited due to eccentricity of the orbit (Figure 5-1(c)). A presence of any cross motion appears to induce small perturbations in the planar librations, however, the analytical approach fails to predict this phenomenon.

As in actual practice, the gravity gradient satellites possess large K_i, normally move in circular or almost circular orbits, and exhibit moderate pointing accuracy, the analytical solution can be applied with confidence, at least for preliminary design purposes.

The effect of eccentricity is indicated in Figure 5-2, which compares the numerically generated response of a

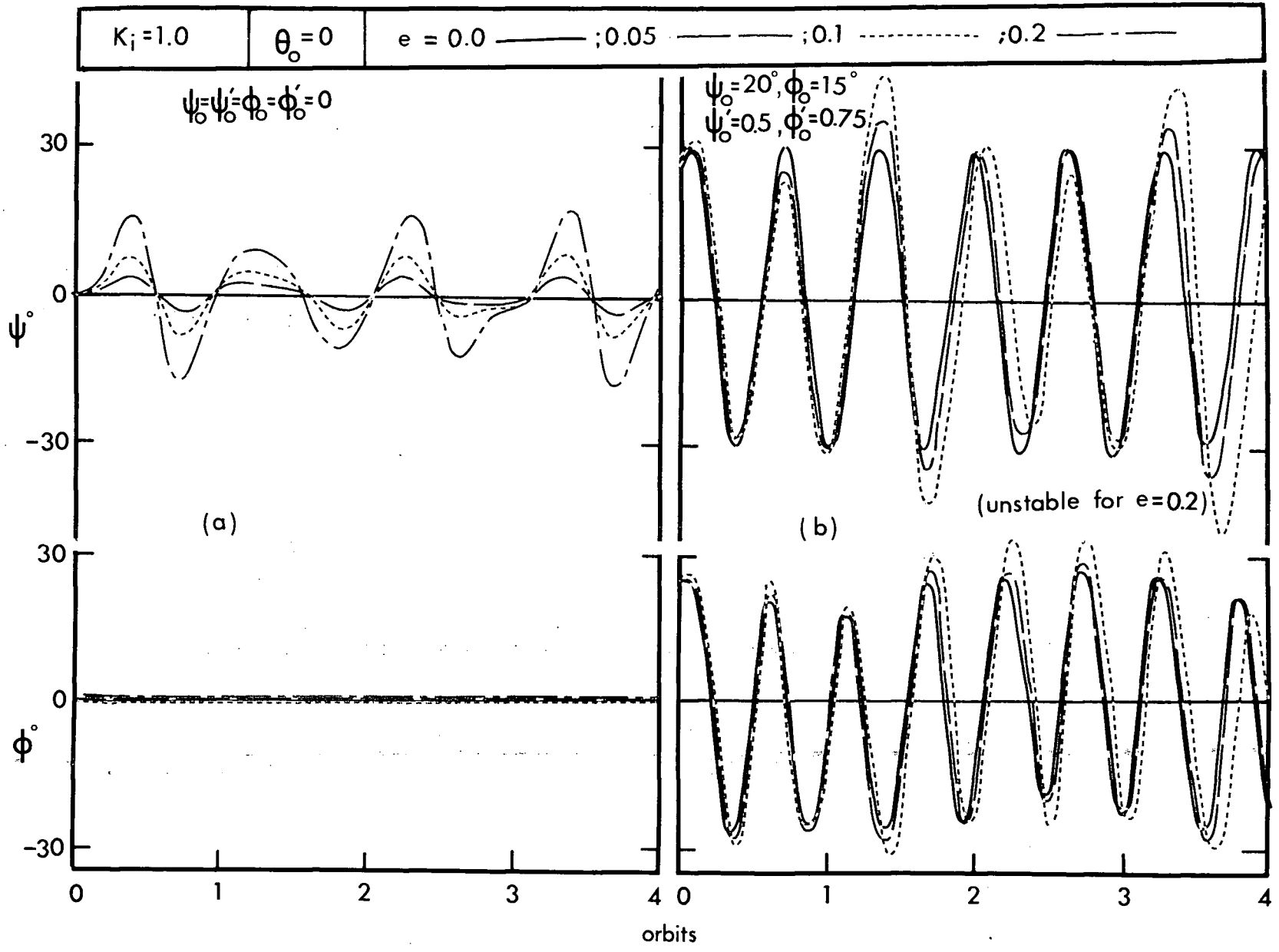

Figure 5-2 Numerical results indicating the effect of orbit eccentricity on the satellite response: (a) no disturbance; (b) large disturbance

dumbbell satellite. Although, in a circular orbit no motion is excited in absence of disturbances, appreciable planar motion, which grows with eccentricity, is noticed in elliptic trajectories. Considerable amplitude modulations at higher eccentricities, particularly of the motion in the orbital plane, suggest an increased tendency towards instability for the satellite subjected to an arbitrary disturbance.

5.4 Stability Bound

5.4.1 Analytical Approach

With obvious limitations of the Butenin method one can hardly expect it to be suitable for any stability study in the large. However, it was gratifying to observe that, in spite of rather drastic simplifications, the method successfully establishes trend for the influence of system parameters.

The form of the solution as given by the variation of parameter method (equation 5.11) suggests that the stability of the system is governed by the amplitude of the harmonic terms. The stability criteria, therefore, become

$$|a| + 2e/(3K_1 - 1) \leqslant \pi/2$$

$$|b| \leqslant \pi/2 \qquad \ldots . (5.13)$$

or, in terms of impulsive disturbance at equilibrium configuration,

$$|\psi_o' - 2e/(3K_i - 1)| \leq (3K_i)^{1/2} \{\pi/2 - 2e/(3K_i - 1)\}$$

$$|\phi_o'| \leq \pi (1 + 3K_i)^{1/2}/2 \qquad \ldots .(5.14)$$

In the ψ_o'-ϕ_o' plane, these correspond to rectangular regions, symmetrical about ψ_o'-axis. It is apparent that a decrease in slenderness of the satellite or an increase in orbit eccentricity would, in general, affect the stability adversely, particularly in the ψ degree of freedom. It is interesting to observe that most satellites should be able to withstand relatively larger +ve planar impulses. At K_i=1/3, the stability bound is not defined and below this critical value, most of the trends mentioned above are reversed.

The Butenin's approach thus yields some qualitative insight into the system stability in the large. However, for quantitative results one has to adopt numerical methods.

5.4.2 Numerical Approach

For autonomous systems, use of the concept of the integral manifold in conjunction with the constant Hamiltonian fascilitated the stability analysis appreciably. Unfortunately, in presence of eccentricity, the concept loses its importance due to the obvious difficulty in representing and interpreting the hyper-surfaces in phase space. Intersection by a phase plane (say, ψ-ψ') no longer represents a cross-section of the hyper-invariant-manifold, and only leads to the scattered

encounter with the trajectories (Figure 5-3). Hence an alternate approach is necessary to get meaningful information about the system stability.

Here the stability bounds are established by analyzing the librational response, over 15-20 orbits, to systematically varied initial conditions, satellite inertia, and orbit eccentricity. The vast amount of information, thus gathered, is condensed in the form of design plots (Figure 5-4), which indicate allowable impulsive disturbances ($\psi_o=\phi_o=0$) at perigee for non-tumbling motion, over a range of K_i and e. For comparison, earlier results with circular orbits are also included.

The effect of even slight increase in eccentricity is to rapidly reduce the stability region, particularly for satellites with smaller K_i. The reduction, in general, is more severe in the plane of the orbit, where the satellite is able to withstand, relatively, large positive disturbance. The plots remain symmetrical about $\phi'=0$ as in the case of autonomous system. The peculiar shape of a stability region with numerous spikes may be attributed to the predominance of various periodic solutions. Of course, at the highest eccentricity for stable motion, the only available solution is a periodic one[9] as indicated by dots in Figure 5-4. The crossing of stability bounds suggest that in some situations, increase in eccentricity may be favourable, locally, in system stabilization.

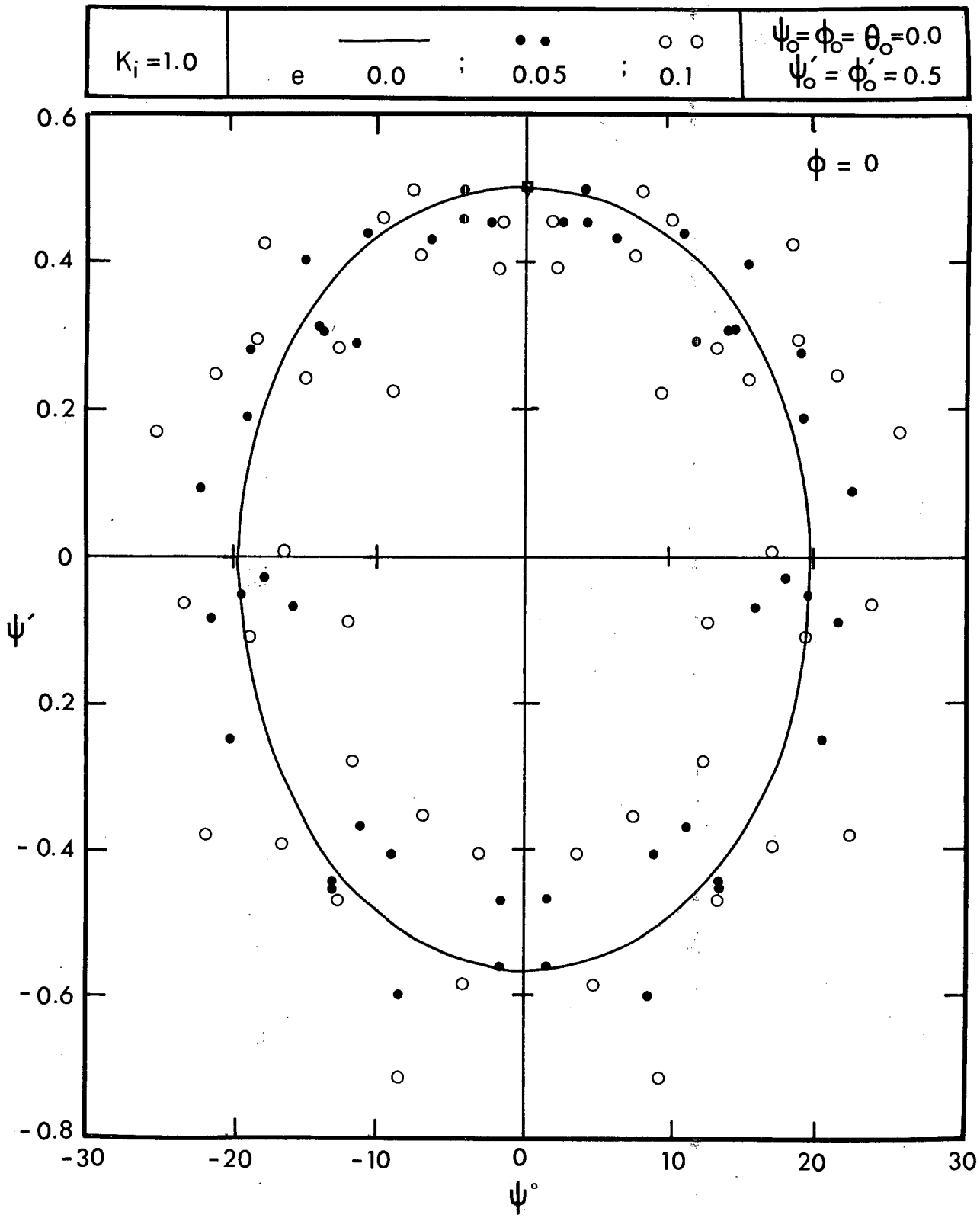

Figure 5-3 Stroboscopic phase plane at $\phi=0$ showing breakdown of the integral manifold concept for non-autonomous system

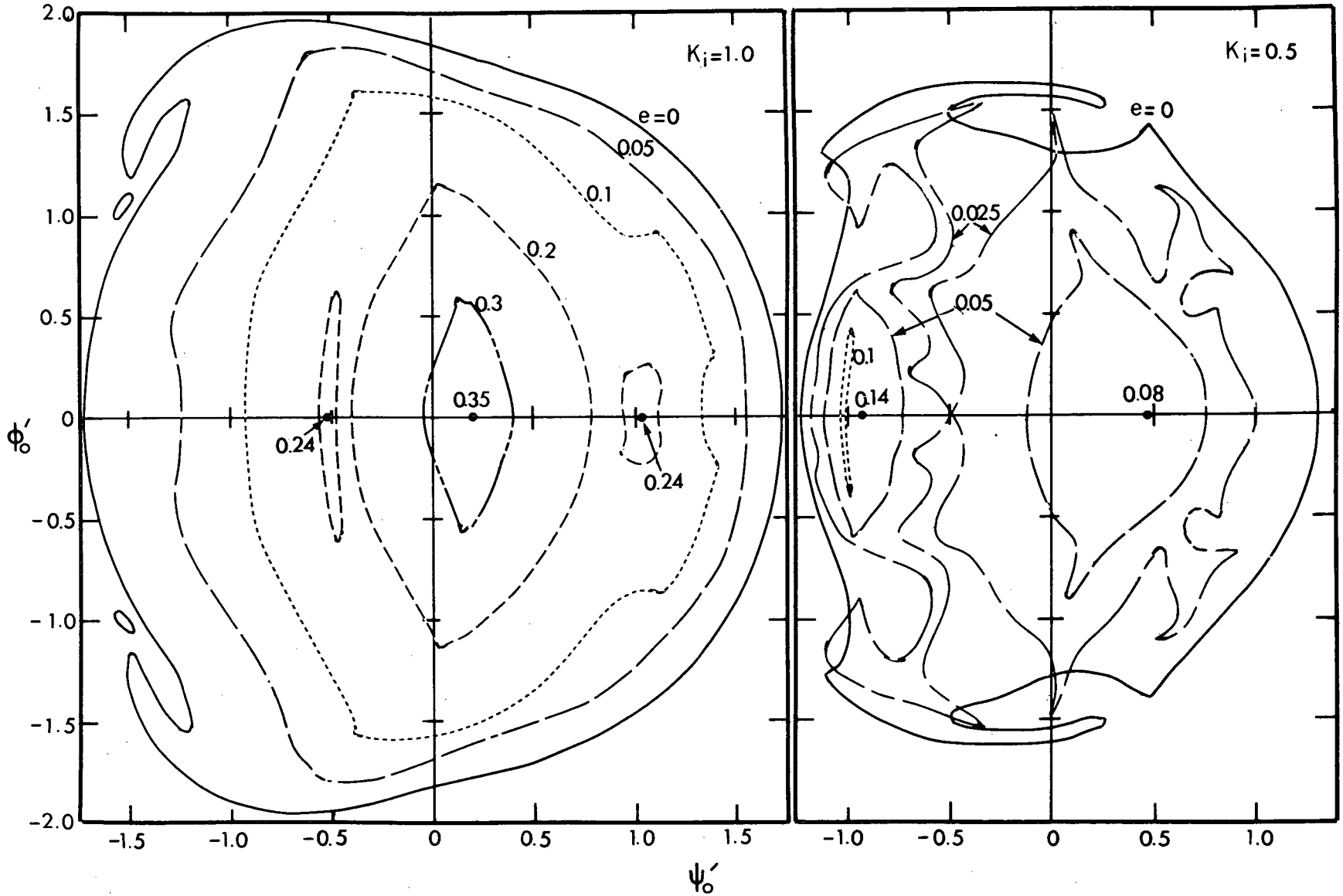

Figure 5-4 Effect of satellite inertia and orbit eccentricity on the allowable impulsive disturbances for stable motion; $\theta_o=\psi_o=\phi_o=0$: (a) K_i=1.0, 0.5

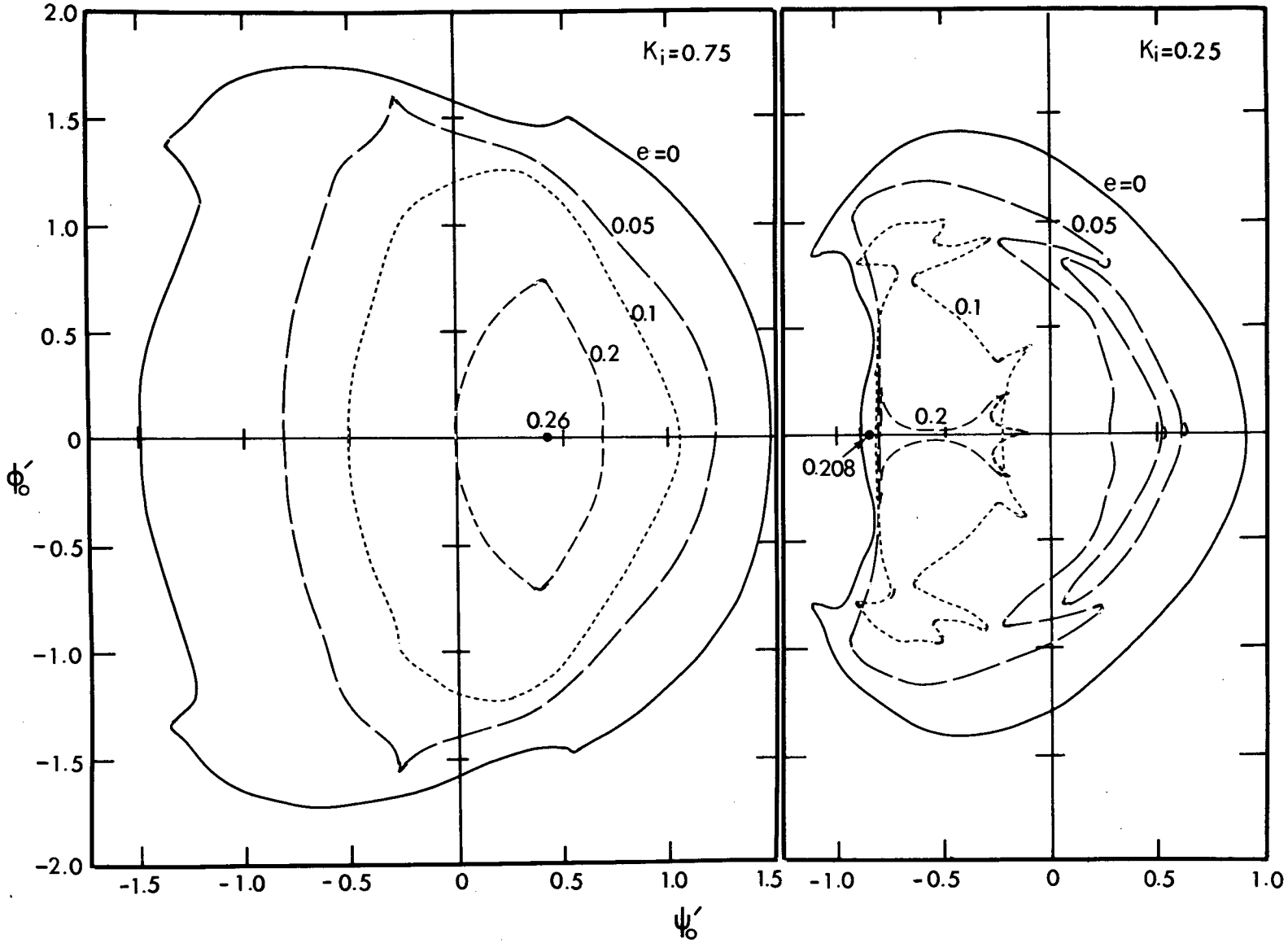

Figure 5-4 Effect of satellite inertia and orbit eccentricity on the allowable impulsive disturbances for stable motion; $\theta_o=\psi_o=\phi_o=0$: (b) $K_i=0.75$, 0.25

Reduction of K_i to 0.25, i.e., a value less than the critical 1/3, reverses some of the trends established above. This is apparent from its better stability characteristics compared to K_i=0.5 in eccentric orbits. A 'shorter' satellite also exhibits an ability to withstand larger negative impulse, $-\psi_o'$.

Although the plots presented here are for disturbances received at perigee, averaging over a large number of orbits suggests their applicability, at least approximately, to any θ in small eccentricity orbits. In principle the system behaviour is similar to planar librations in elliptic orbit[7] and coupled librations in circular orbit. It is important to recognize that presence of cross-plane motion improves the satellite's ability to withstand impulsive disturbances.

5.5 Effect of Aerodynamic Torque on System Response and Stability

5.5.1 Equations of Motion

Using Schaaf and Chambré's approach[66] for a satellite surface in free molecular flow the modified potential function for a cylindrical satellite in a circular orbit was given by equation (3.4). In an elliptic orbit, the change in density and orbital velocity from point to point can be expressed as:

$$\rho = \rho_p \left\{ (r - Re)/(r_p - Re) \right\}^n \quad \ldots . \quad (5.15a)$$

$$v^2 = v_p^2 (v/v_p)^2 = v_p^2 \left\{ (2 r_p - r + r e)/(r + r e) \right\} \quad \ldots . \quad (5.15b)$$

The value of exponent n varies between -5 to -7 in the altitude range of 100-500 miles. The aerodynamic potential, thus becomes:

$$U_a = I\dot{\theta}_p^2 B_{f_p}[\{(r/r_p - Re/r_p)/(1-Re/r_p)\}^n(2r_p/r -1+e)/(1+e)]\{\psi + \sin\psi(\cos\psi + C_1 \sin\psi)\}/2$$

$$(\text{for } |\psi| \leq \pi/2) \quad \ldots . \quad (5.16)$$

where

$$B_{f_p} = \rho_p C_D \epsilon D_o L_o v_p^2/2I\dot{\theta}_p^2 \quad \ldots . \quad (5.17a)$$

$$C_1 = \pi D_o/4L_o = \pi\{(1-K_i)/12(1+K_i)\}^{1/2} \quad (5.17b)$$

It is apparent that, consistent with the assumptions (Section 3.2.1), the governing equation of motion in the ϕ degree of freedom (5.2b) remains unchanged and that in the ψ degree modifies to:

$$\psi''(1+e\cos\theta) - 2e\sin\theta(\psi'+1) - 2\phi'(\psi'+1)(1+e\cos\theta)\tan\phi + 3K_i\sin\psi\cos\psi + B_{f_E}(1+e\cos\theta)(|\cos\psi| + C_1\sin\psi)\cos\psi/\cos^2\phi = 0 \quad \ldots . \quad (5.18)$$

where

$$B_{f_E} = B_{f_p}[\{(1+e)/(1+e\cos\theta) - Re/r_p\}/(1-Re/r_p)]^n(1+2e\cos\theta+e^2)(1+e)^2/(1+e\cos\theta)^4 \quad \ldots . \quad (5.19)$$

Note that the system retains invariant character only under

the transformation (θ,ψ,ϕ) to $(\theta,\psi,-\phi)$.

Increased complexity renders the analytical techniques of questionable value, particularly for motion in the large. Numerical methods, therefore, have to be resorted to.

5.5.2 Equilibrium Configuration

The stable equilibrium position is given as:

$$\psi_e = \tan^{-1}\left\{-B_{f_E} / (3K_i + B_{f_E} C_1)\right\} \quad , \quad \phi_e = 0 \quad . . . \quad (5.20)$$

As B_{f_E} varies with θ, ψ_e changes continuously (Figure 5-5). The symmetry of the plots about $\theta=0$ is of interest. The presence of eccentricity tends to confine the effects of aerodynamic perturbations to the region near perigee. Even for small eccentricity of orbits ($e < 0.1$), the aerodynamic torque becomes negligible for $|\theta| > 60°$. The rate of reduction becomes steeper with increasing e and B_{f_p}, and decreasing K_i.

5.5.3 System Response

A few representative response plots, obtained numerically, for systematically varied inertia, orbit eccentricity, aerodynamic coefficient, and initial conditions are shown in Figure 5-6. As against the librational motion about a constant equilibrium position in circular orbit, presence of a forcing function along with the periodic variation of

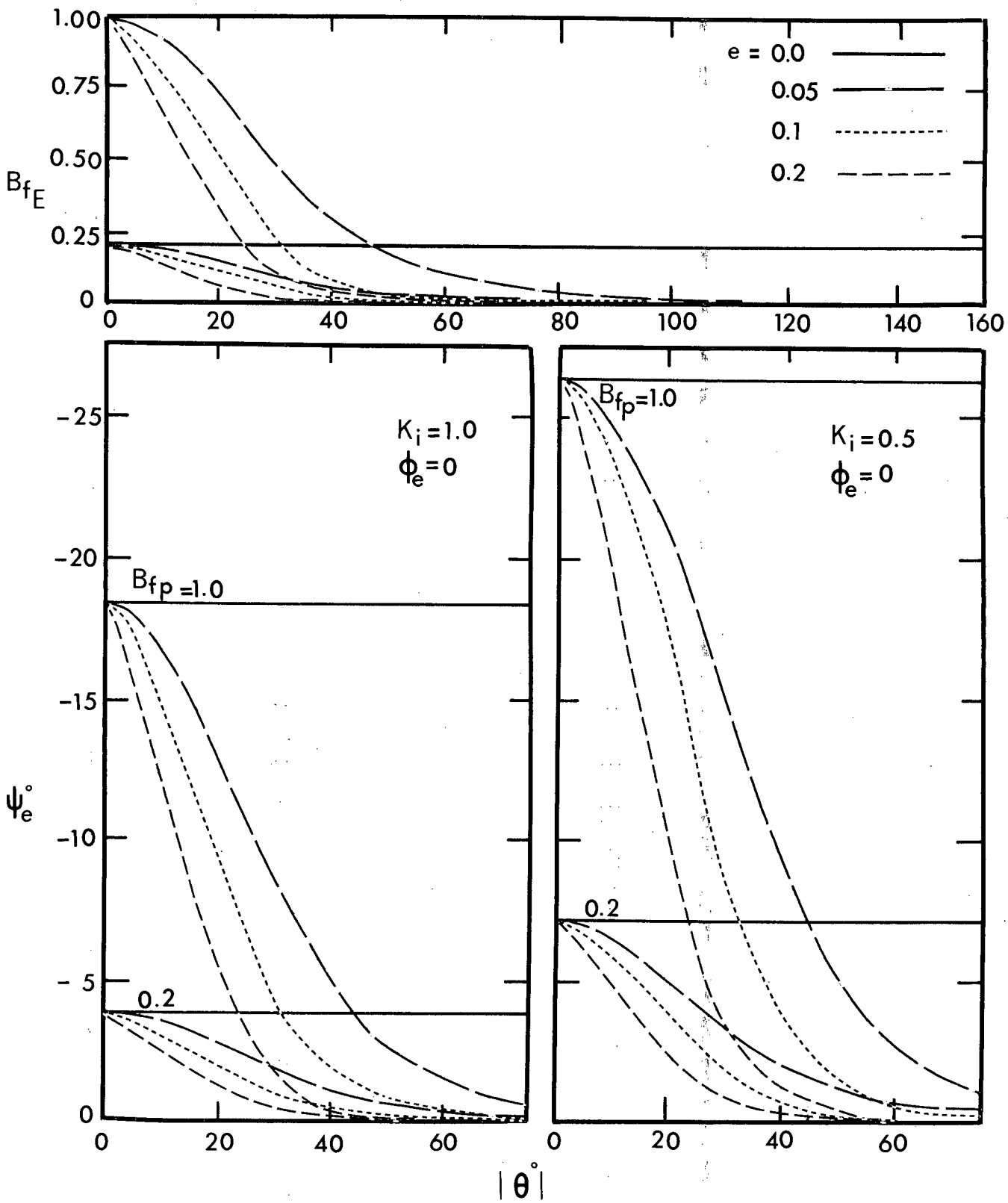

Figure 5-5 Variation of aerodynamic coefficient and stable equilibrium configuration with θ and e

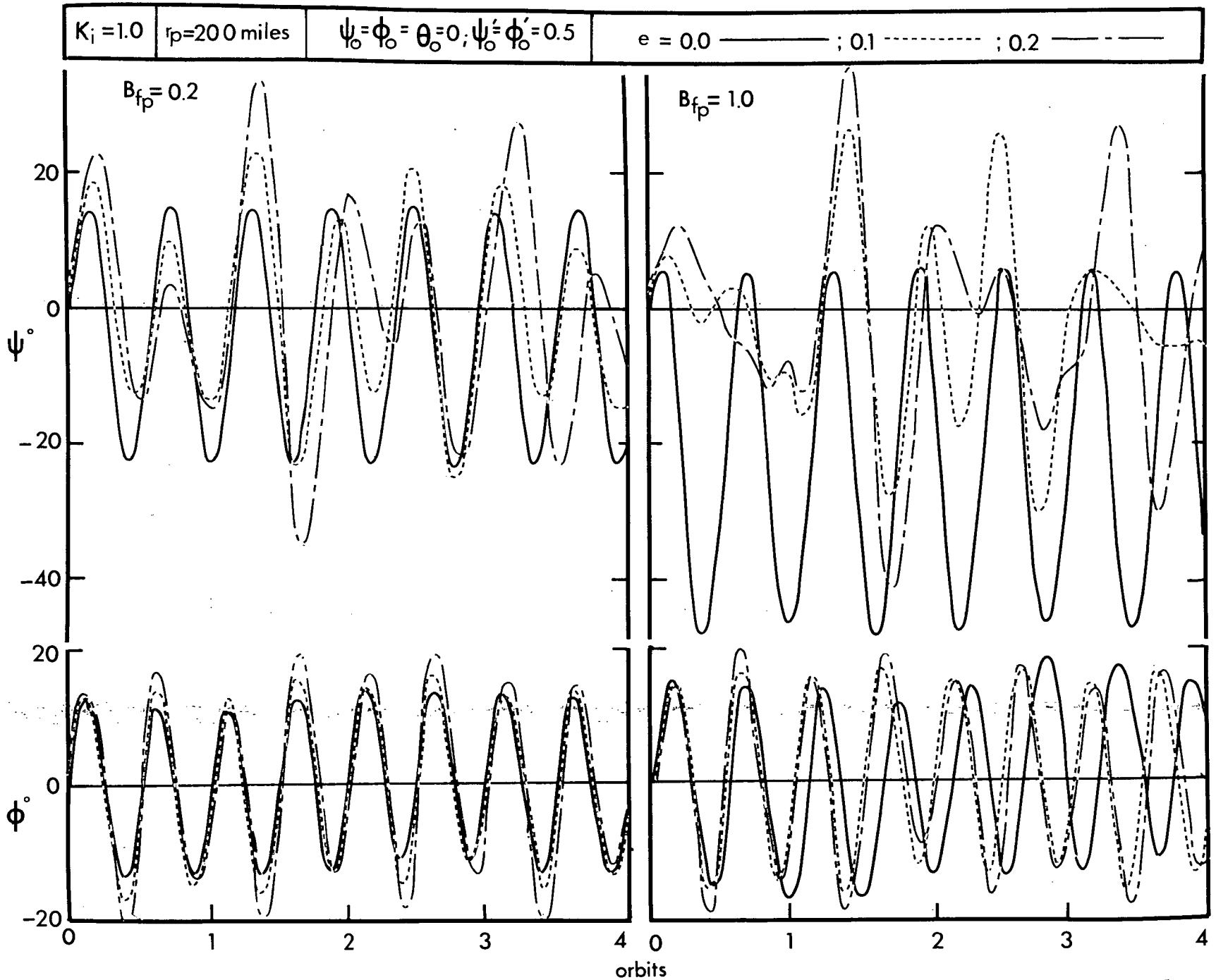

Figure 5-6 Typical system responses showing the effect of orbit eccentricity and (a) atmospheric torque

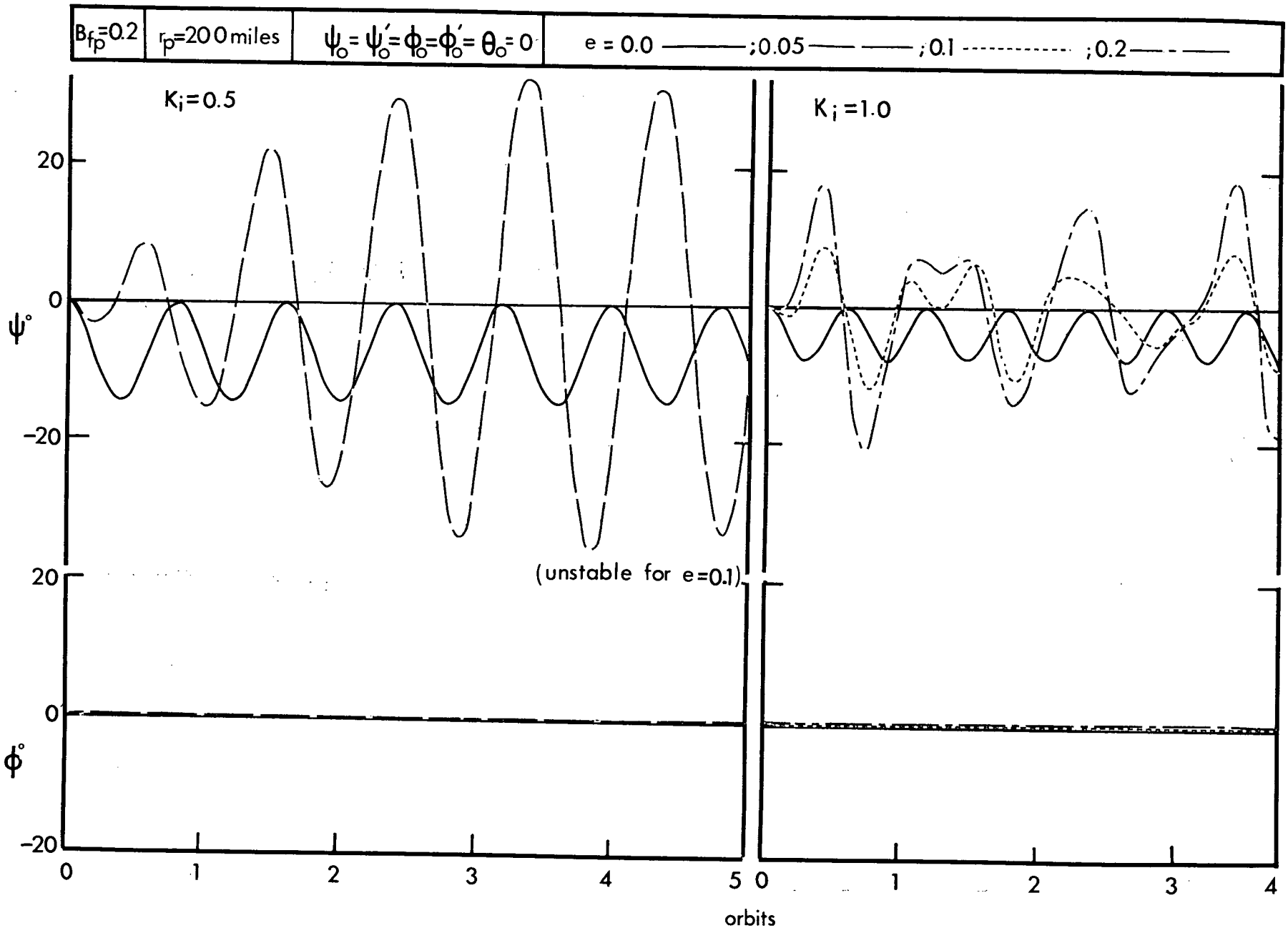

Figure 5-6 Typical system responses showing the effect of orbit eccentricity and (b) satellite inertia

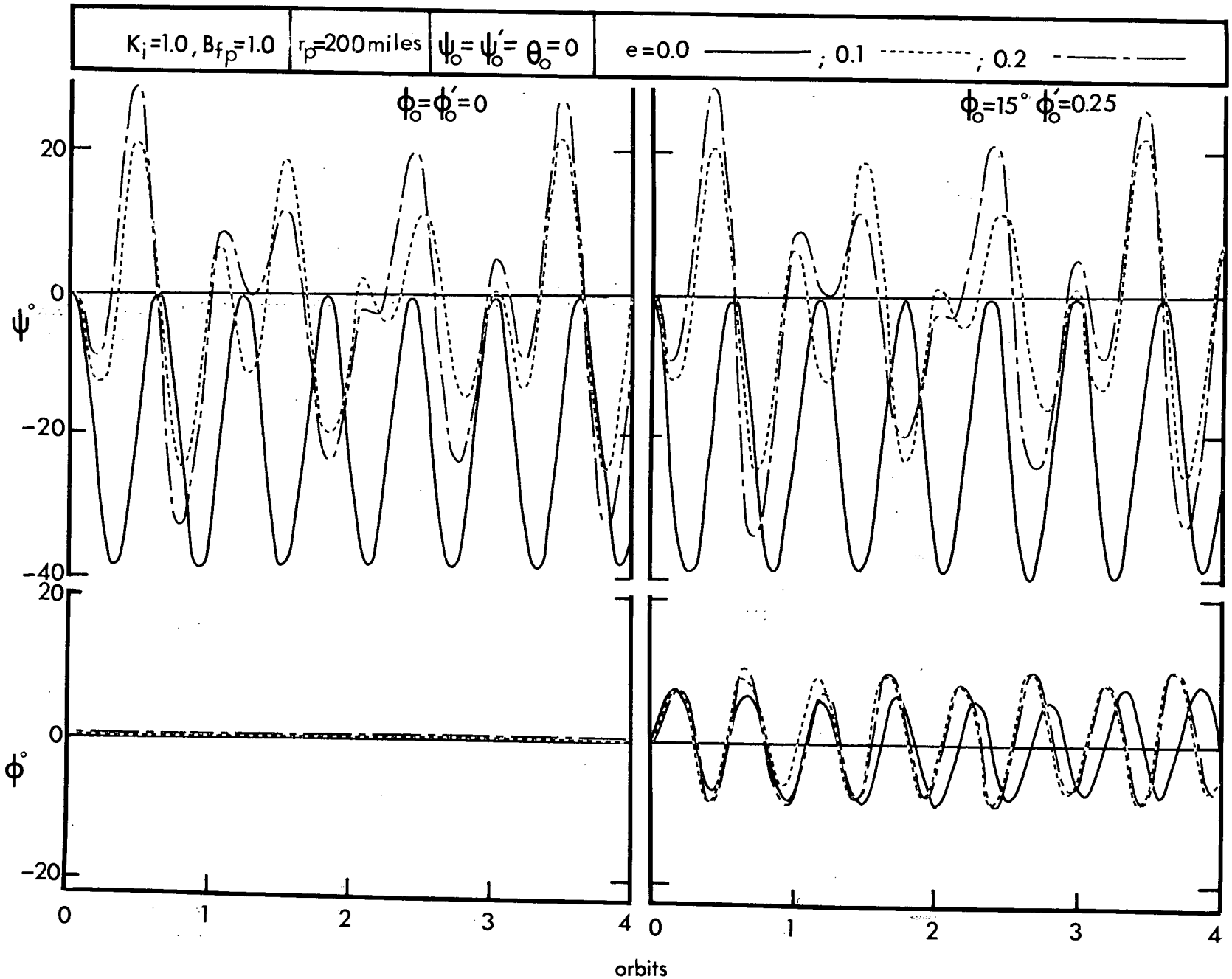

Figure 5-6 Typical system responses showing the effect of orbit eccentricity and (c) initial conditions

aerodynamic torque and equilibrium configuration makes the resulting response quite complex. The modulations, which are more predominant in the planar degree of freedom, grow rapidly with B_{f_p} (Figure 5-6(a)). Even for an identical disturbance in the two degrees of freedom, the planar component appears to be more susceptible to instability. This, in a sense, justifies the earlier simplified model of planar librations used by several authors.[2-9 et al.]

As can be expected, the forcing function arising from orbit eccentricity induces planar librational motion. Due to aerodynamic influence, planar oscillations were noticed in absence of any external disturbance, even in circular orbit. The combined effect of e and B_{f_E} results in a considerably larger planar motion (Figure 5-6(b)), particularly for short satellites. Irrespective of K_i, e or B_{f_E}, a satellite initially positioned correctly along the local vertical executes appreciable librations in the orbital plane. The presence of a cross motion does not affect it noticeably (Figure 5-6(c)). The character of the response suggests possible reduction in the stability region due to aerodynamic torque.

All the response data presented so far, correspond to stable operation of the satellite. Its critical dependence on satellite inertia and orbit eccentricity was shown through stability plots. In Figure 5-7 are shown several examples of instability as functions of K_i, B_f and e. Note that a slender satellite (K_i=1.0), moving in a circular orbit through

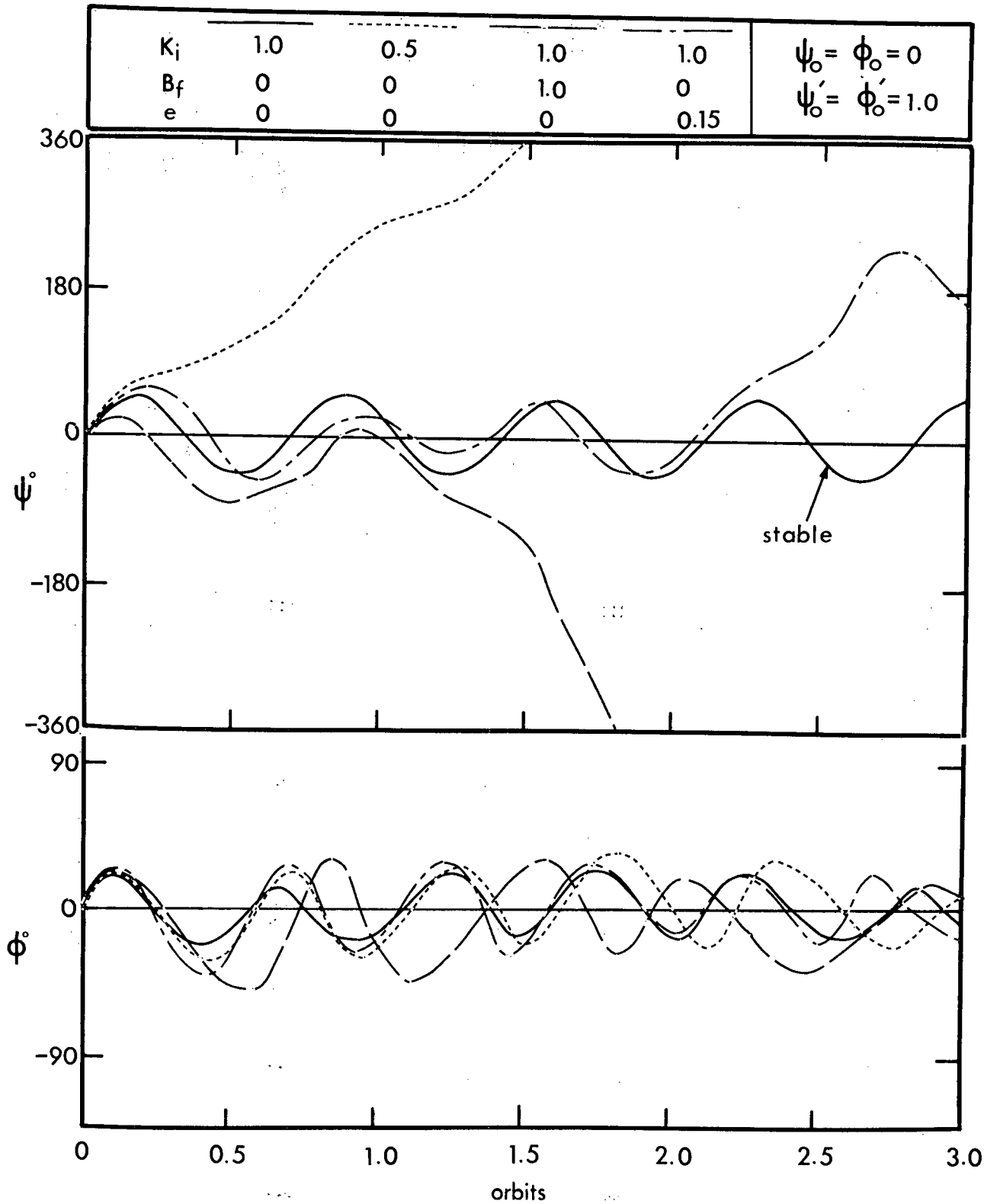

Figure 5-7 Instability excited by change of system parameter

a pure gravity gradient field executes large amplitude stable librations when subjected to a unit impulse ($\psi_o'=\phi_o'=1.0, \psi_o=\phi_o=0$). However, changes in system parameters beyond the critical values lead to tumbling motion. For instance, reduction of K_i to 0.5 or increase of eccentricity to 0.15 lead to instability within a short time. Increase in B_f to a unit value initiates 'clockwise' tumbling in circular orbit itself. It may be pointed out that in all these cases, the motion across the orbit remains bounded. Importance of parametric study of the system, from design considerations, is thus apparent.

5.5.4 Stability Plots

As no known closed form solution is available and the integral manifold technique does not appear to be applicable, the stability of the system is established, as before, through numerically generated response. Design plots again prove useful in condensing an enormous amount of information. The plots (Figure 5-8), symmetrical about $\phi_o'=0$, show all possible combinations of allowable impulsive disturbances for stability. The corresponding results for a circular orbit are also included for comparison. It is apparent that even a small eccentricity of the orbit makes the stability region shrink substantially. The presence of aerodynamic torque further enhances this trend. As in the case of eccentricity, the reduction in the stability margin is predominantly in the ψ degree of freedom. The system shows, in general, better ability to withstand positive

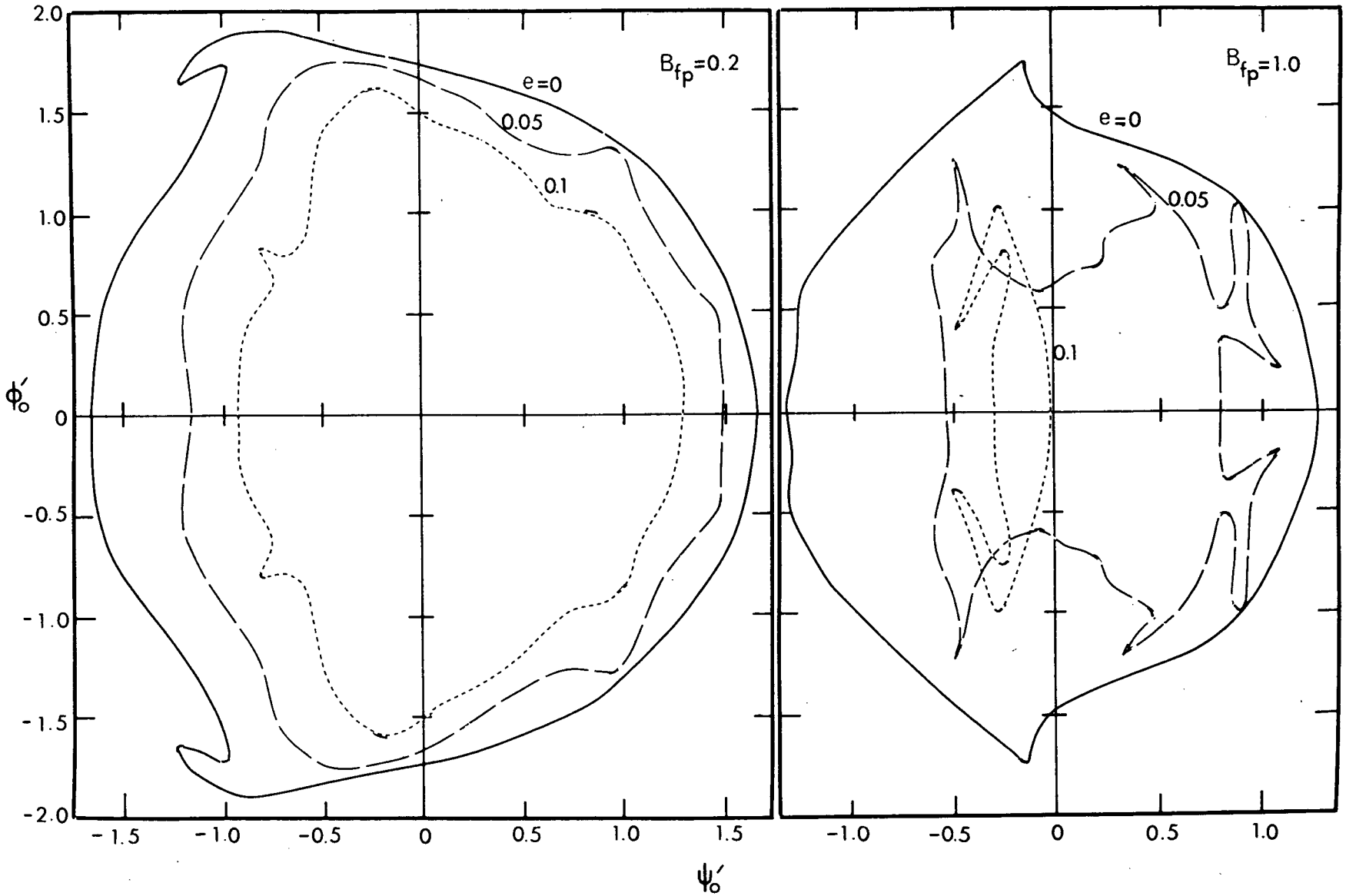

Figure 5-8 Effect of aerodynamic torque and orbit eccentricity on the allowable impulsive disturbance for stable motion; K_i=1.0, $\theta_o=\phi_o=0$, $\psi_o=\psi_e$

planar impulses. The peculiar shapes of the boundary with spikes may be attributed, as before, to coupling effects and the existence of a variety of periodic solutions.

The aerodynamic torque represents a periodic disturbance. Although active only over a relatively small portion of the satellite's eccentric orbit, it has considerable adverse influence on the stability.

The extensive amount of computation involved limited the investigation to only a few representative situations.

5.6 Concluding Remarks

The important aspects of the analysis and more significant conclusions may be summarized as follows:

(i) A simple closed form solution as given by Butenin's variation of parameter method can be used effectively during preliminary design of a satellite.

(ii) In the absence of any disturbance, eccentricity excites a pure planar motion having a period of the same order as the orbital rate. Coupling effects in this case are relatively less significant.

(iii) In the case of the non-autonomous system, the concept of integral manifold in the phase space loses its importance due to obvious limitation of visualization and interpretation of hyper-surfaces.

(iv) The stability region diminishes rapidly with increase in eccentricity. The shrinkage is more significant

in the planar degree of freedom and for shorter satellites (smaller K_i).

(v) The critical eccentricity for stable motion decreases substantially with reduction in K_i. Even in absence of aerodynamic moment, the gravity gradient fails to stabilize the most stable configuration of a dumbbell satellite beyond $e_{cr}=0.35$. The presence of atmosphere affects the situation adversely. The qualitative analysis suggests that at $K_i=1/3$ no stability can be expected. Any reduction of inertia parameter below this critical value reverses the normal trends.

(vi) The presence of aerodynamic torque affects the stable equilibrium configuration which changes periodically with the position of the satellite in eccentric orbit. The torque leads to rapid degeneration of stability region.

6. AERODYNAMIC DAMPING

6.1 Preliminary Remarks

Having gained some understanding of the behaviour of gravity-oriented systems, the next logical step would be to explore the possibility of controlling the undesirable librations to achieve high pointing accuracy. To this end several damping mechanisms have been evolved and analyzed.

Debra[39] considered use of a sphere moving in a viscous media to damp the general librations. Kamm[40] suggested the Vertistat: a set of two flexible booms put horizontally at right angle to each other to control the motion both in and across the orbital plane. For planar librational control Paul[41] proposed the use of a 'lossy' spring supporting a small mass. Modi and Brereton[42] improved this model through a parametric study. Tschann and Modi[43,44] undertook an optimization of the same model using analytical methods and presented a rigorous performance comparison with the conventional boom dampers.

Use of environmental forces in librational damping and attitude control is not new. Paul et al.[45] showed the feasibility of magnetic field. The application of solar radiation pressure for a space vehicle propulsion during inter-planetary flights has been proposed by several authors including Garwin,[38] who described it as "solar sailing."

Sohn[24] et al. investigated specific configurations for satellite stabilization with respect to the sun. More directly, Mallach[46] suggested the use of solar radiation as a damping force for gravity oriented satellites. Recently, Modi et al.[47-49] established the feasibility of using solar radiation pressure for an efficient planar damping and attitude control by adjusting the exposed areas of solar pads as a function of librational velocity and angle.

This chapter explores the possibility of utilizing the normally destabilizing aerodynamic moment to advantage. A semi-passive, velocity-sensitive controller provides restoring moment of appropriate magnitude and sense through judicious adjustment of flaps exposed to the free molecular flow. This concept of librational damping through differential lift is essentially an extension of the aircraft stabilization techniques.

6.2 Feasibility of the Concept

Introduction of the aerodynamic force to a gravity-gradient system presents a possibility of center of pressure not coinciding with the center of mass. This leads to the aerodynamic torque which, if controlled efficiently, can provide not only the librational damping but also the attitude control of the satellite. Extending the concept of aircraft attitude control to spacecraft moving in the rarefied atomsphere, consider a satellite, with two identical stabilizing 'flaps', as shown in Figure 6-1(a). The flaps, located in

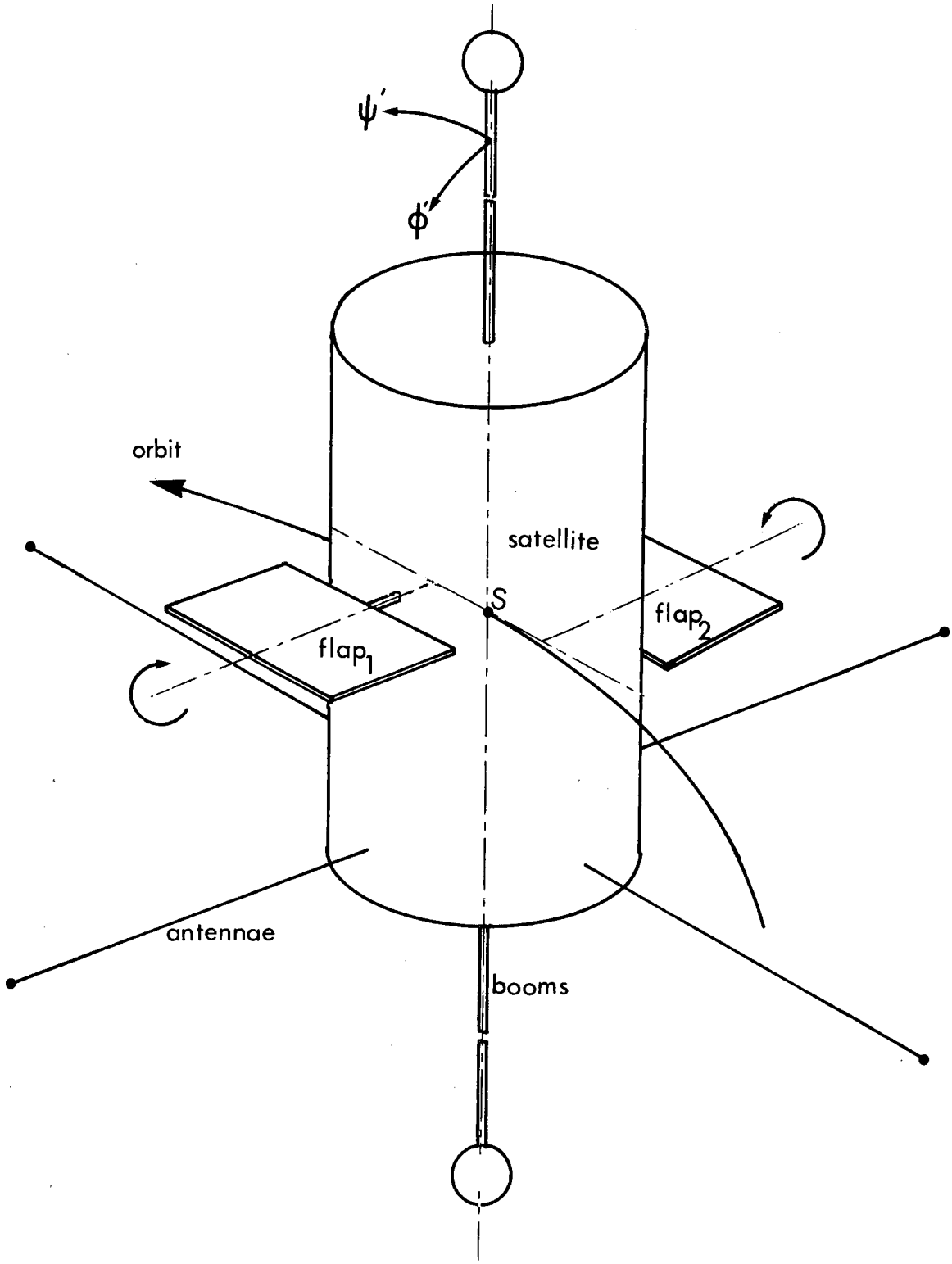

Figure 6-1 Aerodynamic damping and stabilization: (a) satellite configuration

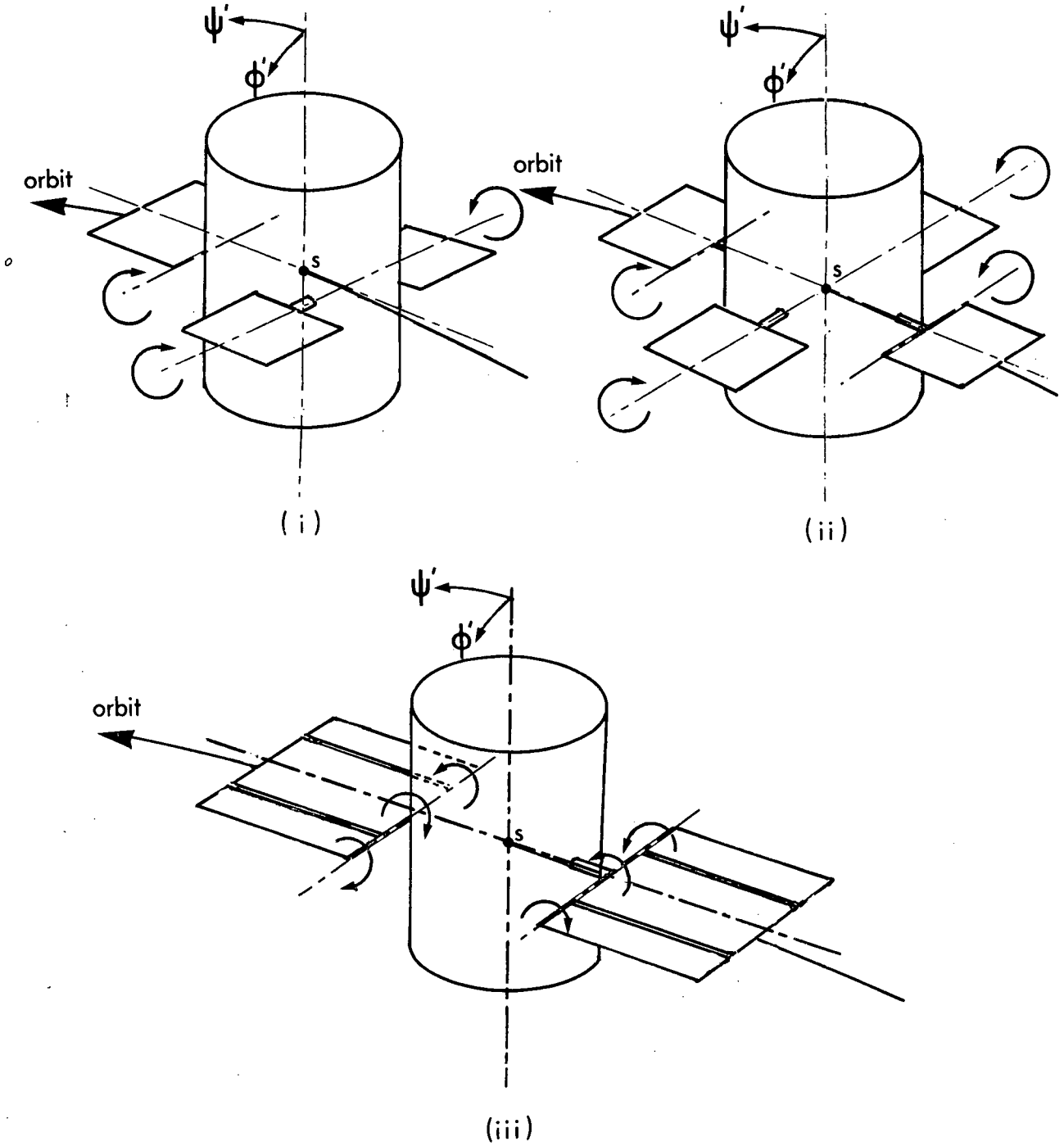

Figure 6-1 Aerodynamic damping and stabilization: (b) possible arrangements of stabilizers

the local horizontal plane passing through the center of mass of the satellite and controlled independently, are free to rotate about the axes perpendicular to the line of symmetry of the satellite. An equal and opposite rotation of the flaps, leads to moment about the center of mass which has stabilizing components in both ψ and ϕ degrees of freedom. Thus with librating satellites, flap orientation can be adjusted continuously to provide suitable correcting torque. The moment due to the forces being balanced, no rotation about the z axis (yaw) is induced. As the satellite, under the action of various disturbances, starts to librate, the flaps are inclined appropriately with respect to the impinging stream to provide a stabilizing torque. The torque, if controlled as a function of satellite's librational velocity, should be able to damp the motion.

Figure 6-1(b) shows some of the alternate schemes for flap arrangement. While the scheme discussed above is likely to be the simplest to construct it has obvious limitations, e.g., lack of control in an individual degree of freedom. The triangular setting (Figure 6-1(b)i), in which the front flap damps the planar motion while the rear two by their opposite movement control the cross-plane librations, provides a way of governing the individual degree of freedom. For maintaining the axi-symmetric character, the rear flaps are appropriately off-set from the center line of the satellite. A further improvement, in terms of symmetry and

magnitude of the restoring moment, is represented by the configuration shown in Figure 6-1(b)ii. Here the off-set is eliminated without affecting independent control of the individual degree. Introduction of a set of split-flaps (Figure 6-1(b)iii) represents another possibility. Here the center sections of each assembly are actuated individually to provide torque for planar control, while the other ones damp the motion in ϕ degree of freedom. Numerous other variations can be thought of by combining these basic arrangements.

The concept during actual design may be faced with several optimization problems:

(i) The atmospheric density as well as the lift coefficient reduce rapidly with increase in altitude. On the other hand, the life time of the satellites diminishes with their closeness to the earth. Thus a compromise is indicated.

(ii) The flaps should be light yet sufficiently rigid and large to generate enough lift. Furthermore, the drag should be small to minimize orbital perturbations.

(iii) The flaps should be so located as to avoid interference with the operation of antennae, cameras and solar cells.

(iv) The arms supporting the flaps should be long enough for adequate moment without sacrificing lightness

and rigidity. Obviously extensive ground tests would be required.

Angular movement of the well arranged flaps is likely to have little effect on total inertia, axi-symmetric character of the system or the position of the center of mass. Of course, sensing the disturbance and operation of the flaps may involve time delay. This, however, would be of little significance due to long period (order of orbital period) of the librations.

6.3 Response Analysis

With linearly proportional, velocity-sensitive control, the governing equations of motion in a circular orbit modify to:

$$\psi'' - 2\phi'(\psi'+1)\tan\phi + 3K_1 \sin\psi\cos\psi + B_f(|\cos\psi| + C_1\sin\psi)\cos\psi/\cos^2\phi + \mu_1\psi' = 0 \quad \ldots\ldots (6.1a)$$

$$\phi'' + [(\psi'+1)^2 + 3K_1\cos^2\psi]\sin\phi\cos\phi + \mu_2\phi' = 0 \quad \ldots\ldots (6.1b)$$

where μ_1 and μ_2 are positive proportionality constants and B_f is the constant aerodynamic coefficient for the satellite without flaps. Due to axi-symmetric arrangement, the stabilizers do not induce rotations about the z axis. The foregoing ignores any variations in damping torque due to small λ oscillations caused by coupling effects (equation (2.1c)).

The physical size and location of the flaps would also impose a limit on the stabilizing torque, i.e.,

$$|\mu_1 \psi'| \leq \tau_{1_{max}}$$

$$|\mu_2 \phi'| \leq \tau_{2_{max}} \qquad \ldots . (6.2)$$

where,

$$\tau_{i_{max}} = \rho v^2 A_{f_i} C_{L_{max}} l_{m_i} / 2I\dot{\theta}^2 \qquad \ldots . (6.3)$$

For example, a satellite, with I=600 slug. ft^2, in a circular orbit at 200 miles altitude ($\rho \simeq 3.0 \times 10^{-13}$ slug/ft^3 - ARDC 1959)[68] and provided with two 3' x 3' flaps with moment arm of 5' each, has the maximum coefficient of lift equal to about 0.2[66] and the associated $\tau_{i_{max}}$ becomes 2.0. The condition (6.2) implies that the flaps would maintain their orientation for torque requirement beyond $\tau_{i_{max}}$.

Figure 6-2 shows, over 3 orbits, the effect of controller proportionality constants (μ_1, μ_2) and system parameters on librational response. A slender satellite with a small aerodynamic coefficient B_f, undergoes substantially large motion in absence of damping. However, a small stabilizing torque in either ψ or ϕ direction causes a quick reduction in amplitude (Figure 6-2(a)). Increase in μ_1, μ_2 considerably improves the damping efficiency. The time index may be as small as the orbital period.

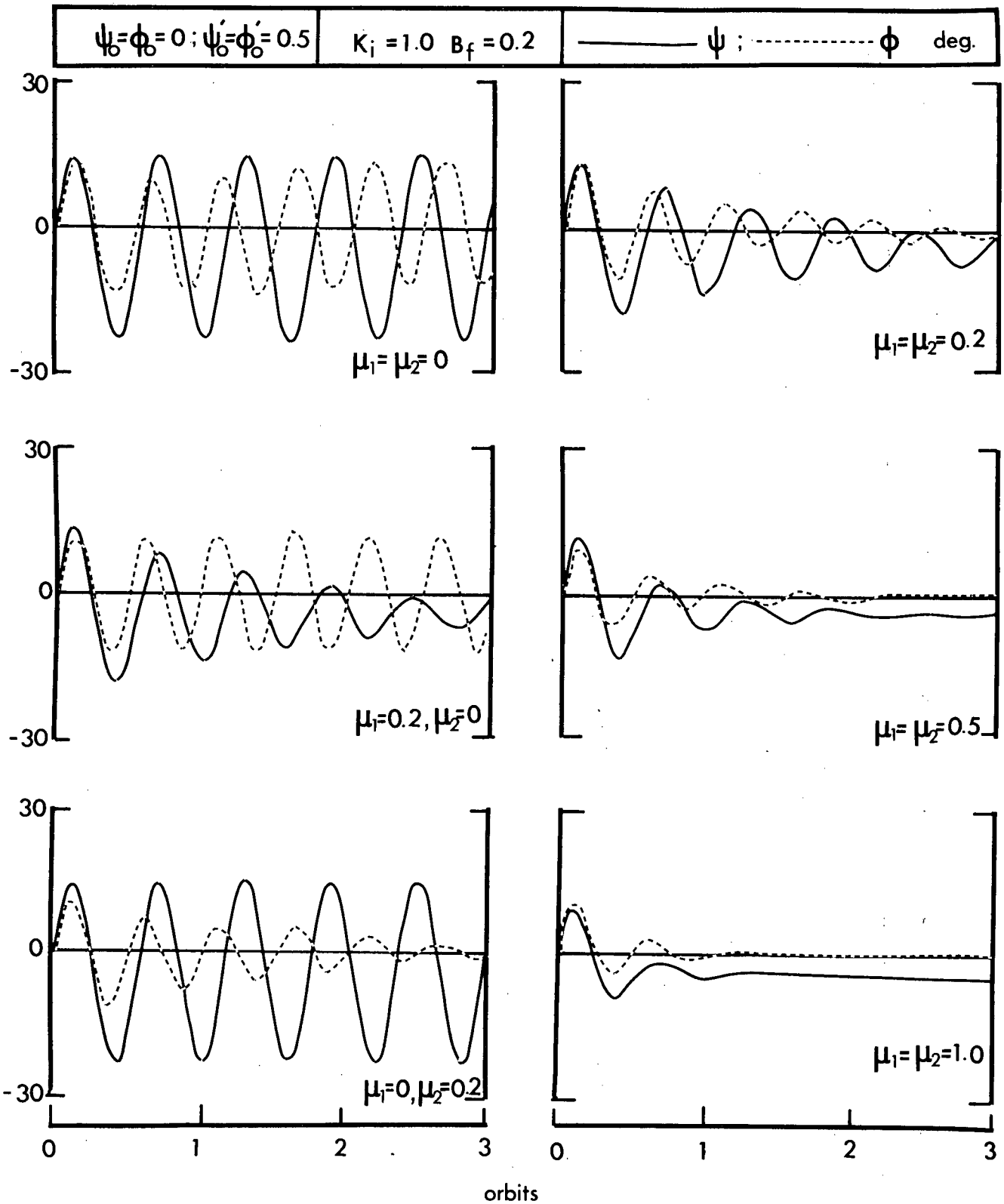

Figure 6-2 Aerodynamically damped response ($\tau_{i_{max}}$=2.0) showing the effects of:
(a) proportionality constants

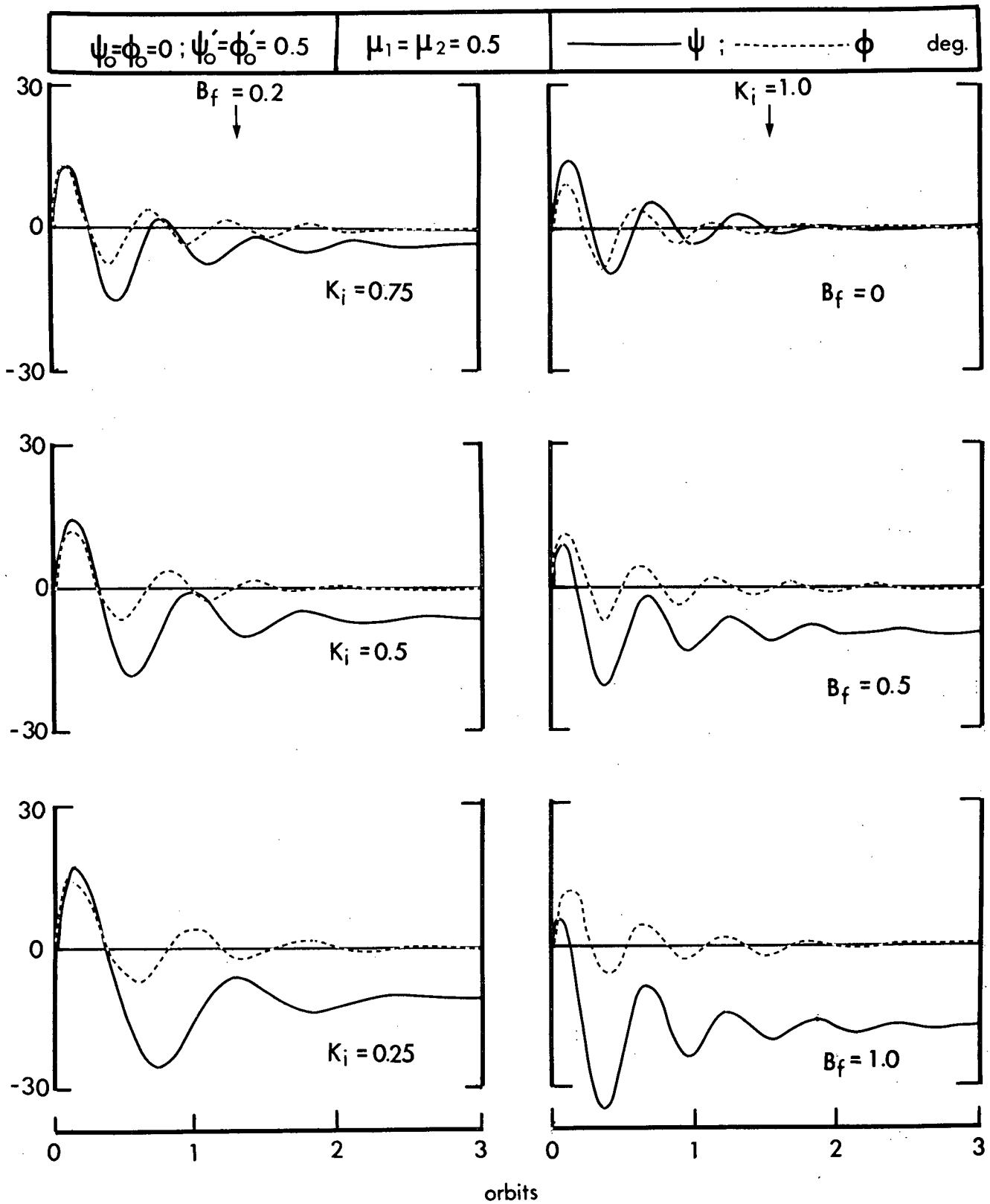

Figure 6-2 Aerodynamically damped response ($\tau_{i_{max}}$=2.0) showing the effects of:
(b) satellite inertia and aerodynamic torque

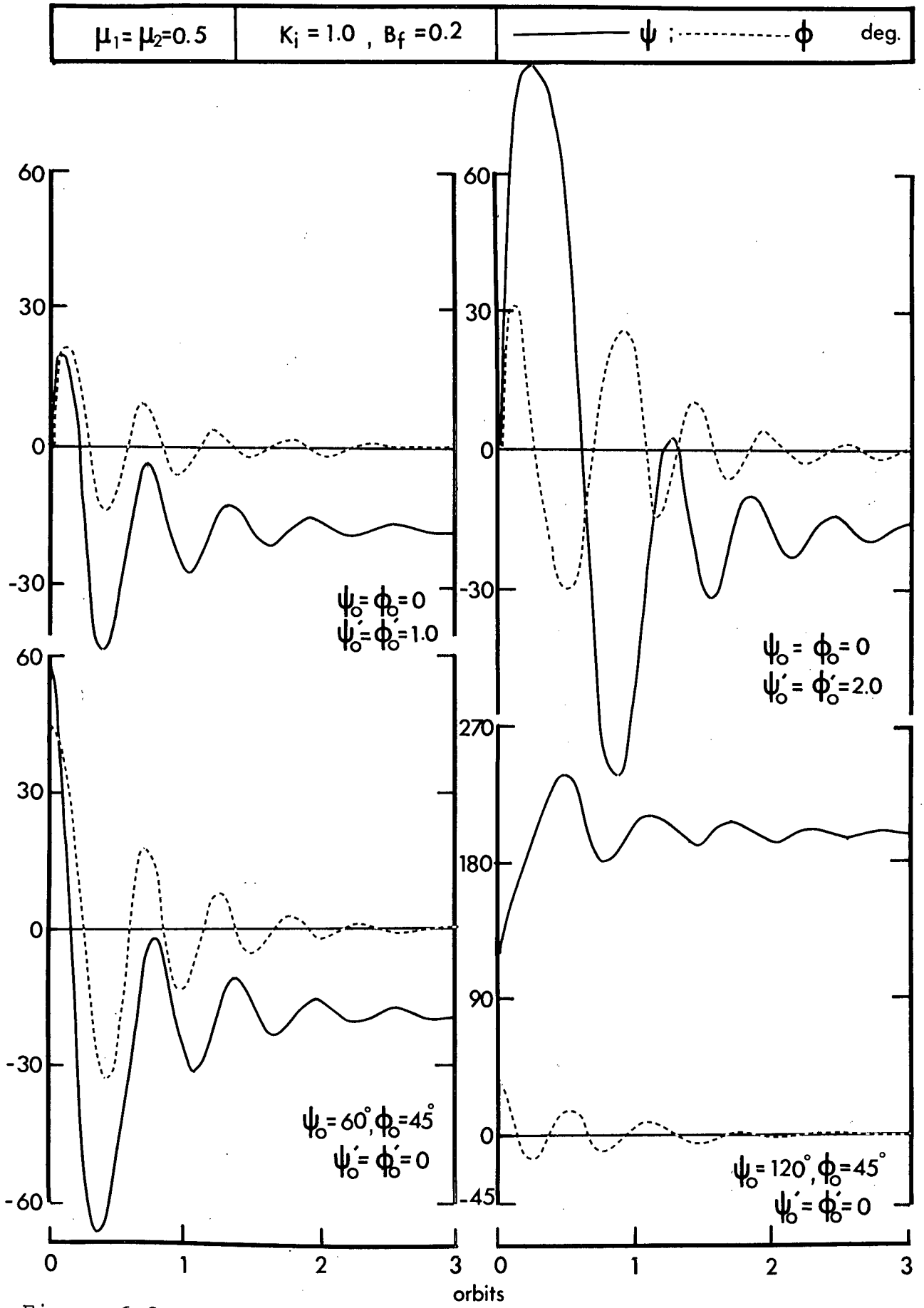

Figure 6-2 Aerodynamically damped response ($\tau_{i_{max}}$=2.0) showing the effects of:
(c) initial conditions

The effectiveness of this aerodynamic damping concept with reference to satellites of different K_i and B_f is suggested by Figure 6-2(b). It appears that irrespective of the transient response, which strongly depends on the system parameters, the time to damp remains relatively unaffected. Final configuration attained in each case is the stable equilibrium position, which depends on K_i and B_f only. As shown in Figure 6-2(c) the aerodynamic controller is able to damp large disturbances without changing the proportionality constants. Of course the time index, i.e., time to damp to the prescribed fraction of the initial amplitude, increases with the magnitude of a disturbance, yet even in the worse situation considered it is limited to three orbits. Bounded response to the normally destabilizing disturbance of $\psi_o'=\phi_o'=2.0$ (Figure 6-2(c)) suggests improved stability.

The mechanism appears to be quite effective in librational damping of near-earth satellites. Its efficiency in controlling general motion appears to be, at least, equal to that of conventional viscous dampers[44] and solar pressure stabilization[47-49] in planar motion.

It is interesting to note that if B_f, which involves several variable parameters, were adjusted appropriately or the stabilizing torque were controlled not only as a function of librational velocity but also of its angular displacement, the mechanism could stabilize the satellite at any desired orientation. This would represent a simple yet powerful method

of attitude control.

For eccentric orbits, steady state performance, i.e., time to damp as well as the limit cycle amplitudes would be of interest. Here also the general effectiveness of the controller appears to be promising.

6.4 Concluding Remarks

Aerodynamic damping of librational motion appears to be quite promising. A velocity-sensitive, semi-passive controller can damp even large amplitude motion, both in and across the orbital plane, in less than two orbits. The final configuration attained is the stable equilibrium one. The time index depends mainly on the proportionality constants and disturbances encountered. The stability bound is likely to be enlarged substantially.

Several optimization problems arising from mechanics, aerodynamics, control, and structual strength considerations do exist, however, they appear to be within the reach of the present level of technology.

7. CLOSING COMMENTS

7.1 Summary

As indicated at the outset, the main objective of this study has been to gain some insight into the librational response and stability of the gravity oriented satellites as affected by system parameters and aerodynamic forces. Emphasis, throughout, has been on generating information suitable for design purposes.

The thesis establishes several useful approaches to investigate the problems of autonomous and non-autonomous character with particular reference to the librational dynamics. Among the few analytical techniques available for the study of non-linear coupled problems, Butenin's variation of parameter method appears to fare well, at least for motion in the small. The success of the method in predicting amplitude and frequency with acceptable accuracy for both autonomous and non-autonomous systems makes it ideally suited to the planning of the satellite control system.

A precise,real time simulation using an analog computer is of considerable importance where cost is the over-riding consideration. It may prove to be of particular significance to the countries like Brazil and India which are involved in the design of communication satellites to be used for social reforms.

The study emphasizes the usefulness of zero velocity curves arising from constant Hamiltonian associated with the autonomous system. It provides bounds of librations, leads to approximate closed form solution for system response and constraints for guaranteed and conditional stability.

The concept of integral manifold used so successfully by Modi et al.[7-9, 27-29] in the stability study of the planar system can also be utilized in analyzing an autonomous, coupled system. It provides all possible combinations of external disturbances to which a satellite can be subjected, at any point in its orbit, without causing it to tumble. The fact that the degeneration of the invariant surface leads to a periodic solution further enhances the importance of the method. Application of the Floquet theory to the fourth order system helps to establish stability of the periodic motion as well as the critical disturbance leading to a tumbling motion.

Of considerable interest are the three distinctly different solutions - regular, island type, and ergodic - in the guaranteed stability domain. The regular stability region being the only one usable from practical considerations, its detailed study and the resulting design charts represent innovations of far reaching implication.

With the study of the non-autonomous case of elliptic orbits we take a modest step forward in a field that has remained, so far, unexplored. The addition of atmospheric

effects clearly emphasize the penalty, in terms of reduced stability, one must pay to achieve longer life.

Finally the utilization of aerodynamic forces to advantage through a semi-passive controller represents the first recorded attempt. The concept presents exciting possibilities of efficient librational damping and attitude control.

It is believed that the information presented here adds to our understanding of satellite attitude dynamics and should prove useful during spacecrafts' design.

7.2 Recommendations for Future Work

The investigation reported here brings to light numerous possibilities for extension and innovations. Some of the more important problems are listed below:

(i) The dynamical study of an arbitrarily shaped, non-rigid satellite would make the analysis more realistic and complete. The magnitude of the difficulties, however, increases substantially as the inertia parameter becomes a time dependent function and λ, the rotation about the long axis, no longer remains a cyclic coordinate.

(ii) Slow orbital decay and local variations in atmospheric conditions make the aerodynamic coefficient a function of time, even in near-circular orbits. This together with the influence of other environmental disturbances, such as solar and earth radiations,

on the general motion of satellites merit investigation.

(iii) In spite of the complex character of the problem, the approximate closed form solutions, in general, have proved to be of considerable practical use. Hence all efforts should be made to improve their accuracy. The use of modified generating functions, better representation of coupling effects, series solution, extension of W.K.B.J. Method to fourth order systems, etc., all appear promising.

(iv) As periodic solutions represent degeneration of integral manifolds, the possibility of reconstructing them from known periodic solutions should be explored. The stability analysis of periodic solution as given Modi and Brereton[8,9] may form a starting point for any such attempt.

Recognizing the important role played by periodic solutions in stability study, their determination for the non-autonomous case represents logical extension to the study in Chapter 4. The corresponding solution for motion in a circular orbit being known, perturbation analysis may prove effective, at least for small eccentricity orbits.

(v) For non-autonomous, coupled, conservative system, the concept of the integral manifold failed to provide useful information, primarily because of the diffi-

culty in visualizing a surface in more than a three dimensional domain. This, indeed, presents a challenging problem. Probably, the method of adiabatic invariants using slowly varying Hamiltonian may prove to be of some use.

(vi) The concept of librational damping using aerodynamic forces should be extended:

(a) to cover non-autonomous situation

(b) to explore its effectiveness in attitude control by adding displacement sensitive terms.

This presents an interesting possibility of changing satellite orientation in the orbit.

BIBLIOGRAPHY

1. 'Communication Satellites - a New World Now' special issue Astronautics and Aeronautics, AIAA, Vol. 6, No. 4, April 1968, p. 32, 71.

2. Klemperer, W.B. "Satellite Librations of Large Amplitude," ARS Journal, Vol. 30, No. 1, January 1960, pp. 123-124.

3. Baker, R.M., Jr., "Librations on a Slightly Eccentric Orbit," ARS Journal, Vol. 30, No. 1, January 1960, pp. 124-126.

4. Beletskiy, V.V., "The Libration of a Satellite on an Elliptic Orbit," Dynamics of Satellites, edited by M. Roy, Academic Press, New York, 1963, pp. 219-230.

5. Schechter, H.B., "Dumbbell Librations in Elliptic Orbits," AIAA Journal, Vol. 2, No. 6, June 1964, pp. 1000-1003.

6. Zlatousov, V.A., Okhotsimsky, D.E., Sarghev, V.A., and Torzhevsky, A.P., "Investigation of Satellite Oscillations in the Plane of an Elliptic Orbit," Proceedings XI International Congress of Applied Mechanics, edited by H. Görtler, Springer-Verlog, Berlin, 1964, pp. 436-439.

7. Brereton, R.C., and Modi, V.J., "Stability of Planar Librational Motion of a Satellite in Elliptic Orbit," Proceedings XVII International Astronautical Federation Congress, Gorden and Breach Science Publishers, Inc., New York, 1967, pp. 179-192.

8. Modi, V.J., and Brereton, R.C., "Periodic Solutions Associated with the Gravity-Gradient Oriented System; Part I: Analytical and Numerical Determination," AIAA Journal, Vol. 7, No. 7, July 1969, pp. 1217-1225.

9. Modi, V.J., and Brereton, R.C., "Periodic Solutions Associated with the Gravity Gradient Oriented System; Part II: Stability Analysis," AIAA Journal, Vol. 7, No. 8, August 1969, pp. 1465-1468.

10. Brereton, R.C., "A Stability Study of Gravity Oriented Satellites," Ph.D. Thesis, University of British Columbia, November 1967.

11. Thomson, W.T., "Spin Stabilization of Attitude Against Gravity Torque," The Journal of Astronautical Sciences, Vol. 9, No. 1, January 1962, pp. 31-33.

12. Kane, T.R., and Barba, P.M., "Attitude Stability of a Spinning Satellite in an Elliptic Orbit," Journal of Applied Mechanics, June 1966, pp. 402-405.

13. Wallace, F.B., Jr., and Meirovitch, L., "Attitude Instability Regions of a Spinning Symmetric Satellite in an Elliptic Orbit," AIAA Journal, Vol. 5, No. 9, September 1967, pp. 1642-1650.

14. Modi, V.J., and Neilson, J.E., "Roll Dynamics of a Spinning Axi-Symmetric Satellite Using the W.K.B.J. Method," Aeronautical Journal, the Royal Aeronautical Society, Vol. 72, No. 693, September 1968, pp. 807-810.

15. Modi, V.J., and Neilson, J.E., "Roll Dynamics of a Spinning Axi-Symmetric Satellite in an Elliptic Orbit," Aeronautical Journal, the Royal Aeronautical Society, Vol. 72, No. 696, December 1968, pp. 1061-1065.

16. Modi, V.J., and Neilson, J.E., "Attitude Dynamics of Slowly Spinning Axi-Symmetric Satellites Under the Influence of Gravity Gradient Torques," Proceedings XX International Astronautical Federation Congress, Mar-del Plata, Argentina, October 1969, (in press).

17. Modi, V.J., and Neilson, J.E., "On the Periodic Solution of Slowly Spinning Gravity-Gradient System," to be presented at XXI International Astronautical Federation Congress, Constance, German Federal Republic, October 1970.

18. Neilson, J.E., "On the Attitude Dynamics of Slowly Spinning Axi-Symmetric Satellites Under the Influence of Gravity-Gradient Torque," Ph.D. Thesis, University of British Columbia, November 1968.

19. Roberson, R.E., "Attitude Control of a Satellite Vehicle - An Outline of the Problem," Proceedings VIII International Astronautical Congress, Wein-Springer-Verlag, Berlin, 1958, pp. 317-339.

20. Wiggins, L.E., "Relative Magnitude of Space-Environmental Torques on a Satellite," AIAA Journal, Vol. 2, No. 4, April 1964, pp. 770-771.

21. Moyer, R.G., and Katucki, R.J., "Gravity-Gradient Stabilization of Communication Satellite Systems," AIAA Communication Satellite System Conference, Washington D.C., May 1966, AIAA paper No. 66-303.

22. Anand, D.K., Whisnant, J.M., Pisacane, V.L., and Sturmanis, M., "Gravity-Gradient Capture and Stability in an Eccentric Orbit," Journal of Spacecrafts and Rockets, AIAA, Vol. 6, No. 12, December 1969, pp. 1456-1459.

23. Flanagan, R.C., and Modi, V.J., Radiation Forces on a Flat Plate in Ecliptic Near-Earth Orbits," Transactions of the Canadian Aeronautics and Space Institute, Vol. 3, September 1970, pp.

24. Sohn, R.L., "Attitude Stabilization by Means of Solar Radiation Pressure," ARS Journal, Vol. 29, No. 5, May 1959, pp. 371-373.

25. Ule, L.A., "Orientation of Spinning Satellite by Radiation Pressure," AIAA Journal, Vol. 1, No. 7, July 1963, pp. 1575-1578.

26. Clancy, T.F., and Mitchell, T.P., "Effects of Radiation Forces on the Attitude of an Artifical Earth Satellites," AIAA Journal, Vol. 2, No. 3, March 1964, pp. 517-524.

27. Modi, V.J., and Flanagan, R.C., "Effect of Environmental Forces on the Attitude Dynamics of Gravity Oriented Satellites; Part I: High Altitude Orbits," Aeronautical Journal, the Royal Aeronautical Society, (in press).

28. Modi, V.J., and Flanagan, R.C., "Effect of Environmental Forces on the Attitude Dynamics of Gravity Oriented Satellites; Part II: Intermediate Orbits Accounting for Earth Radiations," Aeronautical Journal, the Royal Aeronautical Society, (in press).

29. Flanagan, R.C., and Modi, V.J., "Effect of Environmental Forces on the Attitude Dynamics of Gravity Oriented Satellites; Part III: Close-Earth Orbits Accounting for Aerodynamic Forces," Aeronautical Journal, the Royal Aeronautical Society, (in press).

30. Flanagan, R.C., "Effect of Environmental Forces on the Attitude Dynamics of Gravity Oriented Satellites," Ph.D. Thesis, University of British Columbia, July 1969.

31. Schrello, D.M., "Aerodynamic Influence on Satellite Librations," ARS Journal, Vol. 31, No. 3, March 1961, pp. 442-444.

32. Debra, D.B. "The Effect of Aerodynamic Forces on Satellite Attitude," The Journal of Astronautical Sciences, Vol. 6, 1959, pp. 40-45.

33. Beletskiy, V.V., "Motion of an Artifical Earth Satellite About its Center of Mass," Artificial Earth Satellites, Vol. 1, edited by L.V. Kurnosova, Plenum Press, New York, 1960, pp. 30-59.

34. Evans, W.J., "Aerodynamic and Radiation Disturbance Torques on Satellites Having Complex Geometry," Journal of Astronautical Sciences, Vol. 9, 1962, pp. 93-99.

35. Garbar, T.B., "Influence of Constant Disturbance Torques on the Motion of Gravity Gradient Stabilized Satellites," AIAA Journal, Vol. 1, No. 4, 1963, pp. 968-969.

36. Meirovitch, L., and Wallace, F.B., Jr., "On the Effect of Aerodynamic and Gravitational Torques on the Attitude Stability of Satellites," AIAA Journal, Vol. 4, No. 12, December 1966, pp. 2196-2202.

37. Nurre, G.S., "Effect of Aerodynamic Torque on an Asymmetric Gravity Stabilized Satellite," AIAA Journal, Vol. 6, No. 9, September 1968, pp. 1046-1050.

38. Garwin, R.L., "Solar Sailing - A Practical Method of Propulsion Within the Solar System," Jet Propulsion, Vol. 28, No. 3, March 1958, pp. 188-190.

39. Debra, D., "The Large Attitude Motions and Stability due to Gravity of a Satellite with Passive Damping in an Orbit about an Oblate Body," Ph.D. Thesis, Stanford University, June 1962.

40. Kamm, L.J., "Vertistat: an Improved Satellite Orienting Device," ARS Journal, Vol. 32, No. 6, June 1962, pp. 911-913.

41. Paul, B., "Planar Librations of an Extensible Dumbbell Satellite," AIAA Journal, Vol. 1, No. 2, February 1963, pp. 411-418.

42. Modi, V.J., and Brereton, R.C., "The Planar Motion of a Damped Gravity Gradient Stabilized Satellite," Transactions of the Canadian Aeronautics and Space Institute, Vol. 2, No. 1, March 1969, pp. 44-48.

43. Tschann, C., and Modi, V.J., "Linearized Analysis of a Damped Gravity Oriented Satellite," Aeronautical Journal, the Royal Aeronautical Society, (in press).

44. Tschann, C., and Modi, V.J., "A Comparative Study of two Classical Damping Mechanisms for Gravity Oriented Satellites," Transactions of the Canadian Aeronautics and Space Institute, (in press).

45. Paul, B., West, J.W., and Yu, E.Y., "A Passive Gravitational Attitude Control System for Satellites," The Bell System Technical Journal, Vol. 42, September 1963, pp. 2195-2238.

46. Mallach, E.G., "Solar Pressure Damping of Librations of Gravity Gradient Oriented Satellite," AIAA Student Journal, Vol. 4, No. 4, December 1966, pp. 143-147.

47. Modi, V.J., and Flanagan, R.C., "Librational Damping of Gravity Oriented System Using Solar Radiation Pressure," Aeronautical Journal, the Royal Aeronautical Society, (in press).

48. Modi, V.J., and Tschann, C., "On the Attitude and Librational Control of a Satellite Using Solar Radiation Pressure," to be presented at XXI International Astronautical Federation Congress, Constance, German Federal Republic, October 1970.

49. Tschann, C., and Modi, V.J., "Solar Radiation Damping of a Gravity Oriented Satellite Using W.K.B. Method," (presented for publication).

50. Pringle, R., Jr., "Stability of Damped Mechanical Systems," AIAA Journal, Vol. 3, No. 2, February 1965, p. 363.

51. Tschann, C., "On the Librational Dynamics of Damped Satellites," Ph.D. Thesis, University of British Columbia, September 1970.

52. Kane, T.R., "Attitude Stability of Earth-Pointing Satellites," AIAA Journal, Vol. 3, No. 4, April 1966, pp. 726-731.

53. Modi, V.J., and Brereton, R.C., "The Stability Analysis of Coupled Librational Motion of a Dumbbell Satellite in a Circular Orbit," Proceedings XVIII International Astronautical Federation Congress, Pergamon Press, London, 1968, pp. 109-120.

54. Pisacane, V.L., Pardoe, P.P., and Hook, P.J., "Stabilization System Analysis and Performance of GEOS-A Gravity Gradient Satellite (Explorer XXIX)," Proceedings of AIAA/JACC Guidance and Control Conference, AIAA, 1968, pp. 226-237.

55. Auelmann, R.R., "Regions of Librations for a Symmetrical Satellite," AIAA Journal, Vol. 1, No. 6, June 1963, pp. 1445-1446.

56. Krylov, N.M., and Bogoliubov, N.N., Introduction to Non-linear Mechanics, Princeton University Press, 1943.

57. Butenin, N.V., Elements of Non-linear Oscillations, Blaisdell, 1965, pp. 102-137, 201-217.

58. Hamming, R.W., Numerical Methods of Scientists and Engineers, McGraw-Hill Book Co., Inc., New York, 1962, pp. 183-222.

59. Mitropoloskiy, Y.A., "The Method of Integral Manifold in the Theory of Non-linear Oscillations," International Symposium on Nonlinear Differential Equations and Non-linear Mechanics, edited by J.P. LaSalle and S. Lefschetz, Academic Press, New York, 1963, pp. 1-15.

60. Hénon, M., and Heiles, C., "The Applicability of Third Integral of Motion - Some Numerical Experiments," Astronomical Journal, Vol. 69, No. 1, January 1964, pp. 73-79.

61. Jeffreys, W.H., "Some Dynamical Systems of Two Degrees of Freedom in Celetial Mechanics," Astronomical Journal, Vol. 71, No. 5, June 1966, pp. 306-313.

62. Moran, J.P., "Effects of Plane Librations on the Orbital Motion of a Dumbbell Satellite," ARS Journal, Vol. 31, No. 8, August 1961, pp. 1089-1096.

63. Yu, E.Y., "Long-term Coupling Effects Between the Librational and Orbital Motions of a Satellite," AIAA Journal, Vol. 2, No. 3, March 1964, pp. 553-555.

64. Brereton, R.C., and Modi, V.J., "Accuracy of the Numerically Generated Integral Manifolds," AIAA Journal, Vol. 6, No. 7, July 1968, pp. 1415-1417.

65. Cunningham, W.J., Introduction to Nonlinear Analysis, McGraw-Hill Book Co., Inc., New York, 1958, pp. 74-84.

66. Schaaf, S.A., and Chambré, P.L., Flow of Rarefied Gases, Princeton University Press, 1961, pp. 17-24.

67. Cook, G.E., ARC Current Paper No. CP523, Ministry of Aviation, H.M.S.O., London, 1960.

68. Jensen, J., Townsend, G., Kork, J., and Kraft, D., Design Guide to Orbital Flight, McGraw-Hill Book Co., Inc., New York, 1962, pp. 179-264.

69. Ashley, J.R., Introduction to Analog Computation, John Wiley and Sons, Inc., New York, 1963.

70. Minorsky, N., Non-linear Oscillations, D. Van Nostrand Co., Inc., Princeton, 1962, pp. 127-133, 390-415.